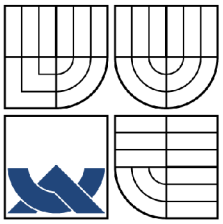

VYSOKÉ UČENÍ TECHNICKÉ V BRNĚ
BRNO UNIVERSITY OF TECHNOLOGY

FAKULTA STROJNÍO INŽENÝRSTVÍ
ÚSTAV MATEMATIKY
FACULTY OF MECHANICAL ENGINEERING
INSTITUTE OF MATHEMATICS

Zobrazovací Reflektometrie

měření optických vlastností tenkých vrstev

Imaging Reflectometry

mesuring thin films optical properties

Disertační práce

Doctoral Thesis

Autor práce
Author — Ing. Tomáš Běhounek

Vedoucí práce
Supervisor — prof. RNDr. Miloslav Druckmüller, CSc.

Brno 2009

Abstrakt

V této práci je prezentována inovativní metoda zvaná *Zobrazovací Reflektometrie*, která je založena na principu spektroskopické reflektometrie a je určena pro vyhodnocování optických vlastností tenkých vrstev .

Spektrum odrazivosti je získáno z map intenzit zaznamenaných CCD kamerou. Každý záznam odpovídá předem nastavené vlnové délce a spektrum odrazivosti může být určeno ve zvoleném bodu nebo ve vybrané oblasti.

Teoretický model odrazivosti se fituje na naměřená data pomocí Levenberg - Marquardtova algoritmu, jehož výsledky jsou optické vlastnosti vrstvy, jejich přesnost, a určení spolehlivosti dosažených výsledků pomocí analýzy citlivosti změn počátečních nastavení optimalizačního algoritmu.

Abstract

An innovative method of evaluating thin film optical properties, the so called *Imaging Reflectometry* based on principles of spectroscopic reflectometry is presented in this thesis. Reflectance spectra of the film is extracted from intensity maps recorded by CCD camera, that correspond to chosen wavelengths, either over selected area or at one point.

A theoretical model of reflectance is fitted to experimental data (the extracted reflectance spectra) by applying Levenberg - Marquardt algorithm in order to determine optical properties, their accuracy and reliability factor used to quantify a convergence successfulness of the reflectance model and hence the quality of the acquired results at given settings in a sense of a sensitivity analysis.

Klíčová slova

Tenká vrstva, optické vlastnosti, reflektometrie, disperzní model, odrazivost, spektrum odrazivosti, nelineární regrese, metoda nejmenších čtverců, Levenberg - Marquardt, analýza citlivosti, faktor spolehlivosti, zpracování obrazu, aditivní šum, obrazový filtr

Key Words

Thin film, optical properties, reflectometry, dispersion model, reflectance, reflectance spectra, nonlinear regression, sum of the least squares, Levenberg - Marquardt, sensitivity analysis, reliability factor, image processing, additive noise, image filter

BĚHOUNEK, T. *Imaging Reflectometry measuring thin films optical properties*, Brno: Vysoké učení technické v Brně, Fakulta strojního inženýrství, 2010. 79 s. Vedoucí disertační práce prof. RNDr. Miloslav Druckmüller, CSc.

Affirmation

I affirm that I created the thesis independently following the supervisor's instructions and with use of the presented literature.

18th November 2009 Tomáš Běhounek

Thanks

My special thanks belong to **prof. RNDr. Miloslav Druckmüller, CSc.** for his expert supervision, useful advices and instructions that contributed to creation of this thesis.

Another special thanks belong to **prof. RNDr. Jiří Spousta, Ph.D.** for introduction of the problematics of materials reflectivity.

Contents

1 Introduction

Many methods determined for measuring optical properties of thin films are known as well as many innovative processes have been developed and applied to improve these methods [1]. Nevertheless, some of the improvements are too specific to be implemented to every method and hence they are often suitable only to a certain method.

One of the methods, so called *Imaging Reflectometry* based on principles of spectroscopic reflectometry [2, 3], enables measuring optical characteristics and morphology of materials within a short time and figures out a reliability of the acquired results even if the measurement is carried out over a marked region of the sample. This method processes intensity images that are created by monochromatic light and recorded by CCD camera where the characteristics of the light are controlled by setting of a measuring assembly depicted in Fig. 1. The images store only a relative reflectance of the sample and because its absolute reflectance is required for the measurement a reference material (i.e. the material with known absolute reflectance [4]) has to be measured (presented in [2]). The absolute reflectance of the sample A_S can be then formulated as:

$$A_S = \frac{I_S}{I_R} \cdot A_R, \tag{1}$$

where I_S and I_R represent the intensities of a light reflected from the sample and reference respectively where the ratio I_S to I_R expresses the relative reflectance of the sample and the A_R denotes the absolute reflectance of the reference.

The calculations of the optical properties of the measured sample are proceeded by Levenberg - Marquardt algorithm [5], [6, pp. 100 - 107]. Apart from measuring experimental data this algorithm is crucial at carrying out a sensitivity analysis where simulated data is proceeded to determine a convergence reliability of the algorithm in order to support or reject the reliability of the calculated results. The analysis deals with the initial setting of the optical characteristics and the global setting of the optimizing algorithm in a sense of detecting sets of initial settings of the optical properties that lead to the desired solutions. By the reason of complexity of the measurement, all procedures concerned with optical properties calculation are included in a REFLECTOMETRY software package.

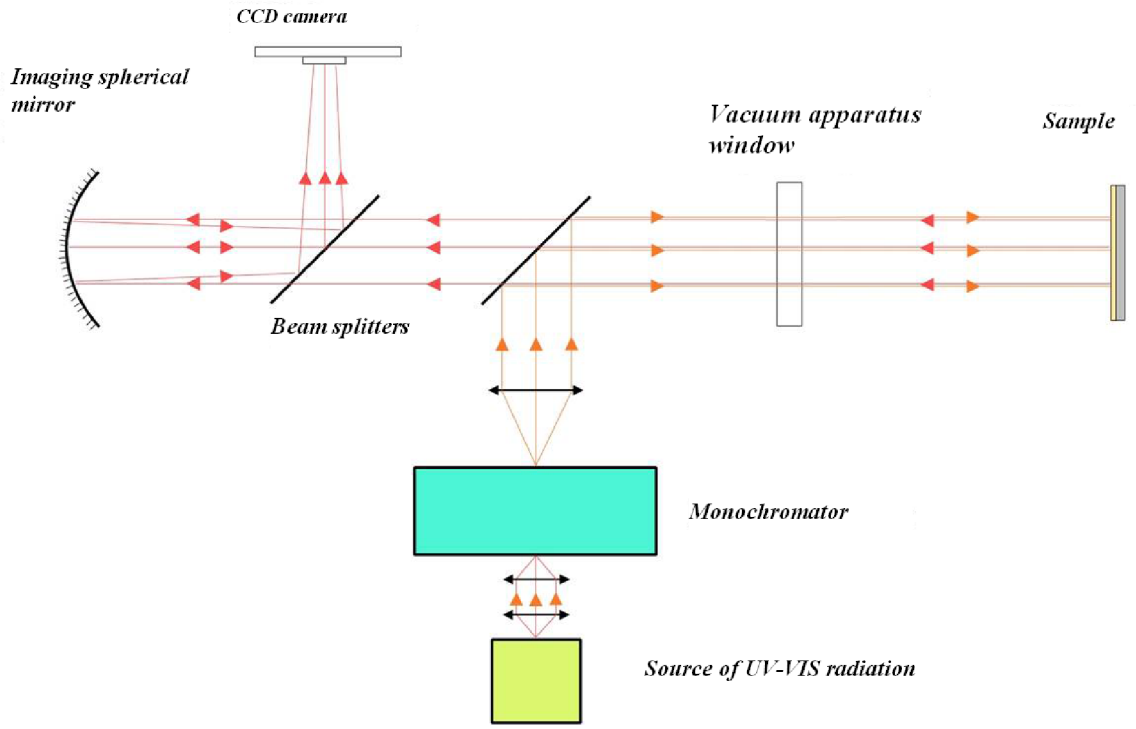

Figure 1: Measuring assembly scheme.

2 Reflectance model

2.1 Model of refractive index

Optical thin films are characterized by the thickness d and complex refractive index [1], [7, pp. 752] $\tilde{N}$

$$\tilde{N} = n + \mathrm{i}k, \tag{2}$$

where n expresses the refractive index of the film and k represents its extinction coefficient (i.e. the coefficient describing the absorption of the material).

The n and k actually describe the material dispersion as they are functions of wavelength λ [7, pp. 752]. The material dispersion is sufficiently defined through the *Cauchy's models* [7, pp. 100] where n and k are expressed in a form of

$$n = A_0 + \frac{A_1}{\lambda^2} + \frac{A_2}{\lambda^4} + \cdots + \frac{A_p}{\lambda^{2p}}, \tag{3}$$

$$k = B_0 + \frac{B_1}{\lambda^2} + \frac{B_2}{\lambda^4} + \cdots + \frac{B_l}{\lambda^{2l}}. \tag{4}$$

Considering second term only is often sufficient enough to describe physical behavior of the material response.

For illustration Cauchy's models [7, pp. 100] of $\tilde{N}$ of several materials are presented bellow and depicted in Fig. 2 where n and k are from [4].

$$\mathrm{SiO_2}: \qquad \tilde{N} = 1.52 + \frac{5000}{\lambda^2},$$

$$\mathrm{SiO_2}: \qquad \tilde{N} = 1.44 + \frac{7000}{\lambda^2} + \mathrm{i}\left(1 \cdot 10^{-5} + \frac{1 \cdot 10^{-10}}{\lambda^2}\right),$$

$$\mathrm{Si_3N_4}: \qquad \tilde{N} = 2.0 + \frac{15000}{\lambda^2},$$

$$\mathrm{PMMA}: \qquad \tilde{N} = 1.38 + \frac{12000}{\lambda^2},$$

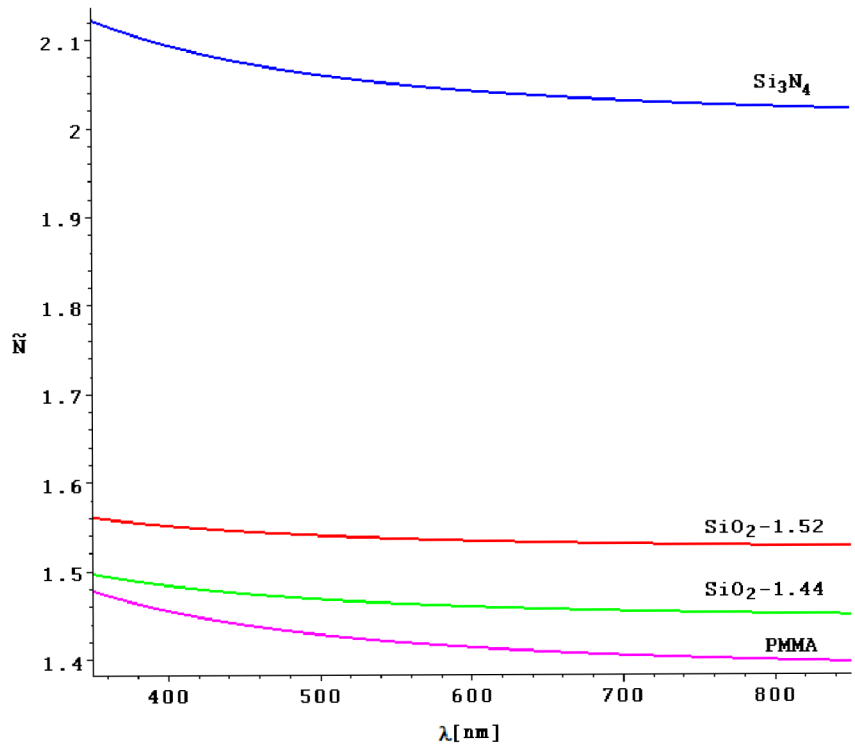

Figure 2: Refractive indices behaviors of several materials.

2.2 Model of reflectance

Each material has an ability to reflect or transmit a portion of incoming light where this property is measured by reflectance and transmittance respectively. The characteristics $\tilde{N}$ and d determine both reflectance and transmittance [7, pp. 45] of the film. In the following, the study will be focused on the reflectance of the films, only.

The light reflection occurs whenever the incident light reaches an interface between different optical media and is described by discontinuity in the complex refractive index $\tilde{N}$ [2]. If the light wave propagated in ambient 1, described by $\tilde{N}_1$, crosses the interface between ambiances 1 and 2, that is described by $\tilde{N}_2$ (see Fig. 3), the reflection is described by *Fresnel coefficient of reflection* r_{12} [1], [7, pp. 737].

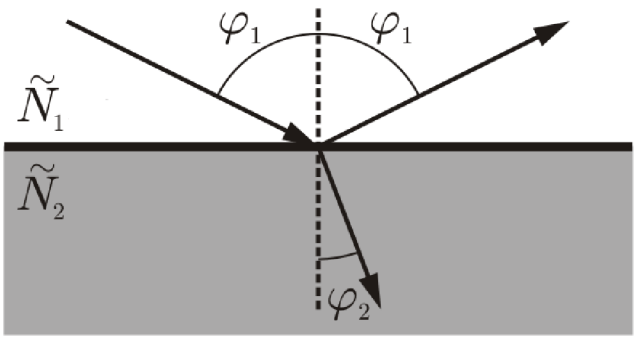

Figure 3: Light reflection at interface of two different optical media.

The relation between the incident angle φ_1 and the angle of propagation φ_2 in the ambient 2 is described by the Snell's law in Eq. (5).

$$\tilde{N}_1 \sin(\varphi_1) = \tilde{N}_2 \sin(\varphi_2) \tag{5}$$

In a case of spectroscopic reflectometry, the incidence of the light is normal. Based on this assumption, the r_{12} is expressed of a ratio of amplitudes of outgoing to incoming light waves. The r_{12} is formulated in Eq. (6).

$$r_{12} = \frac{\tilde{N}_1 - \tilde{N}_2}{\tilde{N}_1 + \tilde{N}_2} \tag{6}$$

The reflectance $\mathcal{R}$ is defined as a ratio of intensities of outgoing to incoming light waves and in the most simple case (as depicted in Fig. 3) it is given by

$$\mathcal{R} = |r_{12}|^2 . \tag{7}$$

To obtain a high reflectance in ambient 1, the material (i.e. the ambient 2) must have either refractive index n_2 very different from n_1 or the extinction coefficient k_2 very different from k_1 [1]. Usually the air is assumed as the ambient 1 where $n_1 = 1$ and $k_1 = 0$. In a case when a single film is deposited on a substrate (Fig. 4), the light reflection is then described by a *total reflection coefficient* r [7, pp. 64 - 65]. That is in this case determined by two Fresnel coefficients of reflection r_{12} and r_{23}, because the light wave has to cross the interfaces between ambiances 1 and 2 and between 2 and 3 as depicted in Fig. 4.

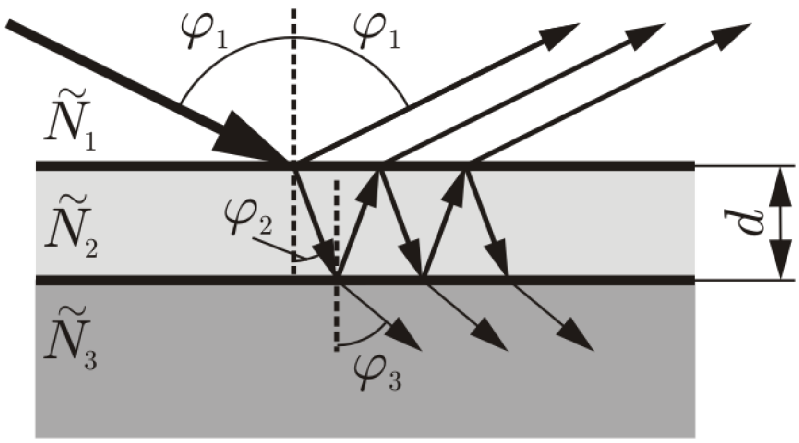

Figure 4: Light reflection from a material with a single film.

The meaning of the total reflection coefficient is the same as of the Fresnel coefficient of reflection in the case of simple reflection and is defined as

$$r = \frac{r_{12} + r_{23}\mathrm{e}^{-\mathrm{i}2\tilde{\beta}}}{1 + r_{12}r_{23}\mathrm{e}^{-\mathrm{i}2\tilde{\beta}}} \tag{8}$$

where the $\tilde{\beta}$ is a phase shift between the top and the bottom of the film [1] defined as

$$\tilde{\beta} = 2\pi\frac{d}{\lambda}\tilde{N}_2\cos(\varphi_2). \tag{9}$$

The reflectance of a substrate with a single film is given by

$$\mathcal{R} = |r|^2. \tag{10}$$

Obviously, if the film thickness equals to 0 then the Eq. (8) reduces to Eq. (6) [1].
In a case of combining depositions of layers of more materials onto each other (the film can be called a multilayer) (Fig. 5), the total reflection coefficient is acquired by stepwise combining of all Fresnel coefficients of the multilayer starting at the top and continuing downwards the bottom as described in [8]. A multilayer consisting of m layers is described by $m+1$ Fresnel coefficients because the incident light has to interact with $m+1$ interfaces. Let $r_{12}, r_{23}, \cdots, r_{mm+1}$ and $r^1, r^2, \cdots, r^m$ be the Fresnel coefficients and total reflection coefficients of the m - level multilayer, respectively. The total reflection of the multilayer can be then formulated as

$$r = r^1 = r_{12}, \quad m = 1, and \tag{11}$$

$$r = r^m = \frac{r^{m-1} + r_{mm+1}\mathrm{e}^{-\mathrm{i}2\tilde{\beta}_m}}{1 + r^{m-1}r_{mm+1}\mathrm{e}^{-\mathrm{i}2\tilde{\beta}_m}}, \quad \forall m = 2, 3, \cdots \tag{12}$$

The reflectance $\mathcal{R}$ is given by Eq. (10). This composition of the reflectance model is evidently more complicated with the higher m. The model is not flexible enough, if the

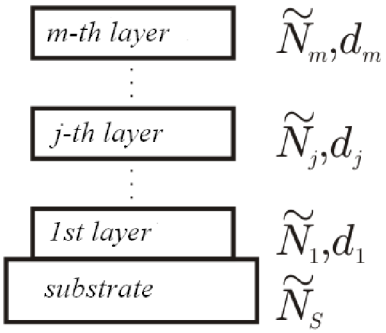

Figure 5: A model of a multilayer.

count of layers is variable because it has to be specifically changed and recalculated for each m. The change would include also expressing and recalculating of all desired derivatives of the model which would lead to store m models for multilayer comprising of 1 to m layers. By these reasons a new model of determining the total reflectance coefficients and hence the reflectance of thin films, especially of the multilayers, based on these principles was developed and presented in [9]. It consists in building an alternative model of r of the multilayer where each layer is treated separately and is defined by its characteristic matrix M_j defined as

$$q_j = \tilde{N}_j \cos(\varphi_j), \tag{13}$$

$$\tilde{\beta}_j = 2\pi \frac{d}{\lambda} q_j, \tag{14}$$

$$M_j = \begin{pmatrix} \cos(\tilde{\beta}_j) & \frac{\mathrm{i}}{q_j} \sin(\tilde{\beta}_j) \\ \mathrm{i} q_j \sin(\tilde{\beta}_j) & \cos(\tilde{\beta}_j) \end{pmatrix} \tag{15}$$

where the q_j in Eq. (13) is substitution simplifying the formulas of $\tilde{\beta}_j$ in Eq. (14), the phase shift between the top and the bottom of the j - th layer, and the characteristic matrix M_j in Eq. (15).
The complete multilayer is then determined by its characteristic matrix

$$\mathbf{M} = \begin{pmatrix} m_{11} & m_{12} \\ m_{21} & m_{22} \end{pmatrix} \tag{16}$$

where $\mathbf{M}$ is defined as a product of particular characteristic matrices

$$\mathbf{M} = M_m M_{m-1} \cdots M_2 M_1. \tag{17}$$

Using the substitution defined in Eq. (13) for the substrate (q_s) and
the ambient (q_a), the r can be formulated (see [9]) more transparently as

$$r = \frac{q_a m_{11} - q_s m_{22} + q_a q_s m_{12} - m_{21}}{q_a m_{11} + q_s m_{22} + q_a q_s m_{12} + m_{21}} \tag{18}$$

where for specification the

$$q_a = n_a \cos(\varphi_a), \tag{19}$$

$$q_s = \tilde{N}_s \cos(\varphi_s) \tag{20}$$

and the reflectance $\mathcal{R}$ is again given by Eq. (10).

Reflectance of SiO_2 during its deposition is presented in Fig. 6 as an example of reflectance variation in dependence on film thickness.

A new method of thin film optical properties measurements based on the principles described in [9] has been developed and presented in [2].

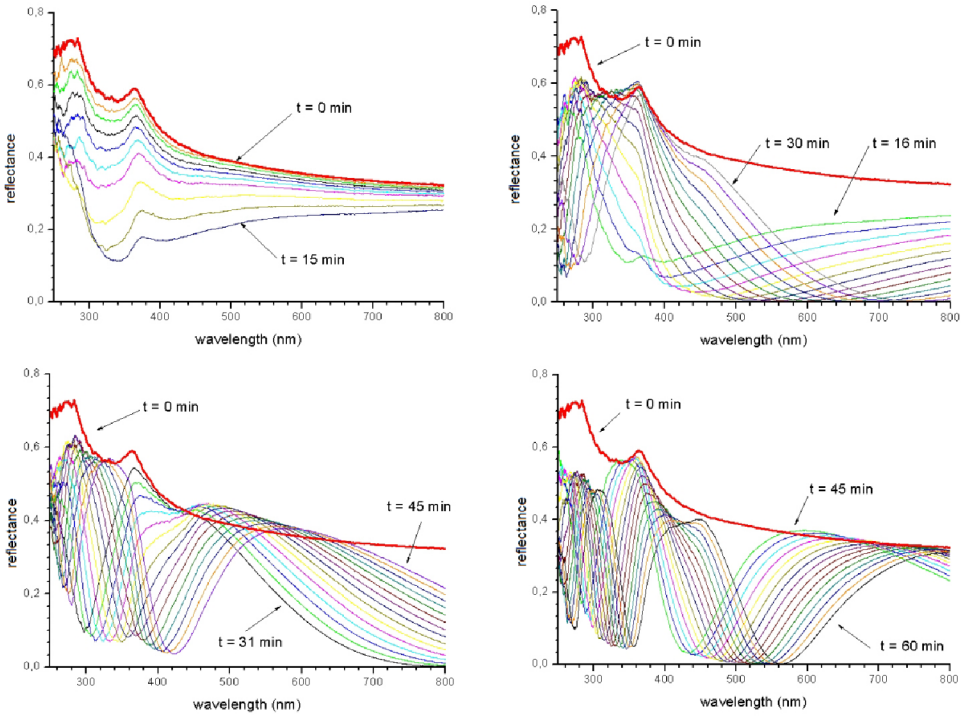

Figure 6: Measured reflectance of SiO_2 growth on a silicon substrate. The reflectance at $t = 0$ min is a reflectance of silicon.

3 Data Analysis

3.1 Regression analysis

An important task in statistics is to find relationships, if any, that exist in a set of variables when at least one is random, being subject to random fluctuations and possibly measurement errors [10, pp. 4 - 6].
One of the variables is called the dependent variable that represents the monitored quantity usually denoted by Y. The other variables $X_1, X_2, \cdots, X_n$ usually predict or explain the behavior of Y [10, pp. 4 - 6]. If it appears that between $\mathbf{X} = (X_1, X_2, \cdots, X_n)$ and Y could be some relationship usually more closely determined by vector of parameters ϑ, the Y can be described by a function f and it would be then written

$$Y \approx f(\mathbf{X}, \vartheta). \tag{21}$$

The symbol $\approx$ is used because the Y is random and the equality can not be satisfied.
The prediction of behavior of Y can be rather formulated (as presented in [10, pp. 4 - 6] and in [11, pp. 189 - 212]) as:

$$Y = f(\mathbf{X}, \vartheta) + \varepsilon, \tag{22}$$

where ε is a random error that is caused by the random fluctuations of the regression coefficients $\vartheta_1, \vartheta_2, \cdots, \vartheta_m$ represented by vector ϑ.
In the case of the reflectance (see chapter 2), the $\mathbf{X}$ is represented by only one variable λ - the wavelength and $(\vartheta_1, \vartheta_2, \cdots, \vartheta_m)$ describe the optical characteristics of the measured thin film such as refractive index and thickness.
Note: *The order of the parameters is the following: at first the coefficients of the refractive index are exploited then coefficients of the extinction coefficient, if any, and at last the ϑ_m corresponds to the thickness d.*
The $f(\mathbf{X}, \vartheta)$ is called the regression function (or a regression model). If the Y can be formulated as a linear combination of all ϑ_j, $j = 1, 2, \cdots, n$, the regression model is called linear, otherwise, it is called nonlinear.
Note: *Since the reflectance model described by Eq. (13) - (17) is complicated function where the regression coefficients appear in arguments of goniometric and exponential functions, the model is nonlinear and hence the linear model description is going to be omitted.*
To describe the behavior of Y as precisely as possible, the vector ϑ should be estimated by a method of maximal likelihood [10, pp. 32 - 33]. If the random errors ε have a normal distribution $N(0, \sigma^2(\sigma^2 > 0))$, the method of maximal likelihood reduces to method of minimizing sum of residual squares [10, pp. 32 - 33], therefore, the method of sum of residual squares is then satisfactory method of estimating the ϑ.

Considering n measurements, each realization of Y can be expressed as

$$y_i = f(\mathbf{x}_i, \vartheta) + e_i, i = 1, 2, \cdots, n \tag{23}$$

where $\mathbf{x}_i$ denotes the realization of $\mathbf{X}$ and e_i expresses the realization of the random error ε at the i - th measurement. To simplify, the $f(\mathbf{x}_i, \vartheta)$ is going to be denoted by $f_i(\vartheta)$, the $\mathbf{f}(\vartheta) = (f_1(\vartheta), f_2(\vartheta), \cdots, f_n(\vartheta))$ and the $\mathbf{y} = (y_1, y_2, \cdots, y_n)$.

The aim of this method is to find vector $\hat{\vartheta}$ that minimizes the sum of residual squares $S(\vartheta)$ where the ϑ^* is considered as the true value of the vector ϑ.

$$\underset{\vartheta}{\text{minimize}} \quad S(\vartheta) \tag{24}$$

$$S(\vartheta) = \mathbf{r}^{\mathrm{T}}(\vartheta)\mathbf{r}(\vartheta) \tag{25}$$

$$\mathbf{r}(\vartheta) = \mathbf{y} - \mathbf{f}(\vartheta) \tag{26}$$

In the following assumptions, the $\hat{\vartheta}$ is considered as a random vector. If the following assumptions 1 - 9 are held, the least square estimator $\hat{\vartheta}$ that minimizes the Eq.(24) exists, is consistent and it has asymptotically normal distribution[10, pp. 563 - 575].
The assumptions presented in [10, pp. 563 - 575] are:

1. The ε_i are i.i.d. with mean zero and variance σ^2 ($\sigma^2 > 0$.)
2. For each i, the $f_i(\vartheta) = f(x_i, \vartheta)$ is a continuous function of $\vartheta \in \Theta$.
3. Θ is a closed and bounded (i.e. compact) subset of $\mathbb{R}^m$.
4. Using

$$B_n(\vartheta, \vartheta_1) = \sum_{i=1}^{n} f_i(\vartheta) f_i(\vartheta_1) \quad and \tag{27}$$

$$D_n(\vartheta, \vartheta_1) = \sum_{i=1}^{n} [f_i(\vartheta) - f_i(\vartheta_1)]^2 \tag{28}$$

as defined in [10, pp. 563 - 575] then the following assumptions can be formulated as:

(a) The $n^{-1}B_n(\vartheta, \vartheta_1)$ converges uniformly for all ϑ, ϑ_1 in Θ to a function $B(\vartheta, \vartheta_1)$ (that is continuous if 2 and 3 hold). This implies by expanding Eq.(28) that $n^{-1}D_n(\vartheta, \vartheta_1)$ converges uniformly to $D(\vartheta, \vartheta_1) = B(\vartheta, \vartheta) + B(\vartheta_1, \vartheta_1) - 2B(\vartheta, \vartheta_1)$.

(b) It is now further assumed that $D(\vartheta, \vartheta^*) = 0$ if and only if $\vartheta = \vartheta^*$ (i.e. the $D(\vartheta, \vartheta^*)$ is positive definite).

It was proved [10, pp. 563 - 575] that with given assumptions 1 - 3 the 4 is sufficient for large n the $\hat{\vartheta}$ and $\hat{\sigma}^2 = \frac{S(\hat{\vartheta})}{n}$ ($\hat{\sigma}^2 = \frac{S(\hat{\vartheta})}{n-m}$ for smaller n) to be strongly consistent estimators of ϑ^* and σ^2 respectively.

5. The ϑ^* is an interior point of Θ (It means that ϑ^* does not lie on the boundary but belongs in an open subset of Θ.) Let Θ^* be an open neighborhood of ϑ^* in Θ.

6. The first and second derivatives $\frac{\partial f_i(\vartheta)}{\partial \vartheta_r}$ and $\frac{\partial^2 f_i(\vartheta)}{\partial \vartheta_r \partial \vartheta_s}$, $r, s = 1, 2, \cdots, m$, exist and are continuous for all $\vartheta \in \Theta^*$.

7. The $\frac{1}{n}\sum_{i=1}^{n} \frac{\partial f_i(\vartheta)}{\partial \vartheta}\left(\frac{\partial f_i(\vartheta)}{\partial \vartheta}\right)^{\mathrm{T}} \quad \left[= \frac{1}{n}\mathbf{F}^{\mathrm{T}}(\vartheta)\mathbf{F}(\vartheta)\right]$ converges to some matrix $\mathbf{\Omega}(\vartheta)$ uniformly in ϑ for $\vartheta \in \Theta^*$ where $\mathbf{F}(\vartheta) = \{\frac{\partial f_i(\vartheta)}{\partial \vartheta}, i = 1, 2, \cdots, n\}$ and $\frac{\partial f_i(\vartheta)}{\partial \vartheta} = \{\frac{\partial f_i(\vartheta)}{\partial \vartheta_j}, j = 1, 2, \cdots, m\}^{\mathrm{T}}$.

8. The $\frac{1}{n}\sum_{i=1}^{n}\left[\frac{\partial^2 f_i(\vartheta)}{\partial \vartheta_r \partial \vartheta_s}\right]^2$ converges uniformly in ϑ for $\vartheta \in \Theta^*$ $(r, s = 1, 2, \cdots, n)$.

9. $\mathbf{\Omega} = \mathbf{\Omega}(\vartheta^*)$ is nonsingular.

If the 1 - 9 hold then

$$\sqrt{n}(\hat{\vartheta} - \vartheta^*) \sim \quad N_m(\mathbf{0}, \sigma^2 \mathbf{\Omega}^{-1}) \tag{29}$$

asymptotically and $\frac{1}{n}\mathbf{F}^T(\vartheta)\mathbf{F}(\vartheta)$ is a strongly consistent estimator of $\mathbf{\Omega}$. And for large n the

$$\hat{\vartheta} - \vartheta^* \sim N_m(\mathbf{0}, \sigma^2 \left[\mathbf{F}^T(\vartheta^*)\mathbf{F}(\vartheta^*)\right]^{-1}) \tag{30}$$

can be figured out approximately [10, pp. 563 - 575].

3.1.1 Confidence intervals

When the estimator $\hat{\vartheta}$ has been found and the assumptions 1 - 9 hold the $\hat{\vartheta}$ converges to ϑ^* and it has an asymptotic distribution

$$\hat{\vartheta} \sim N(\vartheta^*, \sigma^2 \left[\mathbf{F}^{\mathrm{T}}(\vartheta^*)\mathbf{F}(\vartheta^*)\right]^{-1})$$

where $\mathbf{\Omega} = \left[\mathbf{F}^{\mathrm{T}}(\vartheta^*)\mathbf{F}(\vartheta^*)\right]^{-1}$ is a covariance matrix estimated by $\hat{\mathbf{\Omega}} = \left[\mathbf{F}^{\mathrm{T}}(\hat{\vartheta})\mathbf{F}(\hat{\vartheta})\right]^{-1}$ and where its elements express mutual dependences among the regression coefficients and where the $\hat{\sigma}^2 = \frac{S(\hat{\vartheta})}{n-m}$ is an estimate of σ^2 [10, pp. 571]. The diagonal elements $\hat{\sigma}^2\hat{\Omega}_{rr}$ represent estimates of variances of corresponding coefficients ϑ_r^*.
The $\hat{\vartheta}$ itself does not give any information about the accuracy of the current estimate of ϑ^*, therefore, the confidence intervals should be determined in order to present the accuracy of the found estimates.

Based on the variances of all coefficients ϑ_r^* their confidence intervals can be estimated depending on a significance level α which means that only $100\alpha\,[\%]$ of the considerable values of each ϑ_r^* lies outside its confidence interval.
The cofidence intervals are then estimated as:

$$I_{\vartheta_r^*} = \left\langle \hat{\vartheta}_r - t_{n-m}(1-\frac{\alpha}{2})\hat{\sigma}\sqrt{\hat{\Omega}_{rr}}; \hat{\vartheta}_r + t_{n-m}(1-\frac{\alpha}{2})\hat{\sigma}\sqrt{\hat{\Omega}_{rr}} \right\rangle, \tag{31}$$

where $t_{n-m}(1-\frac{\alpha}{2})$ is a critical value of Student's - distribution with $n-m$ degrees of freedom at the significance level α. If $0 \in I_{\vartheta_r^*}$ then ϑ_r^* is considered as a statistically insignificant parameter because the *null hypothesis* $H : \vartheta_r^* = 0$ can not be rejected [11, pp. 192], [12] and the minimization should be recomputed again with the fixed value of ϑ_r at 0.
If at least two different parameters ϑ_r and ϑ_s appear to be statistically insignificant another type of test should be carried out because the parameters do not have to be necessarily insignificant at once therefore, a conjugated hypothesis $H : \vartheta_r = 0 \wedge \vartheta_s = 0$ should be tested [11, pp. 192].

3.1.2 Adequacy of the model

Based on the reflectance theory (see chapter 2), the applied regression model can be considered as adequate.
In spite of that, a constancy of the variance of the errors can be tested in order to check whether the measured data can be considered homoscedastic or not, i.e. whether the variance σ^2 can be constant or a function of $\mathbf{x}$ which can cause the model to be not sufficient for the actual measurement of optical characteristics.
As formulated in [11, pp. 205 - 206], the hypothesis that variances of the errors ε_i are constant: $H : \text{var } \varepsilon_i = \text{const}, \forall i = 1, 2, \cdots, n$ is tested.
At first the vector $\mathbf{x}$ is divided into three vectors $\mathbf{x}_p = \{x_1, x_2, \cdots, x_p\}$,
$\mathbf{x}_M = \{x_{p+1}, x_{p+2}, \cdots, x_{n-q}\}$ and $\mathbf{x}_q = \{x_{n-q+1}, x_{n-q+2}, \cdots, x_n\}$ where only $\mathbf{x}_p$ and $\mathbf{x}_q$ are important and $p > m$, $q > m$, $p + q \leq n$. It is recommended to set $p = q \approx \frac{n}{3}$ [11, pp. 205 - 206]. The vector $\mathbf{y}$ is divided exactly by the same way as the vector $\mathbf{x}$. The $\mathbf{y}_p$ and $\mathbf{y}_q$ are treated as two separate sets of input data and the same regression model is applied to them in order to calculate the residual variances s_p^2 and s_q^2 [11, pp. 205 - 206].

$$s_p^2 = \frac{S(\hat{\vartheta}_p)}{p-m} \tag{32}$$

$$s_q^2 = \frac{S(\hat{\vartheta}_q)}{q-m} \tag{33}$$

$$F_t = \frac{s_p^2}{s_q^2} \tag{34}$$

If the null hypothesis is valid the F_t has $F_{p-m,q-m}$ distribution and if $F_t \geq F_{p-m,q-m}(\frac{\alpha}{2})$ or $F_t \leq F_{p-m,q-m}(1-\frac{\alpha}{2}) = \frac{1}{F_{q-m,p-m}(\frac{\alpha}{2})}$ the hypothesis is rejected [11, pp. 205 - 206].

3.2 Solver

Solving (24) may be very difficult in general, but in spite of that, suitable methods that are rapidly convergent were developed.

However, these methods are seeking the nearest local extreme while a global minimum is required. Since these methods are iterative, the problem of stopping in a local extreme that is not the global minimum may be avoided, if a proper starting point has been chosen [10, pp. pp. 588 - 599], [6, pp. 12 -16].

Due to their character, many methods are based on a *Newton's* [10, pp. pp. 599 - 609], [6, pp. 44 -49] and the *Steepest descent (Gradient)* [10, pp. pp. 594 - 597], [6, pp. 26 -33] methods. The *Newton's* method grants a fast convergence when ϑ is close enough to a local extreme and otherwise, it converges slowly. On the other hand the *Steepest descent* method converges rapidly, if the ϑ is not close enough to the local extreme and otherwise, converges slowly[10, pp. 619 - 627].

Some of the developed methods combine together the advantages of both types of methods and hence they grant a rapid rate of convergence regardless on a distance of ϑ and the nearest local extreme.

Because of its previous successful implementations in solving problems in optics, the *Levenberg - Marquardt* algorithm (see [10, pp. pp. 619 - 627], [6, pp. 95 - 107]) that belongs to the group of mentioned combined methods, was chosen as a solver.

The algorithm is one of so called *Restricted step* methods where step δ, an increment of ϑ, is determined in each iteration [10, pp. pp. 619 - 627], [6, pp. 95 - 107]. Solving (24) by this method is supported by solving a subproblem

$$\underset{\delta}{\text{minimize}} \quad q(\delta), \tag{35}$$

where the $q(\delta)$ is a quadratic approximation of $S(\vartheta+\delta)$ obtained by truncating the Taylor series [6, pp. 95 - 107] and solving (35) means seeking δ_{M} minimizing $q(\delta)$ for all δ within a preset neighborhood of ϑ [6, pp. 95 - 107].

The pivot of this method is to calculate the δ_{M} in each iteration and decide whether it is a convergent step or not (i.e. whether δ_{M} shall be added to ϑ or not).

The δ_{M} is acquired as a solution of (see [13])

$$\left(\mathbf{F}^{\mathrm{T}}\mathbf{F} + \lambda_{\mathrm{M}}\mathbf{D}\right) \cdot \delta_{\mathrm{M}} = -\mathbf{F}^{\mathrm{T}}\mathbf{r}, \tag{36}$$

where $\mathbf{F} = \{F_{i,j} = \dfrac{\partial f(x_i,\vartheta)}{\partial \vartheta_j}\}$ is *Jacobi's matrix*, the factor λ_{M} indicates the character of the algorithm and $\mathbf{D} = \mathrm{diag}\{\mathbf{F}^{\mathrm{T}}\mathbf{F}\} + \mathbf{I}$ is a diagonal matrix that keeps $\left(\mathbf{F}^{\mathrm{T}}\mathbf{F} + \lambda_{\mathrm{M}}\mathbf{D}\right)$

positive definite for all $\lambda_{\mathrm{M}} \geq 0$ [6, pp. 95 - 107]. The smaller is the λ_{M} the closer is the character of the method to the *Newton's* method and on the other hand the greater is the λ_{M} the closer is the character of the method to the *Gradient* method.
When the δ_{M} is known it shall be determined whether to add it to ϑ or not (i.e. if it is a convergent step or not). The control of addition of δ_{M} to ϑ is affected by *actual reduction* ΔS in S on the certain iteration (37) and a corresponding *predicted reduction* Δq (38) [6, pp. 95 - 107].

$$\Delta S = S(\vartheta) - S(\vartheta + \delta_{\mathrm{M}}) \tag{37}$$

$$\Delta q = q(0) - q(\delta_{\mathrm{M}}) = S(\vartheta) - q(\delta_{\mathrm{M}}) \tag{38}$$

$$\mathrm{r}_{\mathrm{M}} = \frac{\Delta S}{\Delta q} \tag{39}$$

The ratio r_{M} in (39) measures the accuracy to which $q(\delta_{\mathrm{M}})$ approximates $S(\vartheta + \delta_{\mathrm{M}})$ in the sense that the r_{M} is closer to 1 the better is the approximation [6, pp. 95 - 107]. The positive r_{M} means that the δ_{M} is a convergent step and hence it is added to ϑ, the non positive r_{M} leaves the ϑ exactly the same because the δ_{M} is classified as a non convergent step and hence it is not added to ϑ.
The quality of the approximation also indicates the character of the method in the following iteration (i.e. it also affects the λ_{M}).
Besides affecting the character of the method the r_{M} implicates setting the size of the neighborhood of ϑ in next iteration by reducing or extending it. Based on L_B and U_B - the preset lower and upper bounds of r_{M} respectively, the neighborhood can be extended only if $\mathrm{r}_{\mathrm{M}} < L_B$ and can be reduced only if $\mathrm{r}_{\mathrm{M}} > U_B$, otherwise the size of the neighborhood stays unchanged. To modify the size of the neighborhood of ϑ in the following iteration means according to value of r_{M} to multiply λ_{M} by E_{M} or R_{M} - the extension or reduction coefficients respectively [6, pp. 95 - 107].
In general the k - th iteration of the algorithm can be summarized in following steps, where ϑ is replaced by its estimate $\mathbf{b}$ as presented in [6, pp. 95 - 107].

1. To given $\mathbf{x}$, $\mathbf{b}^k$, λ_{M}^k calculate $\mathbf{r}(\mathbf{b}^k)$, $S(\mathbf{b}^k)$, $\mathbf{F}^k$, $\mathbf{D}^k$, $((\mathbf{F}^k)^{\mathrm{T}}\mathbf{F}^k + \lambda_{\mathrm{M}}^k\mathbf{D}^k)$ and $(\mathbf{F}^k)^{\mathrm{T}}\mathbf{r}(\mathbf{b}^k)$

2. Solve (36) to give δ_{M}^k

3. Evaluate $S(\mathbf{b}^k + \delta_{\mathrm{M}}^k)$ and $q(\delta_{\mathrm{M}}^k)$ and hence $\mathrm{r}_{\mathrm{M}}^k$ as defined in (39)

4. $\mathrm{r}_{\mathrm{M}}^k \begin{cases} < L_B & \Rightarrow \quad \lambda_{\mathrm{M}}^{k+1} = E_{\mathrm{M}}\lambda_{\mathrm{M}}^k \\ > U_B & \Rightarrow \quad \lambda_{\mathrm{M}}^{k+1} = R_{\mathrm{M}}\lambda_{\mathrm{M}}^k \\ \text{otherwise} & \Rightarrow \quad \lambda_{\mathrm{M}}^{k+1} = \lambda_{\mathrm{M}}^k \end{cases}$

5. $\mathrm{r}_{\mathrm{M}}^k \begin{cases} > 0 & \Rightarrow \quad \mathbf{b}^{k+1} = \mathbf{b}^k + \delta_{\mathrm{M}}^k \\ \leq 0 & \Rightarrow \quad \mathbf{b}^{k+1} = \mathbf{b}^k \end{cases}$

6. $k = k + 1$ and go to 1.

The algorithm is then stopped if any of the following events occurs:

- $S(\mathbf{b}^k) \leq \epsilon$, where ϵ is preset value close to 0 considered as satisfying sum of residual squares
- The number of iterations exceeds the preset maximum k_{max}, i.e. $k > k_{max}$
- The objective function $S(\mathbf{b}^k)$ can not be evaluated
- The λ_{M}^k reaches value very close 0, i.e. the size of neighborhood of $\mathbf{b}^k$ is nearly 0
- The convergence is too slow, i.e. the $\|\delta_{\mathrm{M}}^k\| \approx 0$, if and only if the δ_{M}^k were added to $\mathbf{b}^k$.

Based on the steps 1 - 6, the optimizing algorithm was successfully created and implemented in the REFLECTOMETRY software package developed to measure the optical properties of thin films.

3.3 Sensitivity analysis

Choosing an adequate initial approximation $\vartheta_{\mathbf{0}}$ might guarantee acquiring result $\hat{\vartheta}$ very close to the ideal solution ϑ^*, therefore, the ability of convergence[1] from initial approximations to ϑ^* should be studied.

The more $\vartheta_{\mathbf{0}}$ cause the solver to give such $\hat{\vartheta}$ that can be considered as ϑ^*, the less it depends on setting the initial approximations in order to acquire a very good estimate of ϑ^*.

Based on the ability of convergence, a new method was designed. The aim of this method is to detect a region of interest containing initial approximations that in the most cases grant the solver a convergence to the global minimum.

Detecting the region of interest consists in cropping a chosen set of initial approximations $\mathbf{B}$ to acquire such set $\mathbf{B^I}$ that if any $\vartheta_{\mathbf{0}}$ were chosen from this set it rarely does not converge to the ϑ^*. This can be achieved by studying the character of each acquired result $\hat{\vartheta}$ whether it can be the global minimum or a different local extreme and consequently by calculating a relative frequency (further only "frequency")[2] of convergence from chosen initial approximations to the global minimum.

The initial approximations are separated into groups where at least one coefficient has an arbitrary value from its initial range while the rest of the coefficients remains constant. The frequency of convergence is then calculated as frequency of setting chosen coefficients to certain values regardless on the variable ones, i.e. the frequency of convergence of the group regardless on the omitted coefficients (i.e. the frequency of convergence of a chosen particular setting).

To determine the frequency, the ϑ^* has to be known and a set of initial approximations $\mathbf{B}$ has to be assigned to it[3]. The frequencies are then going to be calculated within this set and the smallest region $\mathbf{B^I}$ that includes all $\vartheta_{\mathbf{0}}$ with very high frequency of convergence is going to be detected.

Each initial approximation $\vartheta_{\mathbf{0}}$ of $\mathbf{B}$ is used as a starting point in the optimizing algorithm and the corresponding acquired result $\hat{\vartheta}$ is compared to ϑ^* to distinguish whether the $\hat{\vartheta}$ can be considered as a global minimum or not. The $\hat{\vartheta}$ is considered as global minimum if and only if:

$$\vartheta^* - \mu \leq \hat{\vartheta} \leq \vartheta^* + \nu, \tag{40}$$

where μ and ν are the lower and upper tolerances of ϑ^* respectively.

If the condition in Eq. (40) holds the $\vartheta_{\mathbf{0}}$ is considered as convergent, otherwise, as non

[1] In a matter of the sensitivity analysis, the convergence is understood as ability to acquire a satisfactory result reasonably close to the global minimum calculated by the optimizing method that started at a chosen initial approximation.

[2] The relative frequency can be also considered as a probability of convergence

[3] It is recommended to choose $\mathbf{B}$ wherein the ϑ^* is a middle point.

convergent. It can be described by a function $\varphi : \mathbb{R}^{\mathrm{m}} \rightarrow \{0, 1\}$ where

$$\varphi(\vartheta_{\mathbf{0}}) = \begin{cases} 1 & \vartheta^* - \mu \leq \hat{\vartheta} \leq \vartheta^* + \nu \\ 0 & \text{otherwise} \end{cases} \tag{41}$$

Apart from that the character of solution should be studied whether it can be a local extreme or not because setting too low limit of iterations can cause the algorithm to stop at a point that might not be an extreme because it would need more steps to reach some. The λ_{M} indicates the character of the acquired result [6, pp. 95 - 107] $\hat{\vartheta}$. The low λ_{M} expresses that the $\hat{\vartheta}$ could be a local extreme and otherwise, the $\hat{\vartheta}$ could not be considered as a local extreme, if the λ_{M} is high. The character of the solution can be described by a function $\gamma(\vartheta_{\mathbf{0}}) : \mathbb{R}^{\mathrm{m}} \rightarrow \{1, 3\}$ where

$$\gamma(\vartheta_{\mathbf{0}}) = \begin{cases} 1 & \lambda_{\mathrm{M}} \leq \Lambda \\ 3 & \text{otherwise} \end{cases} \tag{42}$$

where the Λ is an upper limit still classifying the $\hat{\vartheta}$ as a local extreme.
The frequencies of convergence should be calculated after it has been checked that the most of acquired results are local extremes (i.e. the iteration limit does not cause the algorithm to stop before the $\hat{\vartheta}$ could have reached any local extreme very often).
For more detailed analysis, the convergence and local extreme characteristics are combined together to describe whether the initial approximation $\vartheta_{\mathbf{0}}$ converges to to the global minimum, to a different local extreme or to some other solution. This can be described explicitly by a function $\psi(\vartheta_{\mathbf{0}}) : \mathbb{R}^{\mathrm{m}} \rightarrow \{1, 2, 3, 4\}$ that is defined as:

$$\psi(\vartheta_{\mathbf{0}}) = \gamma(\vartheta_{\mathbf{0}}) + \varphi(\vartheta_{\mathbf{0}}) \tag{43}$$

where the interpretation is the following:

- $\psi(\vartheta_{\mathbf{0}}) = 1$ means that the corresponding initial approximation $\vartheta_{\mathbf{0}}$ is not convergent but the $\hat{\vartheta}$ is close to a local extreme different from ϑ^*.
- $\psi(\vartheta_{\mathbf{0}}) = 2$ expresses that $\vartheta_{\mathbf{0}}$ can be considered as convergent to the global minimum ϑ^*.
- $\psi(\vartheta_{\mathbf{0}}) = 3$ occurs in case when the initial approximation $\vartheta_{\mathbf{0}}$ is not convergent and the acquired $\hat{\vartheta}$ is not close to any local extreme. This can be caused by exceeding maximum of iterations before reaching any extreme.
- $\psi(\vartheta_{\mathbf{0}}) = 4$ should not occur because the $\hat{\vartheta}$ is not considered as a local extreme but in spite of it the corresponding initial approximation $\vartheta_{\mathbf{0}}$ is convergent. However, improper setting of Λ or initial λ_{M} might cause such case because the algorithm can

stop because of reaching satisfying sum of residual squares regardless on the size of λ_M and hence the $\hat{\vartheta}$ close to global minimum can be reached with $\lambda_M \geq \Lambda^4$.

Once all $\psi(\vartheta_\mathbf{0})$ are calculated a projection of the $\psi(\mathbf{B})$ can be carried out by omitting chosen regression coefficients in order to calculate a frequency of each possible result given by ψ at each point of the projection (i.e. at each group of particular initial approximations). The most frequent value of ψ and its frequency form the result of the projection. It means that each point of projection is characterized by modus of the combined characteristics and by its frequency. If the modus of $\psi = 3$ occurs rarely the iteration limit can be considered as large enough and the frequency of convergence can be calculated.
The frequency of convergence is calculated following these steps:

1. A coefficient ϑ_r that is going to be omitted is chosen.

2. All groups of $\vartheta_\mathbf{0}$ have to be checked (see Fig. 7) whether the limit k_{max} is sufficient or not. A first projection $\mathbf{B^p}$ of $\mathbf{B}$ is created without removing any level of $\vartheta_\mathbf{r}$ and where $\mathbf{B^p}$ comprises of all $\vartheta_\mathbf{0}^\mathbf{p}$ where each $\vartheta_\mathbf{0}^\mathbf{p}$ expresses the group of $\vartheta_\mathbf{0}$ with omitted coefficient ϑ_r.

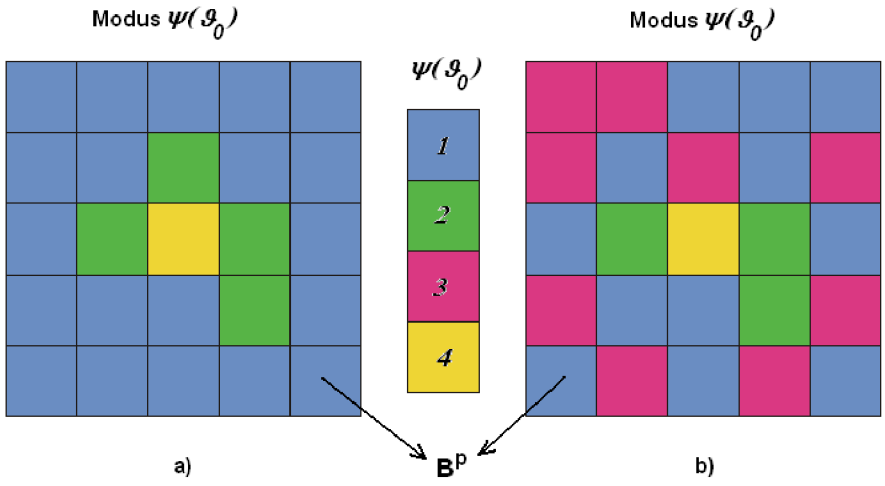

Figure 7: Checking the sufficiency of the iteration limit k_{max}: a) sufficient, b) insufficient.

3. The ϑ_r can be arbitrary value of its initial range $\{\vartheta_r^1, \vartheta_r^2, \cdots, \vartheta_r^{n_r}\}$. The $\mathbf{B}$ is searched level by level until any convergent approximation is found (i.e. the $\psi(\vartheta_\mathbf{0}) = 2$ or 4 or rather the $\varphi(\vartheta_\mathbf{0}) = 1$) starting at the ends of range of the ϑ_r (i.e. starting at $\vartheta_r = \vartheta_r^1$ and at $\vartheta_r = \vartheta_r^{n_r}$).

[4]These cases were very rare in practical detections.

If $\varphi(\vartheta_{\mathbf{0}}) = 0$ for all $\vartheta_{\mathbf{0}}$ from the searched level ϑ_r^i the level ϑ_r^i is removed from the calculations (see Fig. 8).

This procedure reduces the range of ϑ_r to $\{\vartheta_r^k, \vartheta_r^{k+1}, \cdots, \vartheta_r^l\}$ where $k \geq 1$ and $l \leq n_r$.

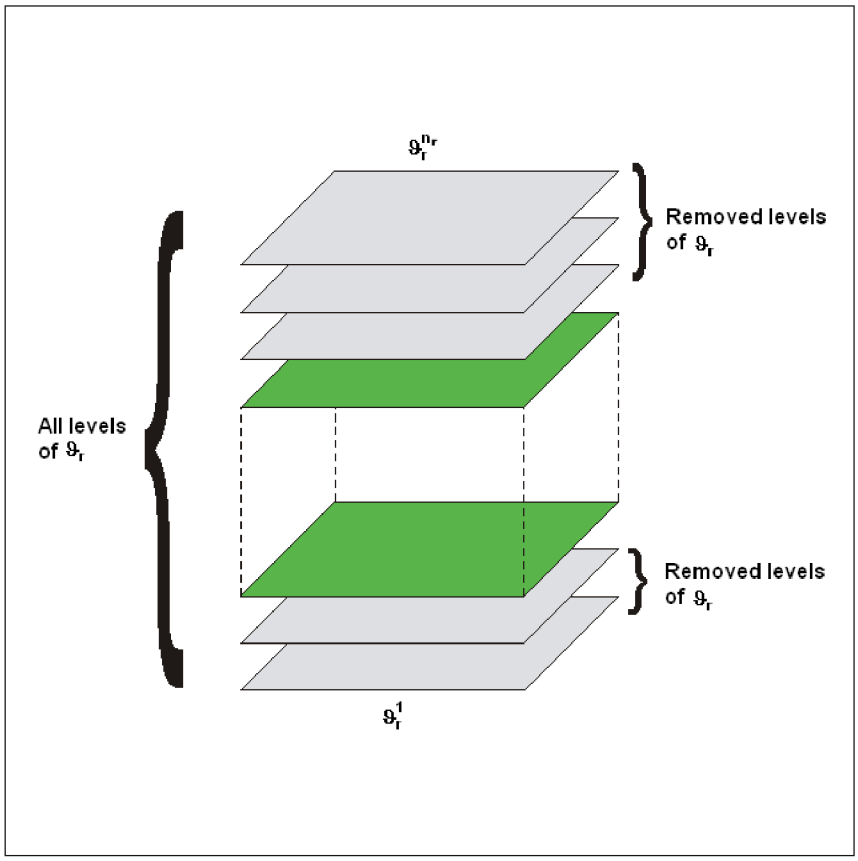

Figure 8: A method of removing levels that do not include any convergent approximation.

4. A repeated projection $\mathbf{B^p}$ of $\mathbf{B}$ is created with all zero - levels of $\vartheta_{\mathbf{r}}$ removed after the step 3.

   The frequency $p(\vartheta_{\mathbf{0}}^{\mathbf{p}})$ of the group $\vartheta_{\mathbf{0}}^{\mathbf{p}}$ is then formulated (see the Eq. (44)) as rate of $\vartheta_{\mathbf{0}}$ from the group where $\varphi(\vartheta_{\mathbf{0}}) = 1$ to all levels that remained after step 3 (see Fig. 9).

$$p(\vartheta_{\mathbf{0}}^{\mathbf{p}}) = \begin{cases} \dfrac{\sum_{\vartheta_r=\vartheta_r^k}^{\vartheta_r=\vartheta_r^l} \varphi(\vartheta_{\mathbf{0}})}{l-k+1} & k \leq l \\ 0 & \text{otherwise} \end{cases} \tag{44}$$

   The situation when $k > l$ means that the set $\mathbf{B}$ does not include any convergent approximation and hence the frequency is 0.

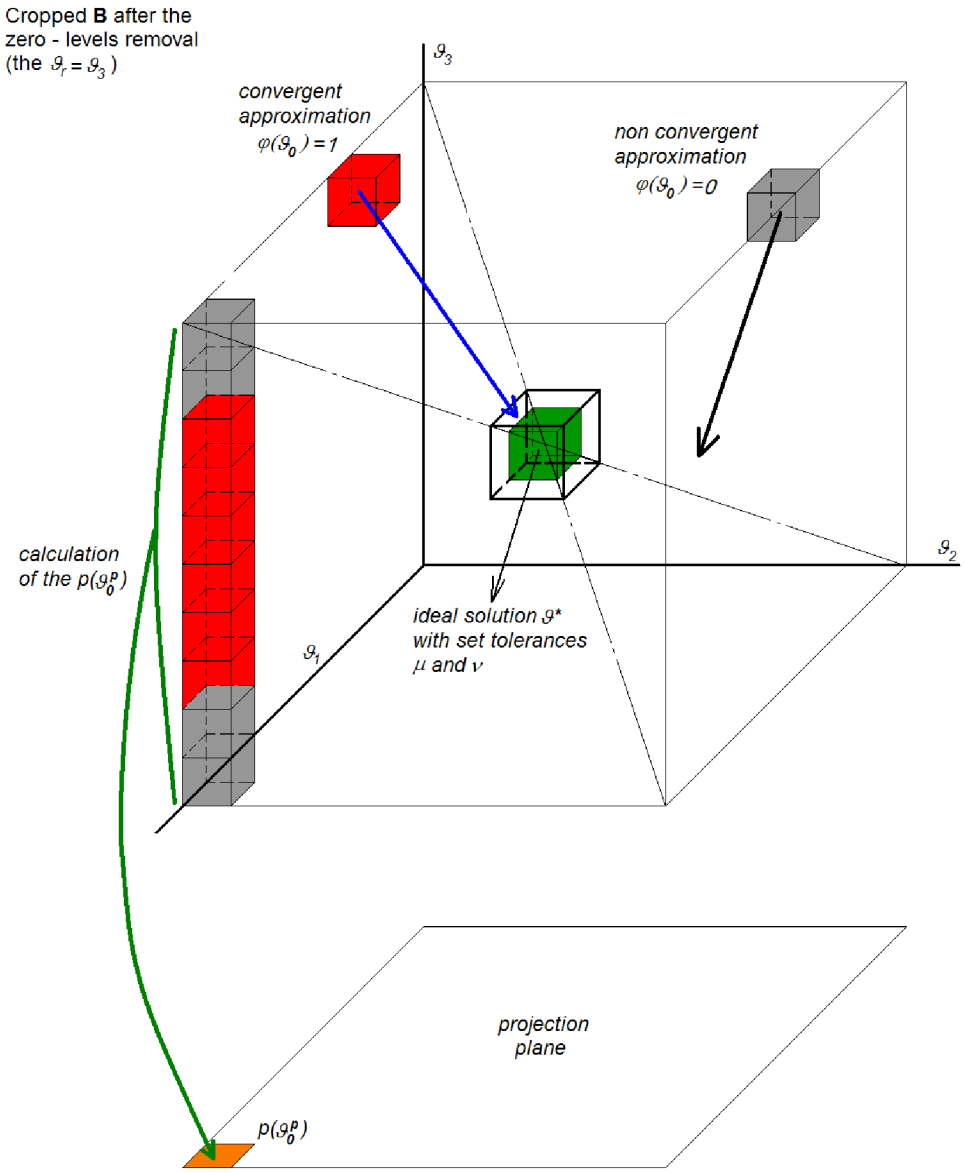

Figure 9: Calculating the frequency of convergence of the group ϑ_0^{P} and its depiction in the projection.

5. A threshold frequency p_t is set to detect the smallest region $\mathbf{B_s^p}$ (selection of $\mathbf{B^p}$) that includes all such $\vartheta_\mathbf{0}^\mathbf{p}$ that

$$p(\vartheta_\mathbf{0}^\mathbf{p}) \geq p_t, \quad \forall \vartheta_\mathbf{0}^\mathbf{p} \in \mathbf{B^p}. \tag{45}$$

It means to crop the intervals of the remaining coefficients following the step 3 where $\vartheta_\mathbf{0}^\mathbf{p}$ and $p(\vartheta_\mathbf{0}^\mathbf{p}) \geq p_t$ are used instead of $\vartheta_\mathbf{0}$ and $\varphi(\vartheta_\mathbf{0})$ respectively.
After all intervals I_{ϑ_j} of all coefficients ϑ_j have been cropped the region $\mathbf{B^I}$ is detected as:

$$\mathbf{B^I} = I_{\vartheta_1} \times I_{\vartheta_2} \times \cdots \times I_{\vartheta_m}. \tag{46}$$

The $\mathbf{B^I}$ can be determined after the $\mathbf{B_s^p}$ has been detected because the cropped interval I_{ϑ_r} is already known. An example of detection of $\mathbf{B_s^p}$ is depicted in Fig. 10.

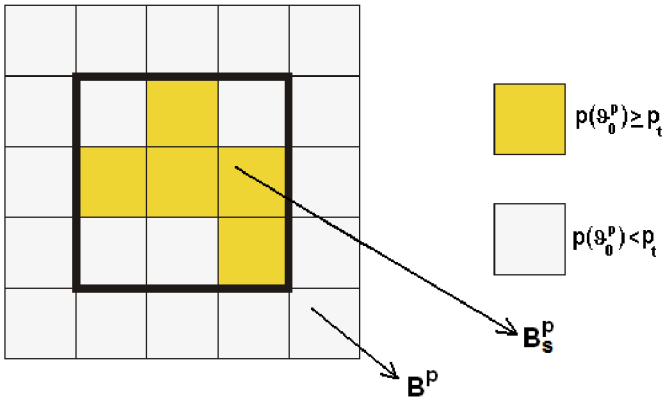

Figure 10: A detection of $\mathbf{B_s^p}$ within the $\mathbf{B^p}$.

The region $\mathbf{B^I}$ can be characterized by a *Reliability factor* $\mathbf{R_f}$ that expresses a mean frequency $\bar{p}$ with that the initial approximation $\vartheta_\mathbf{0}$ chosen from the $\mathbf{B^I}$ converges to the global minimum ϑ^*.
If a region $\mathbf{B^I}$ characterized by higher $\bar{p}$ is required a higher p_t should be set and the step 5 should be repeated with the increased p_t.
An example of the $\mathbf{R_f}$ calculation is shown in Fig. 11.

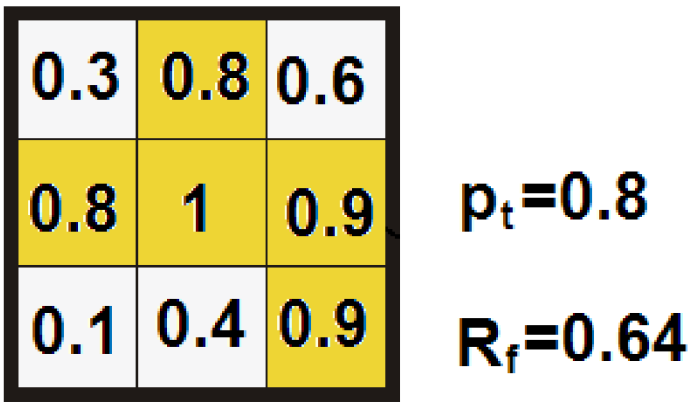

Figure 11: The *Reliability factor* $\mathbf{R_f}$ calculation within the region $\mathbf{B^I}$ with $p_t = 0.8$.

This analysis was successfully implemented in the REFLECTOMETRY software package to support the optical properties measurements by determining a reliability of the acquired results.

4 Image Processing

4.1 Digital space

From [14, pp. 49], [15, pp. 7]:

1. Definition – multiindex:

Let $I_k = \{0, 1, \ldots, i_k, \ldots, m_k\} \in N_0$ be a set of indices. Then the set $\mathbf{I}^{(n)} = \times_{k=1}^{n} I_k$ is called multiindex.

2. Definition – space support:

Let $J_k = \langle a_k; b_k)$ be intervals. Then the set $\mathbf{J}^{(n)} = \times_{k=1}^{n} J_k$ is called nD space support.

3. Definition – equidistant multipartitioning:

Let $D_k = \{x_0^k, x_1^k, \ldots x_{i_k}^k, \ldots x_{m_k}^k\}$ be the equidistant partitioning of intervals $J_k = \langle a_k; b_k)$. Then the set $\mathbf{D}^{(n)} = \times_{k=1}^{n} D_k$ is called the equidistant multipartioning of space support $\mathbf{J}^{(n)}$.

4. Definition – digital space, resolution:

Let $\mathbf{J}^{(n)} = \times_{k=1}^{n} J_k$ be a support of space $\mathbf{D}^{(n)} = \times_{k=1}^{n} D_k$ and D_k its equidistant multipartioning. The ordered pair $\mathcal{D}^{(n)} = (\mathbf{J}^{(n)}; \mathbf{D}^{(n)})$ is called nD digital space. The ordered n-tuple $\mathbf{r} = (m_1, m_2, \ldots, m_k \ldots, m_n)$ is called the resolution of space $\mathcal{D}^{(n)}$.

Digital geometry may be defined as a **mathematical** discipline, which studies characteristics of digital space.

In n - dimensional space $\mathcal{D}^{(n)} = (\mathbf{J}^{(n)}; \mathbf{D}^{(n)})$ are at call:

sets of indices	**intervals**	**interval partitioning**
$I_k = \{0, 1, \ldots, i_k, \ldots, m_k\}$	$J_k = \langle a_k; b_k)$	$D_k = \{x_0^k, x_1^k, \ldots x_{i_k}^k, \ldots x_{m_k}^k\}$

k=0,1...,n

Multiindices $\mathbf{i}, \mathbf{j} \in \mathbf{I}^{(n)}$ are expressed as $\mathbf{i} = [i_1, i_2, \ldots, i_k, \ldots, i_n]$, $\mathbf{j} = [j_1, j_2, \ldots, j_k, \ldots, j_n]$, zero – multiindex is then expressed as $\mathbf{0} = [0, 0, \ldots, 0]$. Then it is able to express the items $M, N \in \mathbf{D}^{(n)}$ as:

$M = [x_{i_0}^0, x_{i_1}^1, \ldots, x_{i_k}^k, \ldots, x_{i_n}^n]$, $\quad N = [x_{j_0}^0, x_{j_1}^1, \ldots, x_{j_k}^k, \ldots, x_{j_n}^n]$,

or $M = A_{[i_1, i_2, \ldots, i_k, i_n]} = A_{\mathbf{i}}$; $\quad N = A_{[j_1, j_2, \ldots, j_k, j_n]} = A_{\mathbf{j}}$.

4.2 Physical domain, physical space

From [14, pp. 50], [15, pp. 8]:

1. Definition – physical domain

The subset $\mathbf{F}^{(n)} \subset \mathbf{J}^{(n)}$ of digital space $\mathcal{D}^{(n)} = (\mathbf{J}^{(n)}; \mathbf{D}^{(n)})$ is called the physical nD domain, if and only if $\mathbf{F}^{(n)} = \times_{k=1}^{n} \langle x_{i_k}^k; x_{i_k+1}^k \rangle$. It is written as $\mathbf{F}^{(n)} = \times_{k=1}^{n} \langle x_{i_k}^k; x_{i_k+1}^k \rangle = \mathbf{F}_{[i_1,i_2,\ldots,i_n]}^{(n)} = \mathbf{F}_{\mathbf{i}}^{(n)}$. The number $v_i^k = x_{i_k+1}^k - x_{i_k}^k; i_k \in \mathbf{i}$ is called $k-tuple$ dimension of physical nD domain $\mathbf{F}_{\mathbf{i}}^{(n)}$.

2. Theorem

$k-tuple$ dimensions v_i^k of all physical nD domains $\mathbf{F}_{\mathbf{i}} \in \mathcal{D}^{(n)}$ are equal.

Proof: The statement is implied by assumed equidistance of partitioning of D_k.

Note:

The theorem enables to ignore the multi index at the dimensions of physical nD domain, i.e. to write only v^k. If no misunderstanding occurs the dimensionality specification of nD domain can be also ignored, i.e. domain will be written instead of nD domain.

3. Theorem

Set $\mathcal{F}^{(n)} = \{\mathbf{F}^{(n)} = \times_{k=1}^{n} \langle x_{i_k}^k; x_{i_k+1}^k \rangle; i_k \in I_k\}$ of all physical domains of support $\mathbf{J}^{(n)}$ of digital space $\mathcal{D}^{(n)} = (\mathbf{J}^{(n)}; \mathbf{D}^{(n)})$ is called the fragmentation of digital space support $\mathbf{J}^{(n)}$.

Proof: It is necessary to prove following three statements:

a)$\forall \mathbf{i} \in \mathbf{I}^{(n)} : \mathbf{F}_{\mathbf{i}}^{(n)} \neq \emptyset$. b)$\forall \mathbf{i}, \mathbf{j} \in \mathbf{I}^{(n)} : i \neq j \Rightarrow F_i^{(n)} \cap \mathbf{F}_{\mathbf{j}}^{(n)} = \emptyset$. c)$\bigcup_{\mathbf{i} \in \mathbf{I}^{(n)}} \mathbf{F}_{\mathbf{i}} = \mathbf{J}^{(n)}$

ad a) $\mathbf{i} = [i_1, i_2, \ldots, i_k, \ldots, i_n] \Rightarrow \mathbf{F}_{\mathbf{i}} = \times_{k=1}^{n} \langle x_{i_k}^k; x_{i_k+1}^k \rangle$. Let $s_{i_k}^k$ be set to $\frac{x_{i_k}^k + x_{i_k+1}^k}{2}$. Then $\forall k \in \{1, 2, \ldots, n\} : s_{i_k}^k \in \langle x_{i_k}^k; x_{i_k+1}^k \rangle \Rightarrow [s_0^k, s_1^k, \ldots, s_{i_k}^k, \ldots, s_{n_k}^k] \in \times_{k=1}^{n} \langle x_{i_k}^k; x_{i_k+1}^k \rangle = \mathbf{F}_{\mathbf{i}} \Rightarrow \mathbf{F}_{\mathbf{i}} \neq \emptyset$.

ad b) Let be $\mathbf{i} = [i_1, i_2, \ldots, i_k, \ldots, i_n]; \mathbf{j} = [j_1, j_2, \ldots, j_k, \ldots, j_n]; \mathbf{j} \neq \mathbf{i}$. Then $\exists k \in \{1, 2, \ldots, n\} : i_k \neq j_k \Rightarrow \langle x_{i_k}^k; x_{i_k+1}^k \rangle \cap \langle x_{j_k}^k; x_{j_k+1}^k \rangle = \emptyset \Rightarrow \times_{k=1}^{n} \langle x_{i_k}^k; x_{i_k+1}^k \rangle \cap \langle x_{j_k}^k; x_{j_k+1}^k \rangle = \emptyset \Rightarrow \times_{k=1}^{n} \langle x_{i_k}^k; x_{i_k+1}^k \rangle \cap \times_{k=1}^{n} \langle x_{j_k}^k; x_{j_k+1}^k \rangle = \emptyset \Rightarrow \mathbf{F}_{\mathbf{i}} \cap \mathbf{F}_{\mathbf{j}} = \emptyset$.

ad c)$\bigcup_{i \in I^{(n)}} \mathbf{F}_{\mathbf{i}} = \bigcup_{\mathbf{i_k}} [\times_{k=1}^{n} \langle x_{i_k}^k; x_{i_k+1}^k \rangle] = \times_{k=1}^{n} [\bigcup_{i \in I^{(n)}} \langle x_{i_k}^k; x_{i_k+1}^k \rangle] = \times_{k=1}^{n} \mathbf{J}^k = \mathbf{J}^{(n)}$.□

The following theorem is a direct implication of this proof.

4. Theorem

Let $\mathcal{D}^{(n)} = (\mathbf{J}^{(n)}; \mathbf{D}^{(n)})$ be a digital space and $A, B \in \mathbf{J}^{(\mathbf{n})}$ arbitrary items of its support. The relation $\rho \in \mathbf{J}^{(n)} \times \mathbf{J}^{(n)}$ defined as $\rho(A, B) \Leftrightarrow \exists \mathbf{F_i} \in \mathcal{F}^{(n)} : A \in \mathbf{F_i} \wedge B \in \mathbf{F_i}$ is an equivalence at $\mathbf{J}^{(\mathbf{n})}$.

5. Definition – physical space

The factorial set $\mathsf{F}^{(n)} = \mathbf{J}^{(n)}/\rho$ from previous theorem is called the physical space of support $\mathbf{J}^{(n)}$ like of the space $\mathcal{D}^{(n)} = (\mathbf{J}^{(n)}; \mathbf{D}^{(n)})$. Resolution of physical space $\mathcal{F}^{(n)}$ is considered as resolution of space $\mathcal{D}^{(n)}$.

4.3 Logical domain, logical space, mapping

From [14, pp. 51], [15, pp. 9 - 10]:

1. Definition – logical space, logical domain

Let $\mathsf{F}^{(n)}$ je be a physical space of digital space $\mathcal{D}^{(n)}$ and v_k dimensions of its physical domains. Also let $\mathbf{C} \in \mathbf{J}^{(n)} : \mathbf{C} = [c_1, c_2, \ldots, c_k, \ldots, c_n]; c_k \in \langle 0; v_k)$. The set $\mathcal{L}_{\mathbf{c}}^{(n)} = \times_{k=1}^{n} \{\mathbf{r}_{i_k}^k \in \mathbb{R} | \forall k \in \{1, 2, \ldots, n\} : \mathbf{r}_{i_k}^k \in \langle x_{i_k}^k; x_{i_k+1}^k) \wedge r_{i_k}^k - x_{i_k}^k = c_k\}$ is called the logical space of space $\mathcal{D}^{(n)} = (\mathbf{J}^{(n)}; \mathbf{D}^{(n)})$, its items $L_{\mathbf{c},i}; \mathbf{i} = [i_1, i_2, \ldots, i_k, \ldots, i_n]$, are called logical domains. Resolution of logical space $\mathcal{L}_{\mathbf{c}}^{(n)}$ is in fact resolution of space $\mathcal{D}^{(n)}$.

2. Theorem

Let $\mathsf{F}^{(n)}$ be a physical space and $\mathcal{L}_{\mathbf{c}}^{(n)}$ be a logical space of the same digital space $\mathcal{D}^{(n)} = (\mathbf{J}^{(n)}; \mathbf{D}^{(n)})$. The projection $\varphi_{\mathbf{c}} : \mathsf{F}^{(n)} \rightarrow \mathcal{L}_{\mathbf{c}}^{(n)}$ such as $\varphi_{\mathbf{c}}(\mathbf{F_i}) = L_{\mathbf{c},i} \Leftrightarrow L_{\mathbf{c},i} \in \mathbf{F_i}$, is bijection.

Proof: If $[r_{i_1}^1, r_{i_2}^2, \ldots, r_{i_k}^k, \ldots, r_{i_n}^n] \in \mathcal{L}_{\mathbf{c}}^{(n)}$, then the provable statement is an implication of equivalence: $\forall r_{i_k}^k : r_{i_k}^k \in \langle x_{i_k}^k; x_{i_k+1}^k) \Leftrightarrow [r_{i_1}^1, r_{i_2}^2, \ldots, r_{i_k}^k, \ldots, r_{i_n}^n] \in \times_{k=1}^{n} \langle x_{i_k}^k; x_{i_k+1}^k) = \mathbf{F_i}$ □

3. Definition – physical space mapping, reference point

The projection $\varphi_{\mathbf{c}} : \mathsf{F}^{(n)} \rightarrow \mathcal{L}_{\mathbf{c}}^{(n)}$ from previous theorem is called mapping of physical space $\mathsf{F}^{(n)}$. The point $\mathbf{C} \in \mathbf{J}^{(n)} : \mathbf{C} = [c_1, c_2, \ldots, c_k, \ldots, c_n]; c_k \in \langle 0; v_k)$ is called its reference point.

4. Note:

As the inference of theorem 2, inversive mapping exists to each mapping: $\varphi_{\mathbf{c}} : \mathcal{F}^{(n)} \rightarrow \mathcal{L}_{\mathbf{c}}^{(n)}$, *i.e.* $\varphi_{\mathbf{c}}^{-1} : \mathcal{L}_{\mathbf{c}}^{(n)} \rightarrow \mathcal{F}^{(n)}$. *Then it is able to assign to each physical domain* $\mathbf{F_i}$ *the only one logical domain* $L_{\mathbf{c},i}$ *by mapping* $\varphi_{\mathbf{c}}$ *and on the contrary to each logical domain* $L_{\mathbf{c},i}$ *it is able to assign the only one physical domain* $\mathbf{F_i}$ *by inversive mapping* $\varphi_{\mathbf{c}}^{-1}$.

5. Definition – vertex and central mapping:

Mapping $\varphi_{\mathbf{v}} : \mathcal{F}^{(n)} \rightarrow \mathcal{L}_{\mathbf{v}}^{(n)}$, with its control point $\mathbf{V} = [0, 0, \ldots, 0]$, is called vertex mapping. Mapping $\varphi_{\mathbf{s}} : \mathcal{F}^{(n)} \rightarrow \mathcal{L}_{\mathbf{s}}^{(n)}$, with its control point
$\mathbf{S} = [\frac{v_1}{2}, \frac{v_2}{2}, \ldots, \frac{v_k}{2}, \ldots, \frac{v_n}{2}]$, is called central mapping (see Fig. 12 on the right).

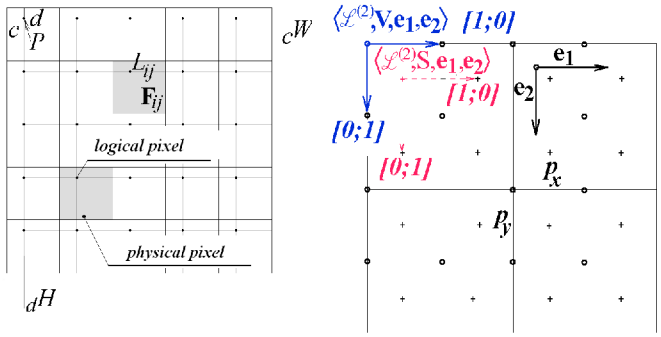

Figure 12: On the left: physical and logical pixels depiction, on the right: central and vertex mapping.

6. Definition – global coordinate system:

Let $\mathcal{D}^{(n)} = (\mathbf{J}^{(n)}; \mathbf{D}^{(n)})$ be a digital space, v^k dimensions of its domains and $\varphi_{\mathbf{c}} : \mathcal{F}^{(n)} \rightarrow L_{\mathbf{c}}^{(n)}$ arbitrary mapping. And let $\mathbf{R}^{(n)}$ be n - dimensional real vector space with base $\{\mathbf{e}_k\}_{k=1}^{n}; \mathbf{e}_k = (0, 0, \ldots, v_k, \ldots, 0)$.

Ordered $(n+2)$ - tuple $\mathrm{L}^{(n)} = \langle \mathcal{L}^{(n)}, S, \mathbf{e}_1, \mathbf{e}_2, \ldots \mathbf{e}_k, \ldots, \mathbf{e}_n \rangle$ is called the global coordinate system of logical space $\mathcal{L}^{(n)}$.

Ordered $(n+2)$ - tuple $\mathrm{F}^{(n)} = \langle \mathcal{F}^{(n)}, S, \mathbf{e}_1, \mathbf{e}_2, \ldots \mathbf{e}_k, \ldots, \mathbf{e}_n \rangle$ is called the global coordinate system of physical space $\mathcal{F}^{(n)}$ induced by mapping $\varphi_{\mathbf{c}}$.

Ordered $(n+2)$ - tuple $\mathrm{D}^{(n)} = \langle \mathcal{D}^{(n)}, S, \mathbf{e}_1, \mathbf{e}_2, \ldots \mathbf{e}_k, \ldots, \mathbf{e}_n \rangle$ is called the global coordinate system of digital space $\mathcal{D}^{(n)}$ induced by mapping $\varphi_{\mathbf{c}}$.

4.4 Image

1. Definition - Physical and logical pixel

The smallest and indivisible[5] displayable object is called a **pixel**[6]. Physical pixel is defined as $2D$ physical domain and logical pixel is then defined as $2D$ logical domain.

Physical pixel is the very small areal element of visualizing output device. This element is controlled directly by hardware of this output device. In practice several smallest elements are put together in order to create one pixel [14, pp. 47 - 48].

For instance:

- Screen - several small elements highlight one pixel
- ink jets - size of pixel corresponds to size of color drop
- laser jets - size of element corresponds to several grains of toner

Logical pixel is scattered point with integer coordinates, which contains integer color value of corresponding physical element [14, pp. 47 - 48]. Logical pixels are representatives of physical pixels (see Fig. 12 on the left).

From [14, pp. 129 - 130], [15, pp. 14 - 16]:

2. Definition – sampling function:

Let $\mathbf{I}^{(n)}$ be support of digital space. Function $g(\mathbf{x})$ defined for every $\mathbf{x} = [x_1, x_2, \ldots, x_n] \in \mathbb{R}^n$ is called sampling function only if $\forall \mathbf{x} \in \mathbf{I}^{(n)}$: $g(\mathbf{x}) = g(Trunc\ (\mathbf{x}))$, where $Trunc(\mathbf{x}) = [Trunc(x_1); Trunc(x_2); \ldots; Trunc(x_n)]$.

3. Definition – Image:

Let $W = \langle 0; w) \subset \mathbb{R}; w \in \mathbb{N} \quad (Width); H = \langle 0; h) \subset \mathbb{R}; h \in \mathbb{N} \quad (Height);$ $V = \langle v_1; v_2) \subset \mathbb{R} \quad (Value\ \ Set)$ be intervals. Let function $I : W \times H \to V$ be called (analog) image. If function I is sampling function then this image is called sampling image. If $W \times H$, the range of definition of function I, is physical (logical) plane then this image is called physical (logical) image. Physical (logical) space resolution is in fact resolution of its support. If function I is sampling function and $H \subset \mathbb{N}$, then the image is called digital image.

Digitizing of image is run in two phases **- sampling and quantizing**. The aim of sampling is transformation of analog image in sampled image. It means to transform the analog image in such way that each pixel in physical plane would carry constant value. Values of pixels are mostly taken from analog image by sampling function. The samples are taken off by high - frequency periodic function with high amplitude. These samples are acquired from original signal in ordinary intervals. In addition to rare exceptions, a

[5]The indivisibility is ignored in special cases.

[6]Pixel is abbreviation of *picture element*.

loss of information occurs. This loss does not have to be significant. However, wrong sampling can deteriorate the image very much [14, pp. 129 - 130] (see Fig. 13 and 14).

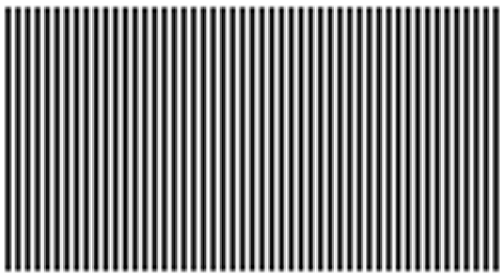

Figure 13: Correctly sampled image.

If Fouriere transformation is applied on the sampled image then its space frequency decomposition is gained. If frequencies higher then the sampling frequencies are significantly present in the image then new low - frequented information is brought into the sampled image, which was not present in the original image. The low - frequented signal within the meaning of Fouriere transformation is called an **alias**. It appears when the maximal image frequency f_{max} is sampled with frequency lower than $2f_{max}$, i.e. below Nyquist's limit [15, pp. 15 - 16]. Alias occurs mostly at sampling of periodic textures or at sampling of images with details that are smaller than size of physical pixel of the output device.

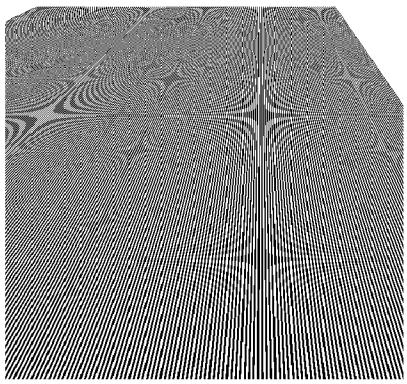

Figure 14: All stripes in this image seemingly contract. When their width underruns the size of physical pixel, the image is under sampled and it contains new structures larger than one pixel.

4.5 Additive noise, its detection

Let R_P be image matrix (perfect image) and let R_S be matrix of the same type as R_P and its elements are stochastically insignificant realizations of random variable X. Let $R = R_P + R_S$, then it is said that R contains additive noise. Characteristics of random variable X are called characteristics of additive noise.
The following two cases of additive noise are distinguished:

1. Additive noise independent on image,
   i.e. R_P and R_S are stochastically independent. In practice it is satisfying, if following weaker condition is fulfilled: $\rho(R_P, R_S) = 0$ where ρ denotes a correlation coefficient or $\mathrm{cov}(R_P, R_S) = 0$, where $\mathrm{cov}(R_P, R_S)$ is covariance of R_P and R_S [16, pp. 526], [15, pp. 16]. Undesirable presence of such noise in an image can be reduced by application of an adequate low pass filter (see section 4.7.1).

2. Noise dependent on image,
   i.e. there exists some stochastic dependence between R_P and R_S that neither disables determining parameters of this noise nor to filter it [15, pp. 16]. In practice some dependences are considered insignificant e.g. the neighboring pixels dependence of CCD chip while recording an image.

Additive noise detection
Assume image $R = R^P + R^S$ as a sum of perfect image R^P and stochastically independent noise R^S. Due to assumption of noise independence on the image, it is possible to estimate a variance (standard deviation) of the noise by using autocovariance function of image relative displacements. For non zero displacements z, the $\mathrm{cov}(R, R_z)$ is not affected by R^S and therefore,

$$\mathrm{cov}(R, R_z) = \mathrm{cov}(R^P, R^P_z), \tag{47}$$

otherwise, $\mathrm{cov}(R, R_0) = \mathrm{var}(R) = \mathrm{var}(R^P) + \mathrm{var}(R^S)$ (see Fig. 15)[7].
The functional dependence of the $\mathrm{cov}(R, R_z)$ on the displacement z is strictly monotonic function, decreasing with growing z and $\mathrm{cov}(R, R_z) \to 0$ for reasonably large z.
Most often, a function $\exp(a \cdot z + b)$ that satisfies these function constraints, is used as determining the autocovariance function. The $\exp(b)$ corresponds to the variance of the perfect image R^P and the $\mathrm{var}(R) - \exp(b)$ corresponds to the variance of the noise image R^S (see Fig. 15). Therefore, the estimate of the additive noise standard deviation is $\sqrt{(\mathrm{var}(R) - \exp(b))}$.
It is recommended to use logarithmic values of the $\mathrm{cov}(R, R_z)$ and of the exponential function because it is easier and quicker to fit a line to data than the exponential function.

[7] If the image R is large enough, the $\mathrm{var}(R)$ and $\mathrm{var}(R_z)$ are considered as equal $\forall z = 0, \cdots, z_{max}$.

Also autocorrelation function can be used instead of the autocovariance function for the noise detection because the autocorrelation function does not exceed 1 and hence the calculations are proceeded within the same range $\langle 0, 1\rangle$ regardless on the dynamic range of the image, i.e. regardless on the highest possible value of the autocovariance function. The additive noise detection was successfully implemented in the REFLECTOMETRY software package.

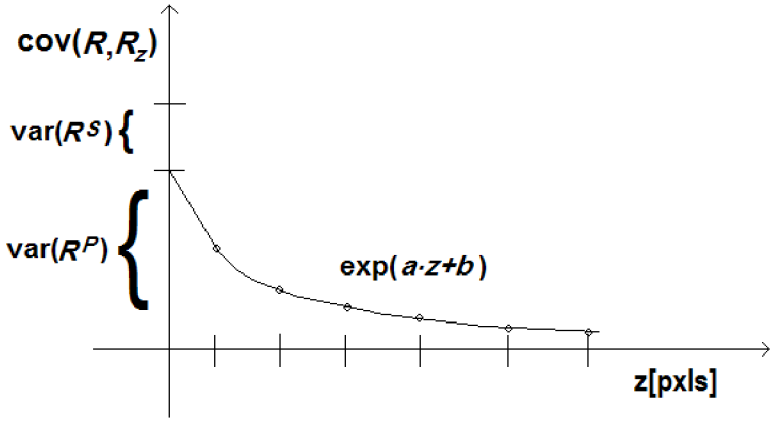

Figure 15: Model of auto covariation characteristics.

4.6 Brightness test

Value of each pixel of the CCD chip depends on the intensity of incoming light. It was empirically found out that bellow a certain intensity limit, the dependence is linear and above this limit, the dependence is nonlinear and a pixel with such value is considered as over exposed. Usually, the linearity of the CCD can be guaranteed within 80 - 98% of the dynamic range of the pixel according to the type of the CCD chip.
Therefore, the image can be considered as over exposed, if it contains more than certain rate limit of the over exposed pixels. The limit rate can be different for each CCD chip. This principle is used in the input data calibration, a necessary component of the REFLECTOMETRY software package.

4.7 Image Filters

From [14, pp. 115 - 125], [15, pp. 17 - 24]:

1. Definition - Image Filter

Image Filter is such operation that changes each pixel of an image by a defined process.

2. Definition - Convolution

nD convolution of two functions $\mathbf{C}(\mathbf{x})$, $g(\mathbf{x})$ defined for every $\mathbf{x} = [x_1; x_2; \cdots, x_n] \in \mathbf{J}^n$ and quadratically integrable on $\mathbf{J}^n$ is defined as an integral

$$\mathbf{C}(\mathbf{x}) \otimes g(\mathbf{x}) = \int_{\mathbf{J}^n} \mathbf{C}(\mathbf{t}) g(\mathbf{x} - \mathbf{t}) d\mathbf{t}. \tag{48}$$

3. Theorem

If $\mathbf{C}(\mathbf{x})$, $g(\mathbf{x})$ are digitalized functions then

$$\mathbf{C}(\mathbf{x}) \otimes g(\mathbf{x}) = \int_{\mathbf{J}^n} \mathbf{C}(\mathbf{t}) g(\mathbf{x} - \mathbf{t}) d\mathbf{t} = \sum_{\mathbf{t}=[-\varepsilon_1;-\varepsilon_2;\cdots;-\varepsilon_n]}^{[\varepsilon_1;\varepsilon_2;\cdots;\varepsilon_n]} \mathbf{C}(\mathbf{t}) g(\mathbf{x} - \mathbf{t}). \tag{49}$$

If $n = 2$ and a physical plane with an unit pixels size is defined on $\mathbf{J}^2$ then for each physical pixel $\mathbf{F}_{ij}$

$$\mathbf{C}(\mathbf{F}_{ij}) \otimes g(\mathbf{F}_{ij}) = \sum_{m=-\varepsilon}^{\varepsilon} \sum_{n=-\varepsilon}^{\varepsilon} \mathbf{C}(\mathbf{F}_{m;n}) g(\mathbf{F}_{i-m;j-n}) = \sum_{m=-\varepsilon}^{\varepsilon} \sum_{n=-\varepsilon}^{\varepsilon} \mathbf{C}(m;n) g(i-m, j-n). \tag{50}$$

According to discrete and finite value domain, the value of calculated convolution has to be rounded or truncated. For $n = 2$ the $\mathbf{C}(m; n)$ of real values is a matrix that can be formally defined as projection

$$\mathbf{C}(m;n) : \{-\varepsilon_1; \cdots; 0; \cdots; \varepsilon_1\} \times \{-\varepsilon_2; \cdots; 0; \cdots; \varepsilon_2\} \to \mathbb{R},$$

nD matrix $\mathbf{C}(\mathbf{t})$ is then $\mathbf{C}(\mathbf{t}) = \times_{i=1}^{n} \{-\varepsilon_i; \cdots; 0; \cdots; \varepsilon_i\} \to \mathbb{R}$.

Filters that can be described by the mentioned convolution assign value to a pixel that is a linear combination of pixels from its rectangular neighborhood. These filters are called **Linear Filters**. Filters that can not be described by this convolution are then called **Nonlinear Filters**.

4. Definition - Convolution matrix

Matrix $\mathbf{C}(m, n)$or $\mathbf{C}(\mathbf{t})$ from theorem 2. is called 2D or nD convolution matrix.

These convolutions are mostly applied to 2D images when their evaluation is interpreted as coloring.

According to chosen matrices $\mathbf{C}$, the filters have a certain characteristics such as **Low pass filters**, **High pass filters** or **Emboss filter**.

4.7.1 Linear Filters

The linear filters assign new value to pixel by linear combination of pixels from its neighborhood. It can be described by the following formula:

$$b_{i,j} = E \sum_{k=-n}^{k=n} \sum_{l=-n}^{l=n} a_{l,k} c_{k-i+2,l-j+2} + D, \tag{51}$$

where $b_{i,j}$ and $a_{i,j}$ are new and old values of a pixel respectively, $\mathbf{C} = (c_{i,j})$ is a square[8] convolution matrix of type $2n+1$, D is an additive constant affecting the image brightness and E is multiplicative constant affecting the image contrast
[14, pp. 117].
In the sense of the Fouriere transformation, high and low space frequencies of an ideal image are uniformly distributed. The high pass and low pass filters prefer representation of only one group of the frequencies to the other.

Low pass filters

Higher representation of low space frequencies causes the image to be blurred because all image details and sharp edges of objects that are represented by high space frequencies are of low contrast [14, pp. 119], [15, pp. 23].
Not only details and sharp edges of objects are the representatives of the high space frequencies but also the additive noise is represented in the image by high frequencies. Hence the low pass filters can decrease the influence of the additive noise by blurring the image.
It is common for typical representatives of low pass filters that $D = 0$ and

$$E = \frac{1}{\sum_{k=-n}^{k=n} \sum_{l=-n}^{l=n} c_{k,l}}.$$

For example

$$\mathbf{C} = \frac{1}{9} \begin{pmatrix} 1 & 1 & 1 \\ 1 & 1 & 1 \\ 1 & 1 & 1 \end{pmatrix}, \quad \mathbf{C} = \frac{1}{5} \begin{pmatrix} 0 & 1 & 0 \\ 1 & 1 & 1 \\ 0 & 1 & 0 \end{pmatrix} \tag{52}$$

are some of the typical representatives of low pass filters [14, pp. 119]. An example of filter application is depicted in Fig. 16 on the left.

[8] Square convolution matrices are the most common in practical use.

High pass filters

The high pass filters enhance the high space frequencies of the filtered image. So the contrast of details and edges of objects is increased. This filter is commonly used to create sharp image or to detect borders of objects. However, these filters also increase a volume of the present additive noise and hence they should be applied with this consideration. The typical representatives of high pass filters are usually presented with $D = 0$ and $E = 1$, where $\{c_{0,0} = A_c + \sum_{(k\neq 0)\vee(l\neq 0)} c_{k,l}, \quad A_c \geq 1\}$ is the only positive element of the convolution matrix, all other elements are non positive. If E is large enough then the filter can be used as border detector [14, pp. 119], [15, pp. 21 - 22]. The Eq. (53) shows two of typical high pass filters and Fig. 16 on the right depicts result of high pass filter application.

$$\mathbf{C} = \begin{pmatrix} -1 & -1 & -1 \\ -1 & 9 & -1 \\ -1 & -1 & -1 \end{pmatrix}, \quad \mathbf{C} = \begin{pmatrix} 0 & -1 & 0 \\ -1 & 8 & -1 \\ 0 & -1 & 0 \end{pmatrix} \tag{53}$$

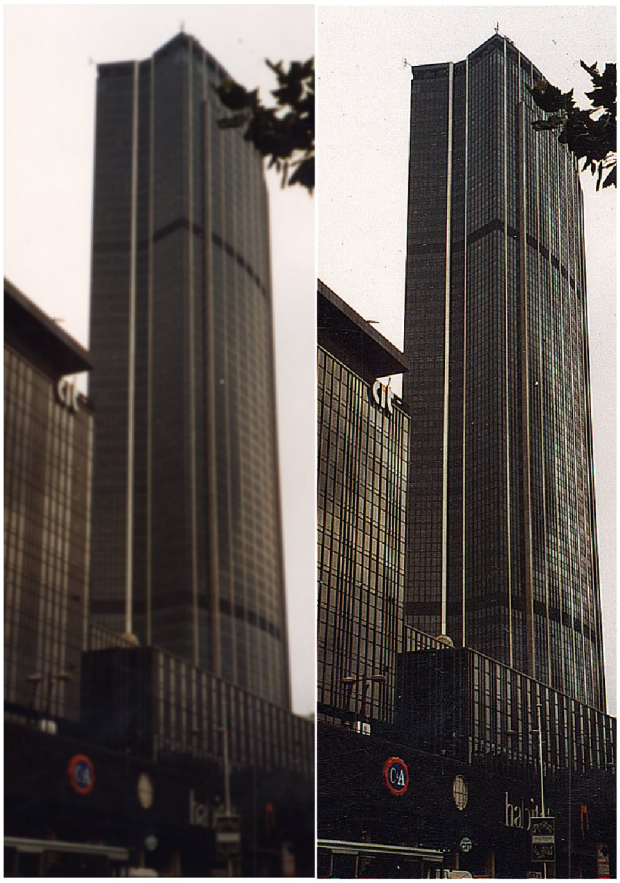

Figure 16: Image on the left - low pass filter application, image on the right - high pass filter application.

Gaussian filters

To enhance image details or decrease the additive noise representation it is better to apply so called **Gaussian filters** because better results of filtering are usually acquired[9]. These filters can be both high pass and low pass and are described by the following formula:

$$c_{m,n} = k \cdot \mathrm{e}^{-\frac{m^2}{\sigma_m^2} - \frac{n^2}{\sigma_n^2}}, \quad m, n = -a, \cdots, a \tag{54}$$

where σ_m^2 and σ_n^2 are chosen variances for directions x and y respectively [14, pp. 119].

Emboss filters

A special case of linear filter where the convolution matrix is written as

$$c_{i,j} = \begin{cases} -1, & i = j, -n \leq i < 0, \\ 1, & i = j, 0 < i \leq n, \\ 0, & \text{otherwise} \end{cases} \tag{55}$$

is called the **Emboss filter** that makes the image to look like it was embossed (see Fig. 17). The filter is the more demonstrative the larger is the n[14, pp. 120] [10].

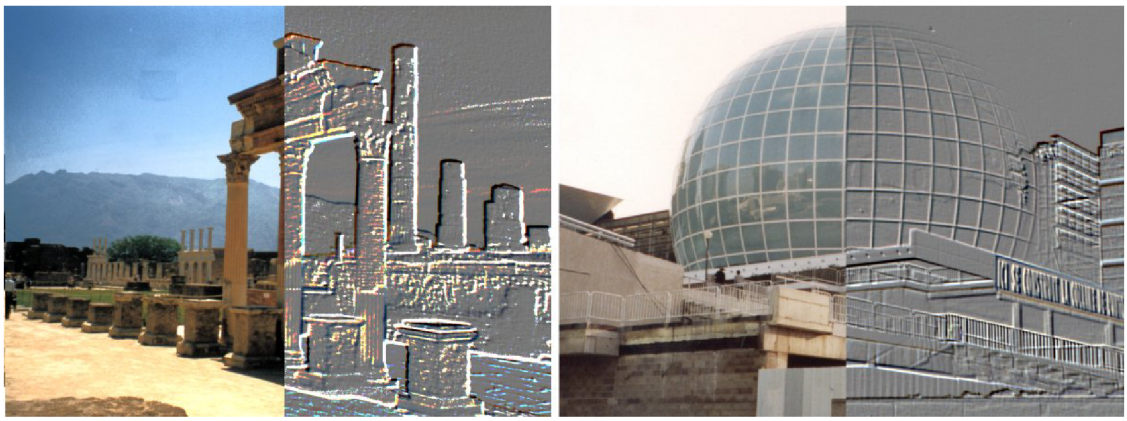

Figure 17: Example of Emboss filters applications.

[9] For some application it is satisfactory to apply the non Gaussian filters.

[10] i.e. the size of convolution matrix is greater

4.7.2 Nonlinear Filters

The nonlinear filters assign the pixel new value by principally different way than linear filters so the new pixel value is not determined by a linear combination. To the group of nonlinear filters belong functions **minimum**, **maximum** or **thresholding** that are used most often.

Minimum

This filter assigns the pixel the lowest value of its chosen neighborhood. In case of gray scale images the minimum is simply defined as minimal gray level, on the other hand in case of colored images the minimum can be defined by several ways, e.g. minimal color can be defined as combination of minima of each color channel, e.g. in RGB images the minimal color C_{min} is then defined by the following sum [14, pp. 120 - 121], [15, pp. 25]:

$$\mathrm{C}_{min} = 256^2 \cdot \mathrm{B}_{min} + 256 \cdot \mathrm{G}_{min} + \mathrm{R}_{min}, \tag{56}$$

$$\mathrm{B}_{min} = \min\{\mathrm{B}_{i,j}\}, \mathrm{G}_{min} = \min\{\mathrm{G}_{i,j}\}, \mathrm{R}_{min} = \min\{\mathrm{R}_{i,j}\},$$

$$\forall [i,j] \in \{\langle I_{min}; I_{max}\rangle \times \langle J_{min}; J_{max}\rangle\} \tag{57}$$

where B_{min}, G_{min}, R_{min} are the minima of blue, green and red channels respectively searched within pixel's neighborhood determined by rectangle
$\{\langle I_{min}; I_{max}\rangle \times \langle J_{min}; J_{max}\rangle\}$, or as minimum of combination of all color channels,
e.g. in RGB images the C_{min} is then defined as

$$\mathrm{C}_{min} = \min\{256^2 \cdot \mathrm{B}_{i,j} + 256 \cdot \mathrm{G}_{i,j} + \mathrm{R}_{i,j}\}, \quad \forall [i,j] \in \{\langle I_{min}; I_{max}\rangle \times \langle J_{min}; J_{max}\rangle\}. \tag{58}$$

A correction of results in the REFLECTOMETRY software package is based on the principle of the minimum filter.

Maximum

Analogically to minimum filter this filter assigns the pixel the highest value of its chosen neighborhood. If in equations (56) and (58) the function min were replaced by max the equations become considerable definitions of maximal color C_{max}.

Filters **Minimum** and **Maximum** are also known as filters **Dilatation** and **Erosion** [14, pp. 121], [15, pp. 25] because they can dilate or erode image objects. Dark objects with light background are dilated by minimum filter and eroded by maximum filter and interpretation of these filters is switched in case of light objects with dark background. Dilatation is also used for connection of objects and erosion is also applied in order to split these objects. For instance if a gap between two objects (at least locally) is lesser than diameter of the chosen neighborhood, the dilatation filter connects these objects and otherwise, if one object that looks like connection of two smaller objects is in place of connection thinner than chosen neighborhood of erosion filter this filter can split the

object into two smaller.
Dilatation and erosion filters are usually combined together, especially in multiple use when one filter is applied k times and then the other is applied same times in order to connect or separate objects with respect to what is demanded. See examples of dilatation and erosion filters application in Fig. 18.

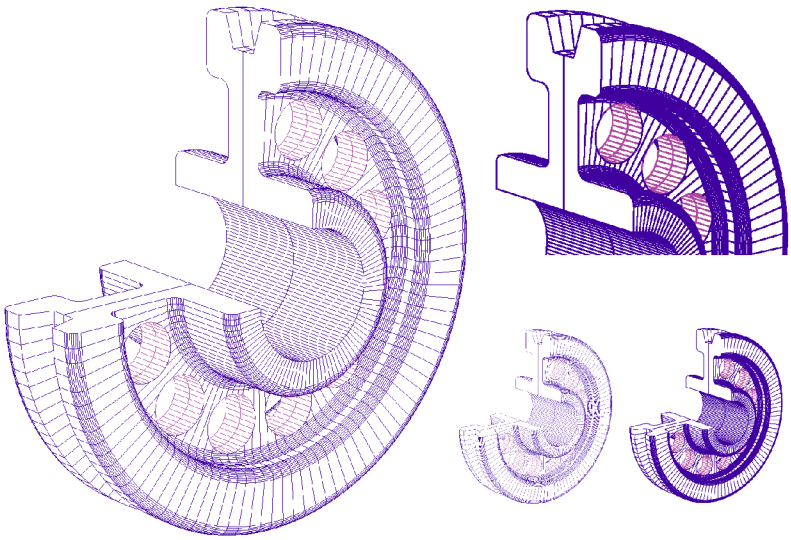

Figure 18: Examples of dilatation and erosion applications. On the left - original image, on the right: on the top - detail of the image after the dilatation has been applied, at the bottom: on the left - scaled down image after erosion filter application, on the right - dilated original image - also scaled down.

Threshold

The **threshold** filter can be applied when objects borders detections are required. Other nonlinear filters that can detect borders of objects are gradient filters [14, pp. 124 - 125]. Threshold filter usually creates an binary image where objects are represented by chosen color and background of objects is represented by different color. The decision factor in this case is directly the threshold. If the pixel is lower than the set threshold it is considered as background and background color is assigned to it, otherwise, it is considered as object and object color is assigned. Then the threshold can be defined as limiting color difference instead of absolute color value and after application, image with depicted borders of objects only can be obtained (see Fig. 19).
The principle of thresholding is used in the sensitivity analysis.

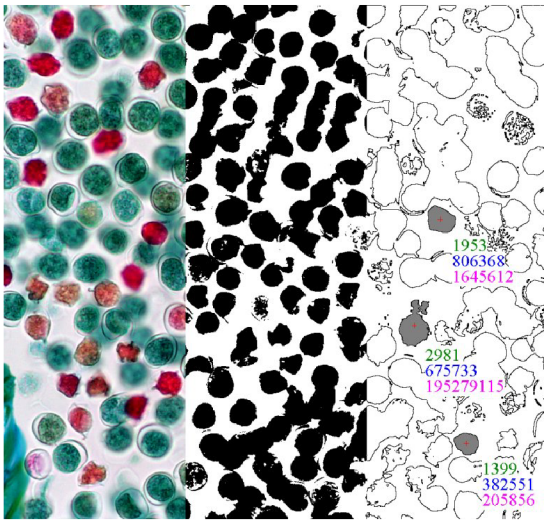

Figure 19: Example of threshold filters applications.

5 Results

A specific software package called REFLECTOMETRY was developed for processing measurements of the thin films optical properties. Apart from the processing the experimental measurements, the program also offers an option to analyze the reliability of acquired results by simulating the reflectance spectra and consequently by detecting the region of interest and by the calculating *Reliability factor*.

5.1 Experimental data acquisition and calibration

The experimental data is acquired as images recorded by CCD camera embodied into the measurement assembly where its model is depicted in Fig. 20. The Fig. 40 in the Figure annex shows the real measuring assembly.

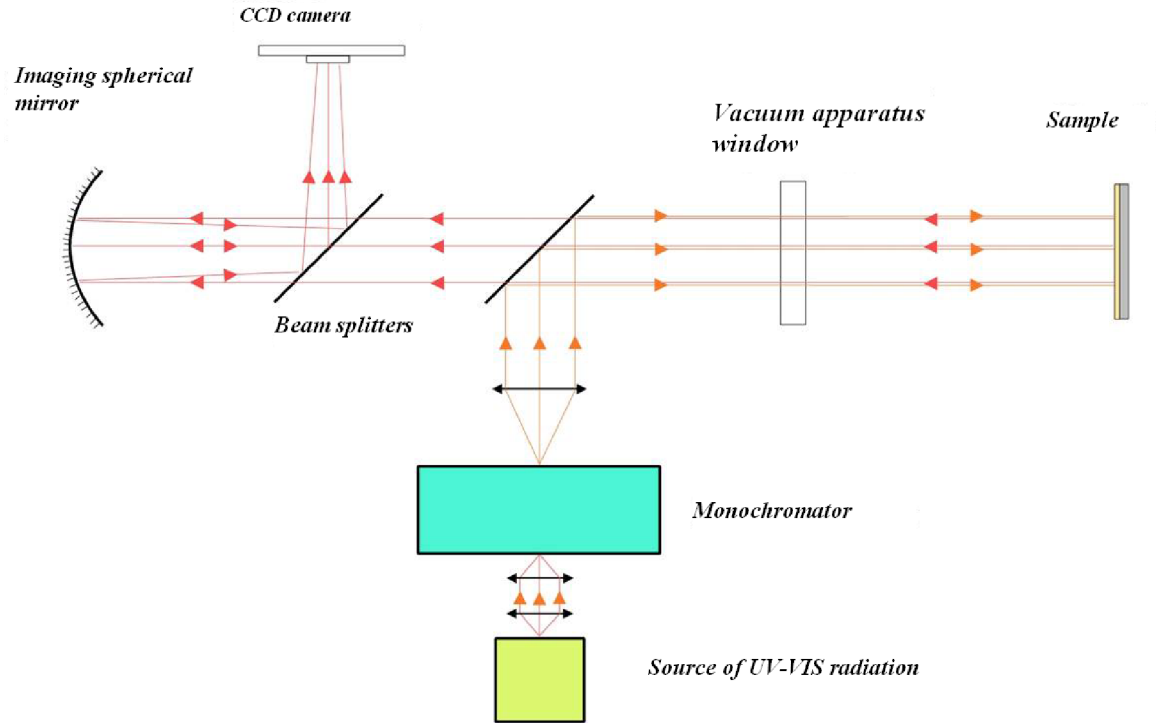

Figure 20: The scheme of the measuring assembly.

Each image stores an intensity information of light reflected from the sample, related to the input intensity I_{in} of the outcoming light from the monochromator and the recorded image corresponds to a wavelength λ set by the monochromator.
The image acquisition has to be carried out at constant I_{in} or each image should be weighted in relation to the input intensity in order to balance all images and to avoid any misinterpretation of the optical characteristics measurements caused by disbalanced measurement conditions which first of all means the wrong reflectance spectra extraction.

The images are specifically separated into categories according to the type of intensity they store. Those can be intensities of the *Reference* material (i.e. a material with known absolute reflectance), the measured *Sample*, the *Background* or the *Noise*.
If the sample (or the reference material) is removed the *Background* images can be acquired. These images store an additional information of intensity of light reflected from the components of the measuring assembly (mainly from the beam splitters).
In addition, if the arc discharge lamp is switched off the camera can record the *Noise* images that could randomly distort the intensity information and hence the *Noise* images should be subtracted from all other images. The Fig. 21 depicts examples of the experimentally measured intensities of the *Sample* and *Reference*, the intensities of *Background* and the *Noise* are too low in comparison to the *Reference* and *Sample* so they would appear just as black images and hence they are not depicted in the thesis.

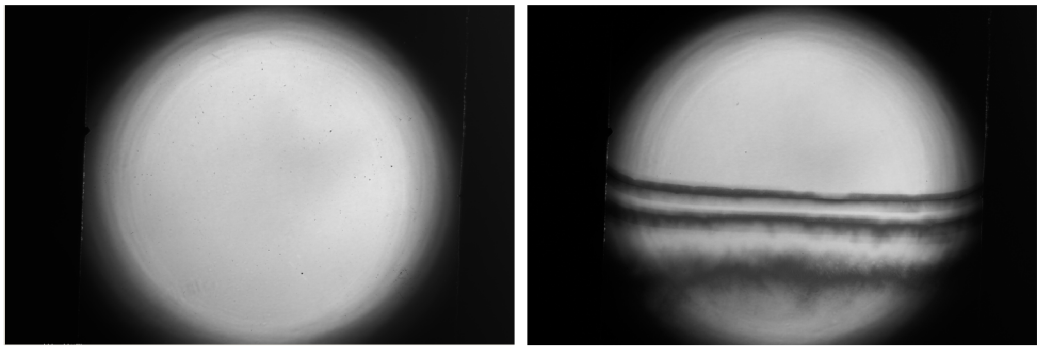

Figure 21: The experimentally measured intensities of the *Reference* (on the left) and the *Sample* (on the right).

The calibration consists in two steps:

- in the brightness test,
- in the additive noise detection.

The brightness test removes the over exposed and related images from further calculations because using these over exposed images could cause significant distortion in the reflectance spectra extraction. See Fig. 22 and Fig. 23 to compare the distort and correct reflectance spectra extraction.

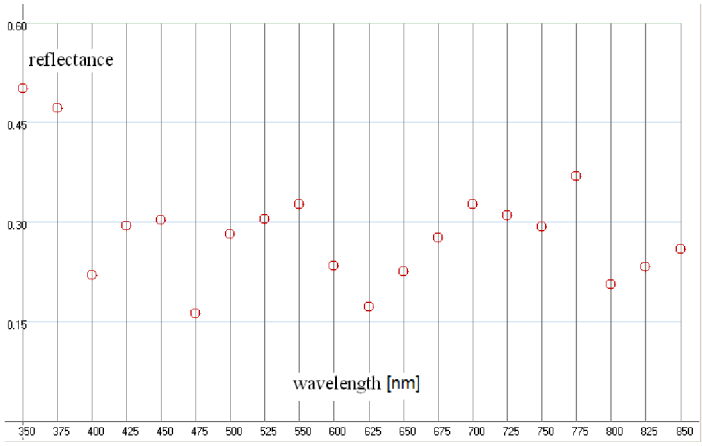

Figure 22: Extracted reflectance spectra including the over exposed intensity information.

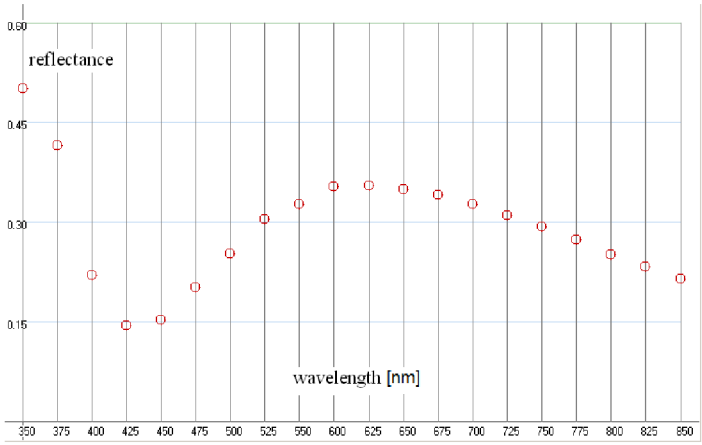

Figure 23: Extracted reflectance spectra without any over exposed image.

All over exposed images and all images corresponding to the same wavelengths as the over exposed images are removed from all data categories.
The additive noise can also distort the calculations, therefore, it is recommended to detect its presence in all images and carry out some correction process such as application of the low pass filter to decrease its affection of the image.
The *Noise* images should be subtracted from the other images before the detection is proceeded in order to possibly decrease the level of the present noise in the images. The example of the additive noise detection is depicted in Fig. 24.

For creating experimental data silicon oxide thin films deposited on silicon wafers were measured, each sample size was 15×15 mm. ST - 7XME CCD camera with chip size 720×576 pixels proved as a reliable recorder because the estimated additive noise standard deviation of each saved image was detected bellow 1% of each image brightness mean (except the *Noise* category) and the setting of the camera enabled all images to satisfy the brightness requirements and hence none of the images was removed.

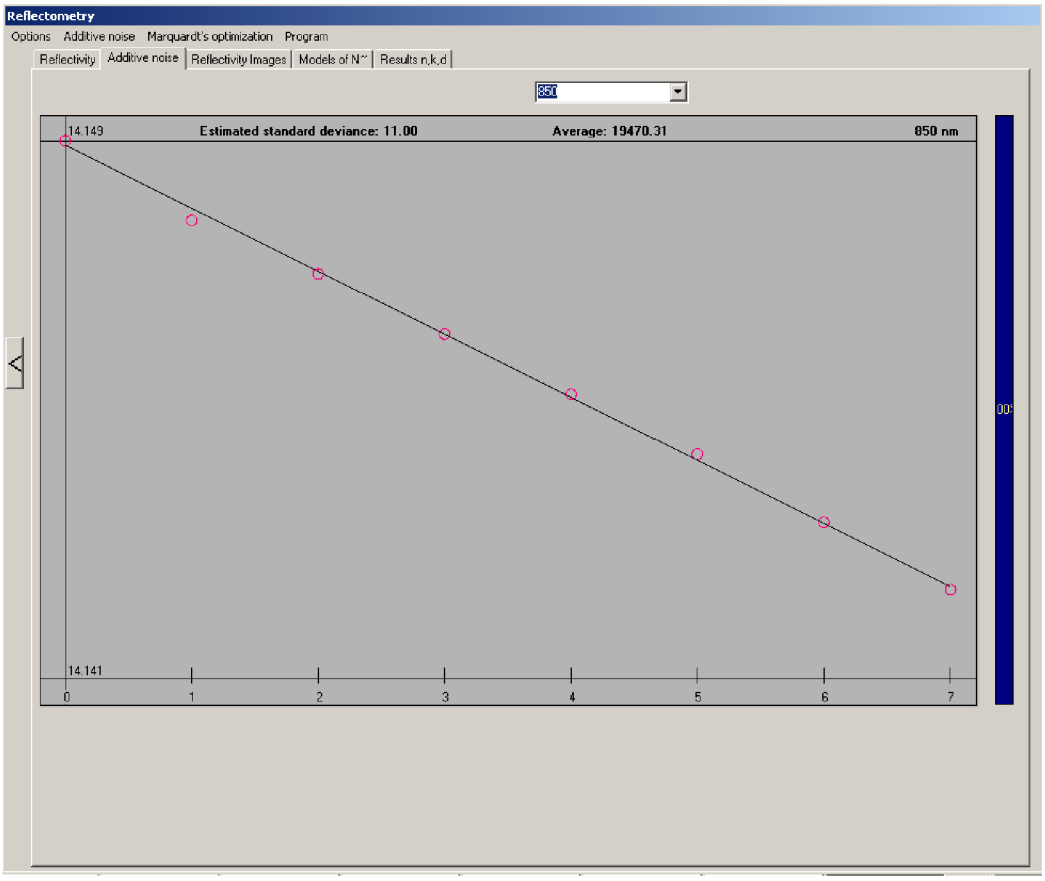

Figure 24: The additive noise detection at *Sample* image corresponding to wavelength 850nm. The estimated standard deviation of the additive noise is very low in comparison to the brightness mean and hence the image is considered as not affected by the additive noise.

5.2 Spectra extraction

The calibrated data with the additive noise decreased to the lowest possible level can be used for the reflectance spectra extraction.
The spectra is extracted at all wavelengths remained after the calibration.
Since each image stores the intensity I of reflected light that can be expressed as fraction of the intensity I_{in}, the absolute reflectance of the sample A_S is formulated as a relative reflectance of the sample related to the reference multiplied by the absolute reflectance of the reference, see Eq. (59) where I_S, I_R and A_R denote the intensity of sample image, intensity of the reference and the absolute reflectance of the reference respectively.

$$A_S = \frac{I_S}{I_R} A_R \tag{59}$$

Since each image comprises a portion of intensity of light reflected directly from the beam splitters, the intensity of the background I_B should be subtracted from the I_S and I_R in order to extract much accurate spectra. The A_S should be then calculated as

$$A_S = \frac{I_S - I_B}{I_R - I_B} A_R \tag{60}$$

Note: *The I_S, I_R and I_B are considered as decreased by the intensity of the Noise data.*
The example of the extracted reflectance spectra is depicted in Fig. 23.
The sample intensities were measured either during the growth of the film or after it has been locally etched by the hydrofluoric acid where the etching created film with stair - like profile (see Fig. 25).

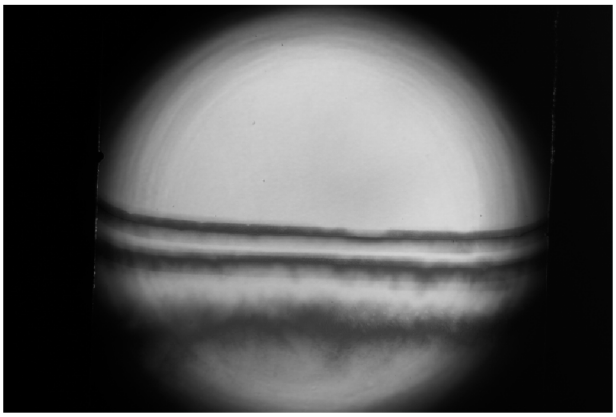

Figure 25: Intensity information of the SiO_2 film etched by hydrofluoric acid.

5.3 Measurement setting

The optical characteristics that indicate the sample reflectance are measured by fitting the experimental spectra to the theoretical model of reflectance. The quality of fitting inter alia depends on the general setting of the optimizing method and on the proper setting of the initial approximation.

The general setting of the method defines conditions of stopping the calculations such as the maximum of iterations k_{max}, the satisfactory limit of sum of the residual squares ϵ or the lowest considerable limit of the speed of convergence $\|\delta^k\|$, and the initial parameter λ_M, whereas the initial approximation defines what kind of material was or could potentially be the thin film made of. The initial approximations are loaded from library of the corresponding dispersion model of $\tilde{N}$. The library can be modified in the sense of adding or removing the models of $\tilde{N}$.

In summary, before the spectra can be fitted to the theoretical model, the type of dispersion model of $\tilde{N}$ and consequently a specific model have to be chosen and the general conditions of the optimization have to be set.

The setting of the method is depicted in Fig. 26.

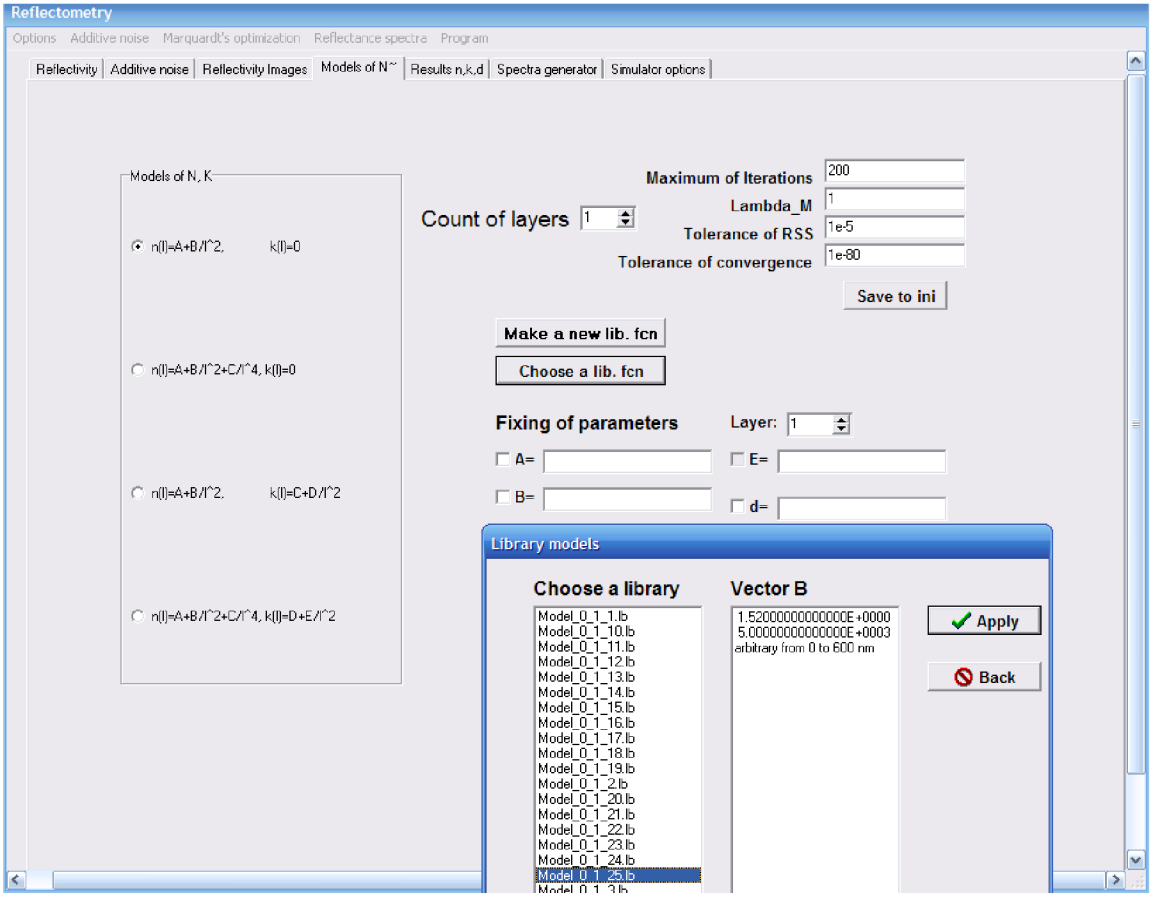

Figure 26: Optimization setting: choosing the dispersion model, setting the global parameters of the optimization, initial setting of coefficients and the option to fix them.

5.4 Measurement

The optical characteristics can be measured either at chosen point (pixel) or at chosen rectilinear area. See Fig. 27 and Fig. 28 where the measurements at the chosen point and the chosen area are shown.

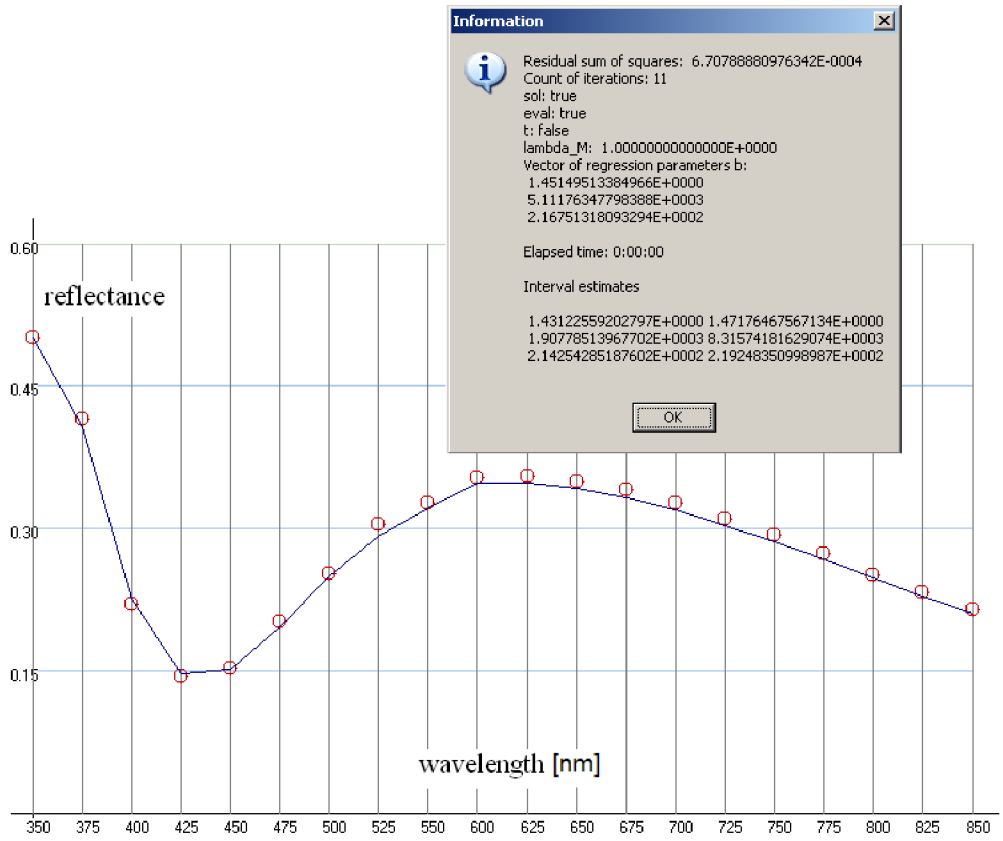

Figure 27: Measured characteristics of SiO_2 film at chosen point. The ring - shaped dots represent the extracted reflectance spectra and the line indicates the fitted model where the results are depicted in the dialog box.

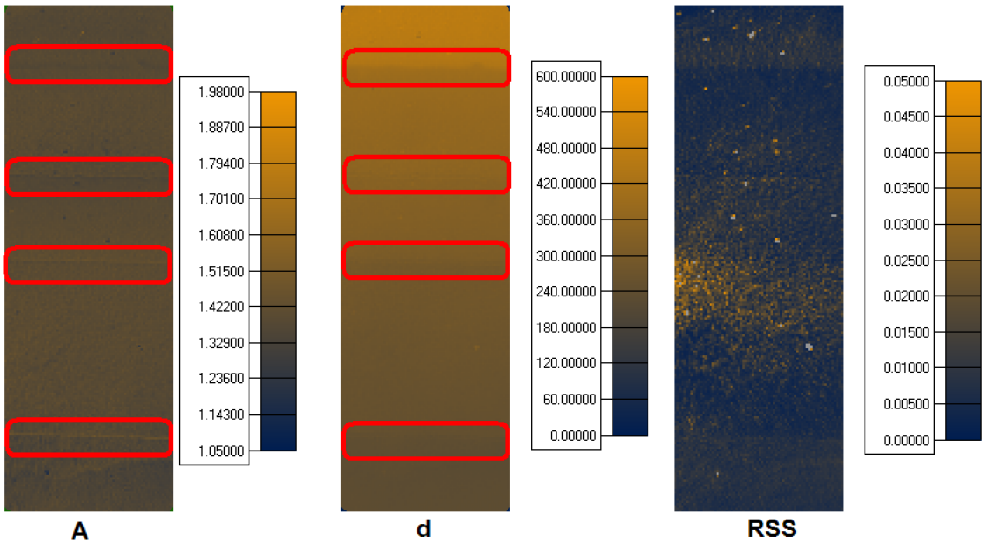

Figure 28: Measured characteristics A, d of SiO_2 film etched by the hydrofluoric acid over a chosen area 143×430 pixels followed by the RSS. The coefficients were unfixed and hence th affection by the mutual correlation between A and d is apparent (see the marked regions). The A is expected to be constant whereas the major change of A follows morphology of the film in the results.

The characteristics measured within the chosen area can be corrected after the fitting has been completed. The correction consists in assigning each point such solution from its neighborhood that gives the smallest sum of residual squares. The surface is considered continuous and hence the neighboring points should give similar results unless something suddenly changes the reflectance of the sample (e.g. very sharp edge or a sharp bounded dust particle, drop of liquid, etc.). The higher is the resolution of the image, the more real is the depiction of the surface and the more difficult is to detect a very sharp edge. Then, if the resolution is high enough, the sudden changes of reflectance are mostly caused by the dust particles or the drops of some liquid, etc. This has to be also considered because the laboratory conditions do not have to be usually too strict.
The neighborhood should be set carefully with respect to the resolution of the image. The higher is the resolution, the larger neighborhood can be set. The calculation of the results within the chosen area ran approximately 28 minutes whereas the correction with neighborhood set to ± 10 pixels ran about 6 minutes.
An example of the results correction is depicted in Fig. 29.

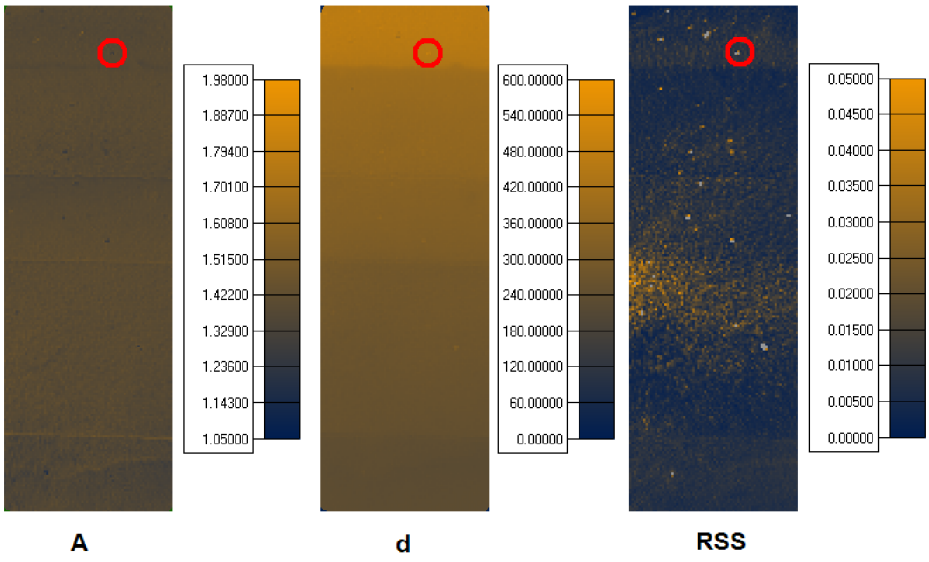

Figure 29: The correction of the results within the chosen area. The correction can modify the results only at few points (see the marked regions), if the calculation was precise enough. Therefore, the results look the same as in Fig. 28.

The other option of the measurement is to estimate the coefficients when all of them stay unfixed or some of them are fixed. Fixing chosen parameters can avoid the affection of mutual correlations among the regression coefficients and hence the measurement can be more precise. The difference of the acquired results is presented in Fig. 30 where the thickness was estimated within the chosen area.

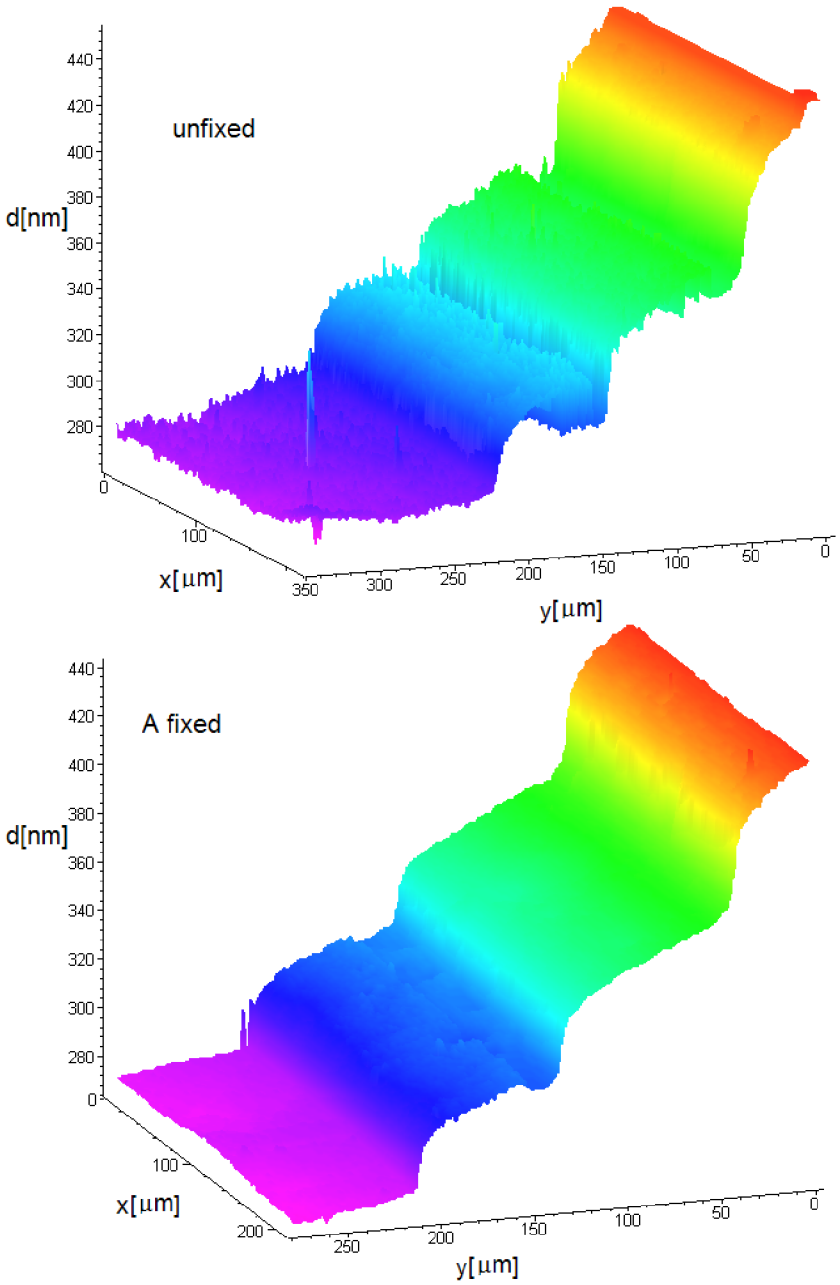

Figure 30: The example of the measurement of SiO_2 film characteristics with and without fixing the coefficients.

5.5 Sensitivity analysis

It is possible to carry out the analysis with various global settings of the method and with option to fix chosen regression coefficients. Three materials, the SiO_2, Si_3N_4 and PMMA with the refractive indices $\tilde{N} = 1.52 + 5000\text{nm}^2/\lambda^2$, $\tilde{N} = 2.0 + 15000\text{nm}^2/\lambda^2$ and $\tilde{N} = 1.38 + 12000\text{nm}^2/\lambda^2$ respectively considered as deposited on silicon substrates were tested in the sense of the defined sensitivity analysis. The global setting of the optimizing method and setting of initial approximation were studied in order to check whether the region $\mathbf{B^I}$ can be different for one material when the global setting changes or the coefficients of the initial approximations are fixed or unfixed.

Note:*Following the theory of the Sensitivity analysis, the* $(\vartheta_1^*, \vartheta_2^*, \vartheta_3^*)$ *and* $(\vartheta_1, \vartheta_2, \vartheta_3)$ *are going to be denoted by* (A_{id}, B_{id}, d_{id}) *and* (A, B, d) *respectively.*

The global setting differed only in the λ_M that was set to values: 0.01, 1 and 100 and the $\tilde{N} = A + B/\lambda^2$ was chosen as type of dispersion model where at most one of the coefficients A, B was fixed. Since the set tolerances of the thickness d were set too tightly, the analysis with fixed d was omitted. The tolerances μ and ν were set to $(\pm 0.07, \pm 3000\text{nm}^2, \pm 1\text{nm})$, the Λ and the p_t were set to 1 and 0.95 respectively and 44 wavelengths λ in the range from 351 to 886nm were chosen for the analysis.

The analysis started at the lowest values of A, B and d that were increased by their increments until they reached their maximal values and the $\mathbf{B^I}$ was detected at each initial setting. The ranges of the coefficients that determine the $\mathbf{B^I}$ are expressed as deviations $(\Delta A_{min}, \Delta B_{min}, \Delta d_{min})$ and $(\Delta A_{max}, \Delta B_{max}, \Delta d_{max})$ of the ideal solution (A_{id}, B_{id}, d_{id}) where $\mathbf{B^I} = \langle A_{id} + \Delta A_{min}, A_{id} + \Delta A_{max}\rangle \times \langle B_{id} + \Delta B_{min}, B_{id} + \Delta B_{max}\rangle \times \langle d_{id} + \Delta d_{min}, d_{id} + \Delta d_{max}\rangle$. The increments of the coefficients were set to $(0.01, 150\text{nm}^2, 2\text{nm})$ when A was fixed and to $(0.03, 150\text{nm}^2, 2\text{nm})$ in other cases.

The ideal thickness d_{id} [nm] was set in all analyzed cases to all values from range $\{100, 105, 110, \cdots, 500\}$, i.e. for every analyzed material and every initial setting.

A good initial setting can be found, if the $\mathbf{B^I}$ is as large as possible and the $\mathbf{R_f}$ is ideally 1 or close to 1 as much as possible. On the other hand, a very small $\mathbf{B^I}$ with very small $\mathbf{R_f}$ means that the initial setting of the coefficients is very difficult to find because it is too case sensitive. The sensitivity analysis is going to be discussed in a matter of finding the initial setting of the regression coefficients or rather the successfulness of the fitting. Each analyzed setting is described by its input and output protocols (the modal and frequency characteristics) that are in a text format (see Fig. 41 - 43 in the Figure annex).

The SiO_2 was analyzed within these ranges of coefficients: $(1.07, 500, 100)$ - $(1.97, 9500, 500)$ when all coefficients were unfixed, $(1.07, 2000, 100) - (1.97, 8000, 500)$ when B was fixed and $(1.45, 500, 100) - (1.59, 9500, 500)$ when A was fixed.

The detected ranges of B and d were exactly the same as the initial ranges set for the

analysis, therefore, the initial setting of the regression coefficients was studied only as setting of the A. Results of the analysis are depicted in Fig. 31 - 33. Considering all cases of fixed and unfixed coefficients A and B, it appeared that the detected range of A is not significantly affected by the initial value of λ_{M}. The range of the initial A tends to contract with growing thickness of the film in the cases when A was unfixed (see Fig. 31) and because the $\mathbf{R_f}$ in these cases (see Fig. 32) is not much variable, it could mean that it is more difficult to fit the model to measured data of films of higher thicknesses than to data of thinner films.

In the case when A was fixed, the range of initial setting of A was detected rather as contracting with decreasing thickness of the film (see Fig. 33 a)). Together with the $\mathbf{R_f}$ (see Fig. 33 b)) which appeared to grow with the thickness of the film, it could mean that it is convenient to use such setting for fitting the reflectance model to data of films of high thicknesses, if the A were reasonably precise.

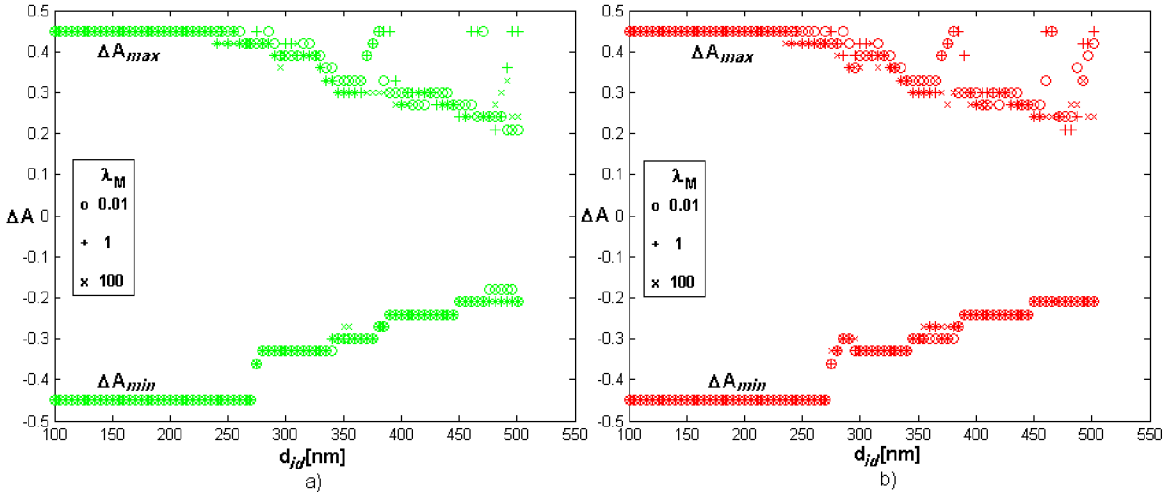

Figure 31: The detected ΔA_{min} and ΔA_{max} of the simulated SiO_2 film when the : a) coefficients were unfixed, b) the coefficient B was fixed. The results are very similar because the variability of B does not affect the $\tilde{N}$ significantly and hence fixing or unfixing B leads to almost the same results.

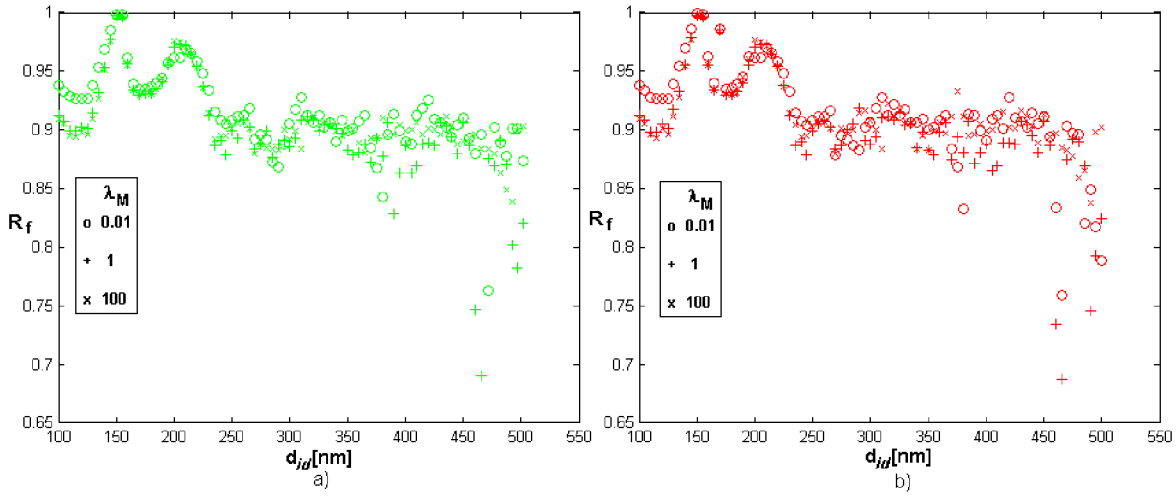

Figure 32: The detected $\mathbf{R_f}$ of the simulated SiO_2 film when the : a) coefficients were unfixed, b) the coefficient B was fixed.

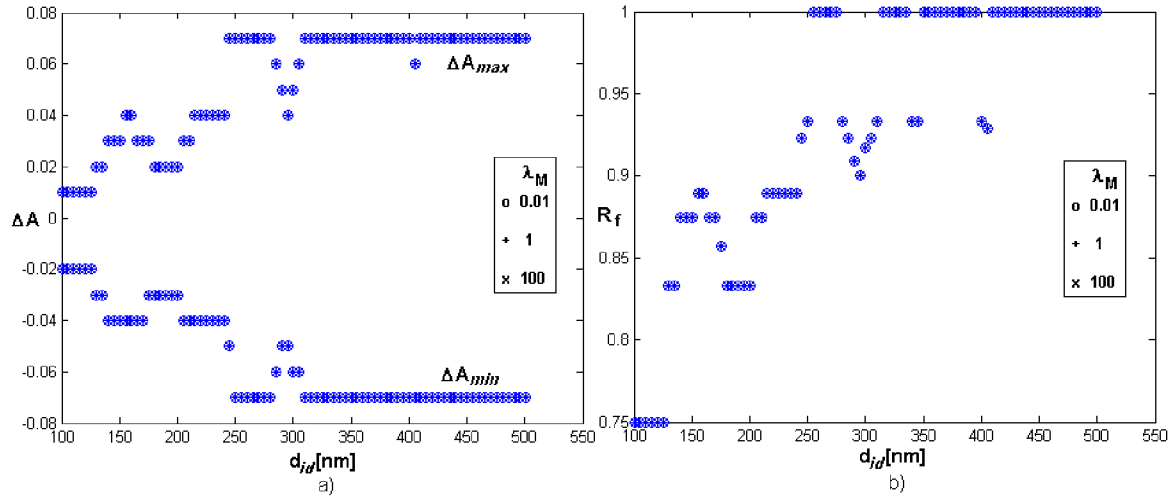

Figure 33: The detected ΔA_{min}, ΔA_{max} and $\mathbf{R_f}$ of the simulated SiO_2 film when the A was fixed.

The analysis of PMMA (see Fig. 34 - 36) was carried out with these settings: $(0.93, 6000, 100) - (1.83, 18000, 500)$ when all coefficients were unfixed,
$(0.93, 9000, 100) - (1.83, 15000, 500)$ when B was fixed and $(1.31, 6000, 100)$ - $(1.45, 18000, 500)$ when A was fixed.
The results are similar to the SiO_2 analysis with a slight difference in a case when A was not fixed where the initial setting $\lambda_M = 100$ gives more precise results than the other settings (see Fig. 34). Anyway, it can be concluded again that for fitting the model to measured data of the PMMA films of higher thicknesses (~ above 400nm) it is more convenient to fix the value of A (see Fig. 36), if the A were known quite precisely, and on the other hand for fitting the model to data of lower thicknesses (~ bellow 200nm), better

results are acquired with A unfixed (see Fig. 34 - 35). Again, the detected ranges of B and d were the same as set before the analysis.

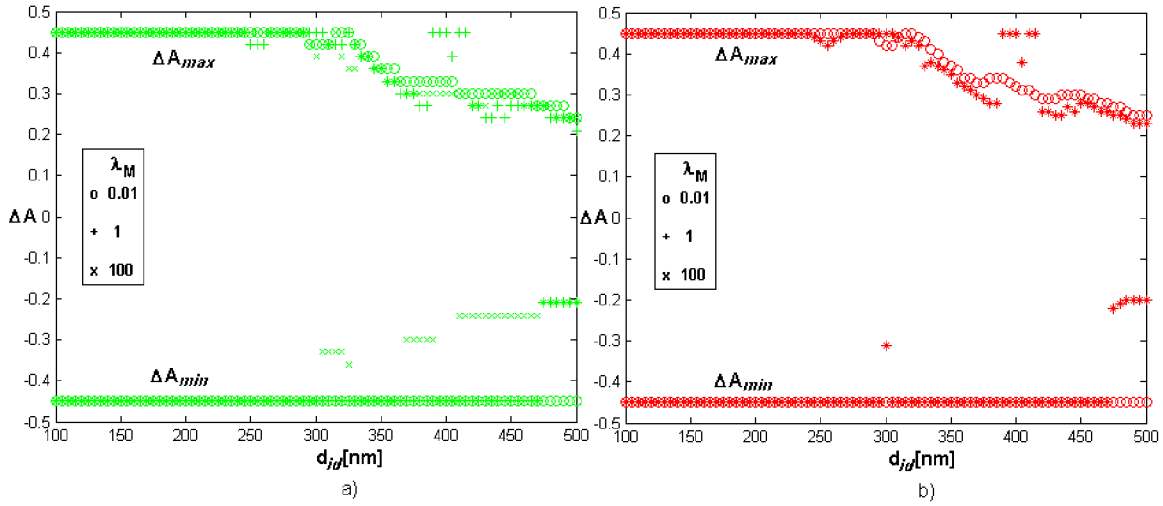

Figure 34: The detected ΔA_{min} and ΔA_{max} of the simulated PMMA film when the : a) coefficients were unfixed, b) the coefficient B was fixed.

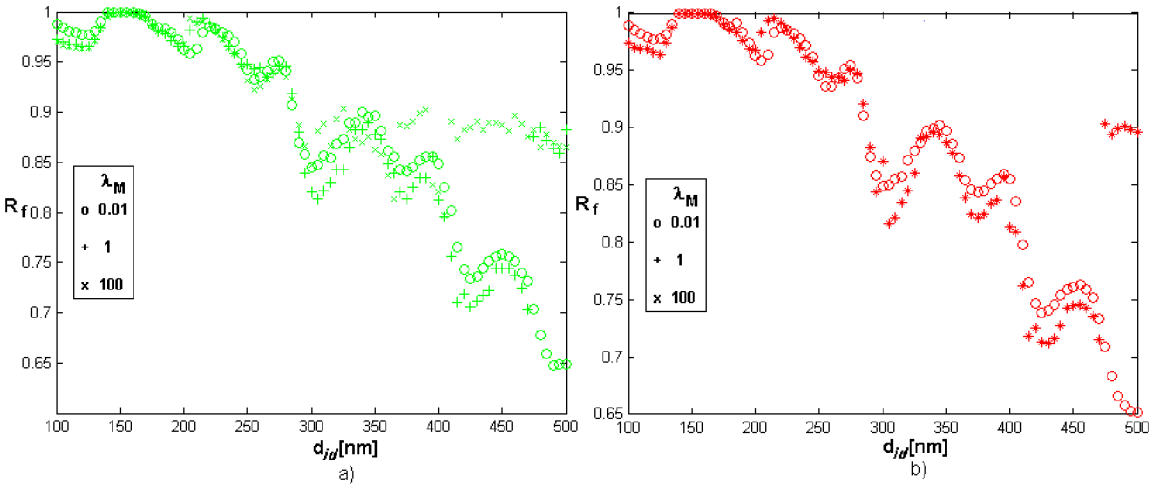

Figure 35: The detected $\mathbf{R_f}$ of the simulated PMMA film when the : a) coefficients were unfixed, b) the coefficient B was fixed.

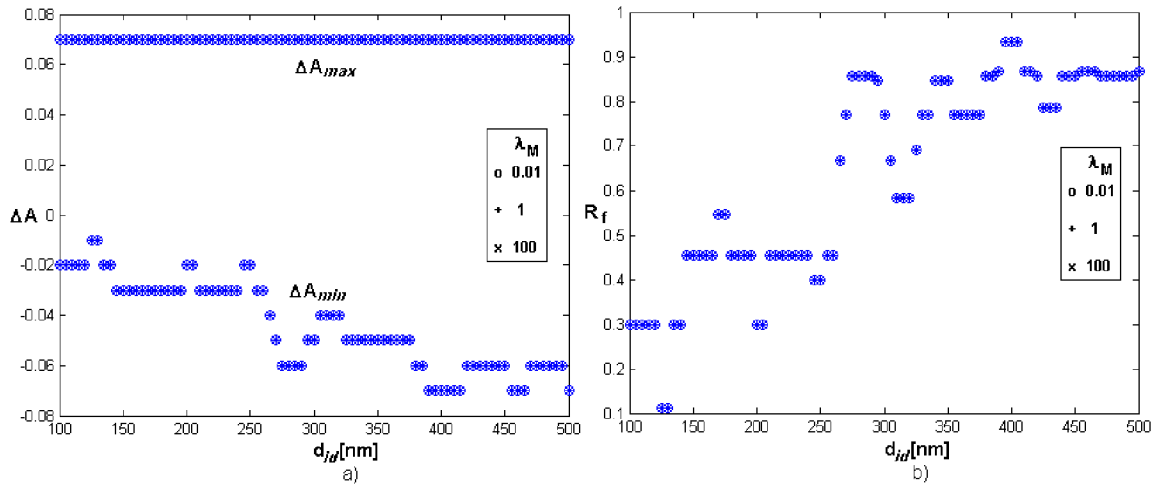

Figure 36: The detected ΔA_{min}, ΔA_{max} and $\mathbf{R_f}$ of the simulated PMMA film when the A was fixed.

And finally, the analysis of the Si_3N_4 (see Fig. 37 - 39) that was carried out within the following ranges of coefficients: $(1.55, 9000, 100) - (2.45, 21000, 500)$ when all coefficients were unfixed, $(1.55, 12000, 100) - (2.45, 18000, 500)$ when B was fixed and $(1.93, 9000, 100) - (2.07, 21000, 500)$ when A was fixed, showed that the model with unfixed A is more convenient for films of lower thicknesses (~ above 150nm) (see Fig. 37 - 38) and the model with fixed A could be used for films of any thicknesses from the analyzed range (see Fig. 39), if the A were reasonably precise. And again, the detected ranges of B and d were the same as set before the analysis.

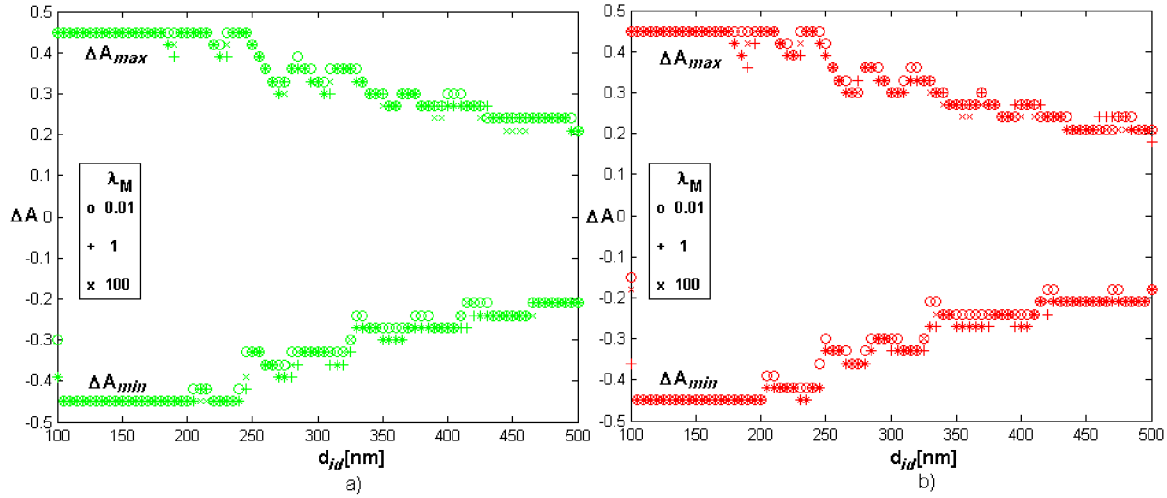

Figure 37: The detected ΔA_{min} and ΔA_{max} of the simulated Si_3N_4 film when the : a) coefficients were unfixed, b) the coefficient B was fixed.

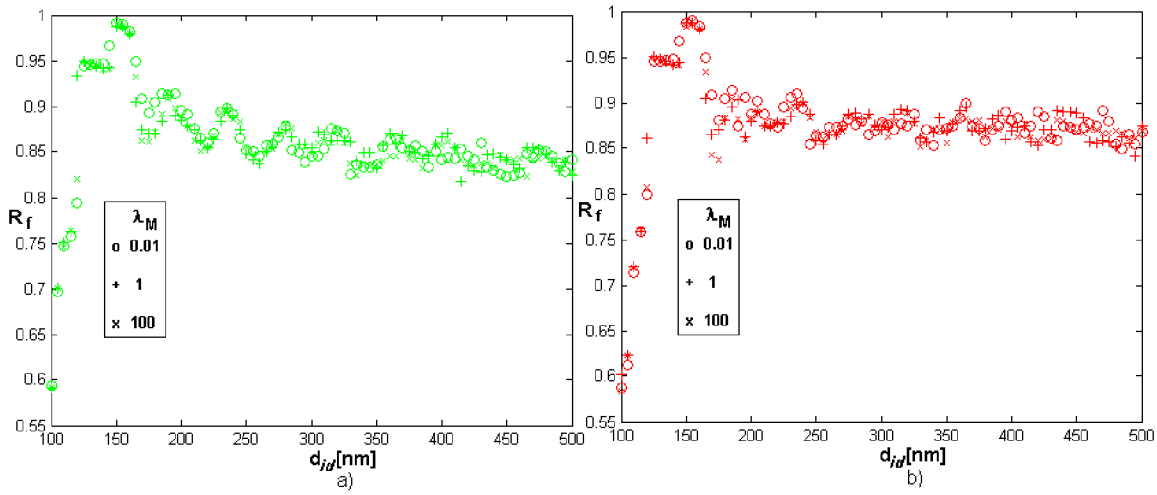

Figure 38: The detected $\mathbf{R_f}$ of the simulated Si_3N_4 film when the : a) coefficients were unfixed, b) the coefficient B was fixed.

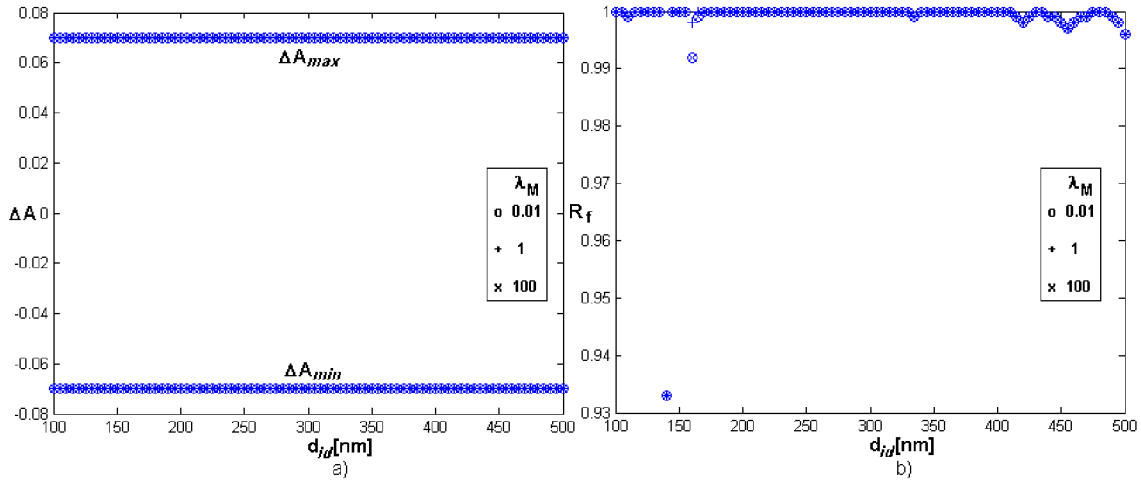

Figure 39: The detected ΔA_{min}, ΔA_{max} and $\mathbf{R_f}$ of the simulated Si_3N_4 film when the A was fixed.

Based on the results of the analysis, the fitting of the films of higher thicknesses requires most of all a reasonably precise setting of A with recommendation to fix this value. And on the other hand, the fitting the model to data of films of lower thicknesses might be better when the A is unfixed.

So knowing A very close to the A_{id} generally does not have to mean to acquire model fitting precise enough. It should be reminded that this conclusion is based on an assumption that the measured data exactly follow the chosen dispersion and reflectance models and any distortion was not implemented into the simulated reflectance spectra.

The fluctuation of B_{id} actually causes an error of $\tilde{N}$ that is up to 2 orders lower than the error caused by fluctuations of A, therefore, the results of sensitivity analysis when all coefficients were unfixed and when the B was fixed are very similar. If the fixing of coefficients is demanded it is recommended to fix rather the A than d because the refractive index is expected to be constant over the measured sample whereas the morphology may be variable.

To analyze the quality of the fitting when the data follows a different model (especially the dispersion model) than the fitted one or when the data is distort (somehow to simulate the real measurement with possible errors), it could be a matter of another research.

Note: *Examples of the projections* $\mathbf{B^p}$ *of chosen* SiO_2, Si_3N_4 *and PMMA simulated films are depicted in Fig. 44 - 55 in the Figure annex.*

6 Conclusion

A new method of thin films optical properties measurements has been presented and tested on the experimental data. The method grants the optical properties being fast calculated because of the advanced processing of the images. Therefore, the thin film can be treated as any of various materials and the optical properties can be quickly recalculated with changed settings.

The options of presented calculations also enable to measure only chosen characteristics, while the other remain fixed where such option can avoid the mutual correlations among the chosen characteristics and hence the measurement can be more precise.

This method was successfully tested on ex situ measurements of coated silicon substrates. New approach has been introduced in sensitivity analysis by defining a tool that figures out and hence verifies the reliability of calculated results.

The reliability of the acquired results was calculated at three chosen materials: the SiO_2, Si_3N_4 and the PMMA, that can be considered as representatives of the low to high refractive index materials and the simulated films of these materials were assumed as deposited on a silicon substrate.

The simulated reflectance spectra were considered as following exactly the chosen model and the reliability of the acquired results was calculated within a reasonably large range of initial settings. It was concluded which setting of the global parameters of the optimizing method and which setting of the regression coefficients in the matter of their fixing or precision could lead to acquire very precise and high reliability results, if the data followed the chosen regression model. The setting of the initial regression coefficients appeared to be crucial in the setting of the refractive index coefficients, primarily the coefficient A and its option to be fixed or unfixed. The other coefficients could be set more liberally. Most of all, the settings differed in measuring thinner (~200nm) and thicker (~400nm) films.

References

[1] Tompkins, H., G., McGahan, W., A., *Spectroscopic ellipsometry and reflectometry: a user's guide.* John Wiley & Sons, New York, 1999,pp. 54 - 61.

[2] Urbánek, M., Spousta, J., Běhounek, T., Šikola, T., Imaging Reflectometry In situ, *Applied Optics*, 46 (25) (2007), pp. 6309 - 6313.

[3] Urbánek, M., Spousta, J., Navrátil, K., Fiedor, M., Chmelík, R., Buček, M., Šikola, T., *Instrument of Thin Films Diagnostics by UV Spectroscopic Reflectometry*, Poster presentation at ECASIA 03, Berlin, October 2003, Book of Abstracts, pp. 89.

[4] Edwards, D., F., Silicon (Si), In Palik (ed.), E., D., *Handbook of Optical Constants of Solids*, Academic Press, New York, 1991, pp. 547 - 569.

[5] Marquardt, W., D., An algorithm for least squares estimation of nonlinear parameters, J. Soc. Ind. *Appl. Math.* 11, 1963, pp. 431 - 441.

[6] Fletcher, R., *Practical methods of optimization*, John Wiley & Sons Ltd., Chichester, 1993.

[7] Born M., Wolf, E., *Principles of Optics*, (7^{th} ed.), Cambridge University Press, 1999.

[8] Vašíček, A., *Optika tenkých vrstev,* ČSAV, pp. 182 - 186.

[9] Furman, Sh., A., Tikhonravov, A., V., *Basics of Optics Multilayer Systems*, Edition Frontiers, Gif - sur Yvette, 1992, pp. 21.

[10] Seber, G., A., F., Wild, C., J., *Nonlinear regression*, John Wiley & Sons Inc., Hoboken, 2003.

[11] Anděl, J., *Statistické metody*, Matfyzpress, Praha 1993.

[12] Dowdy, S., Wearden, S., *Statistics for research*, John Wiley & Sons Ltd., Toronto, 1983, pp. 176 - 179.

[13] Celý, J., *Programové moduly pro fyzikální výpočty*, rektorát UJEP, Brno 1985, pp. 18 - 80.

[14] Martišek, D., *Matematické principy grafických systémů*, Litera, Brno 2002.

[15] Běhounek, T., *Vícerozměrné filtry a jejich použití*, diplomová práce, Ústav Matematiky FSI VUT v Brně, Brno 2004.

[16] Jaroslavskij, J., Bajla, I., *Metódy a systémy číslicového spracovania obrazov*, Alpha, Bratislava 1989, pp. 526.

7 Symbol list

A	refractive index coefficient
A_{id}	ideal value of A
A_R	absolute reflectance of a reference
A_S	absolute reflectance of a sample
ΔA_{min}, ΔA_{max}	lower and upper detected deviances of A_{id} respectively
$\mathbf{b}$	vector of the calculated regression coefficients
B	blue component of color
B	refractive index coefficient
B_{id}	ideal value of B
ΔB_{min}, ΔB_{max}	lower and upper detected deviances of B_{id} respectively
$\mathbf{B}$	set of initial approximations
$\mathbf{B^I}$	region of interest (sensitivity analysis)
$\mathbf{B^p}$	projection of the $\mathbf{B}$
$\mathbf{B^p_s}$	selection of the $\mathbf{B^p}$
$\mathbf{C}$	reference point of mapping
$\mathbf{C}(\mathbf{x})$	convolution function,
$\mathbf{C}(m,n)$	$m \times n$ 2D convolution matrix
C_{max}	maximal color
C_{min}	minimal color
$\mathbf{C}(\mathbf{t})$	nD convolution matrix
d	thickness of the film
d_{id}	ideal value of d
D	additive constant of linear filter
D_k	equidistant partitioning
$\mathbf{D}^{(n)}$	equidistant multipartitioning
$\mathcal{D}^{(n)}$	nD digital space
$\mathrm{D}^{(n)}$	global coordinate system of digital space
Δd_{min}, Δd_{max}	lower and upper detected deviances of d_{id} respectively
$\mathbf{D}$	diagonal matrix induced by Jacobi's matrix
E	multiplicative constant of linear filter
E_{M}	extension of the searched region
$f(\mathbf{X}, \vartheta)$	regression function
$2f_{max}$	minimal sampling frequency - Nyquist's limit
F	tested statistics, critical value of the F - distribution
$\mathbf{F}(\vartheta)$	Jacobi's matrix
$\mathbf{F}^{(n)}$	physical domain

$\mathcal{F}^{(n)}$	fragmentation of digital space support
$\mathsf{F}^{(n)}$	physical space
$\mathrm{F}^{(n)}$	global coordinate system of physical space
$\mathbf{F}_{ij}$	physical pixel
G	green component of color
$g(\mathbf{x})$	sampling function
H	image height
I	image
$I_{\vartheta_r^*}$	confidence interval of the regression coefficient ϑ_r
I_B, I_N	intensity of the light reflected from the background and the intensity of the black background considered as noise respectively
I_R, I_S	intensities of light reflected from reference and sample respectively
I_k	a set of indices
$\mathbf{I}^{(n)}$	multiindex
$\mathbf{I}$	elementary matrix
$\mathbf{J}^{(n)}$	nD space support
k	extinction coefficient, index of a matrix/vector element[11]
k_{max}	maximum of iterations
$\mathcal{L}_{\mathbf{c}}^{(n)}$	logical space
$\mathrm{L}^{(n)}$	global coordinate system of logical space
L_B	lower bound of the optimizing algorithm decision factor
m	matrix/vector element index, matrix/vector dimension[11]
M_j	characteristic matrix of the j - th layer
$\mathbf{M}$	characteristic matrix of the complete multilayer
$\tilde{N}$	complex refractive index
n	refractive index, the real part, matrix/vector dimension[11]
n_a	ambient refractive index
p	vector index
$p(\vartheta_{\mathbf{0}}^{\mathbf{P}})$	relative frequency of convergence of the $\vartheta_{\mathbf{0}}^{\mathbf{P}}$
q	vector index
q_a, q_j, q_s	substitutions
Δq	predicted reduction in the optimization step
r_{12}	Fresnel coefficient of reflection

[11] The symbols subjected to the different meanings are used separately, each in different section, so the misunderstanding in their explanation is avoided.

r	total reflection coefficient, index[11]
$\mathbf{r}$	vector of residuals,
	resolution of digital space[11]
$\mathrm{r_M}$	decision factor of the optimizing algorithm
R_M	reduction of the searched region
$\mathbf{R_f}$	reliability factor
$\mathcal{R}$	reflectance of the film
R	blue component of color
R	image
R_z	image R displaced about z pixels
	according to its initial position
R^P	perfect image
R^S	image representing an additive noise
s_p^2, s_p^2	residual variances
$\mathbf{S}$	control point - center
$S(\vartheta)$	objective function - the residual sum of squares (RSS)
ΔS	actual reduction in the optimization step
t	critical value of the Student's distribution
U_B	upper bound of the optimizing algorithm decision factor
v_i^k	$k-tuple$ dimension of physical nD domain
$\mathbf{V}$	control point - vertex
V	value set (definition of an image)
W	image width
$\mathbf{x}$	vector of realized measurements settings
X	random variable
$\mathbf{X}$	vector of independent random variables
Y	random variable
$\mathbf{y}$	vector of realizations of the random variable Y
β	phase shift between the top and the bottom of the layer
$\gamma(\vartheta_\mathbf{0})$	local extreme decision function
δ, δ_M	vectors of the regression coefficients increments
ε	random error
ϵ	satisfactory limit of the RSS
φ_1, φ_2, φ_3	angles of light propagation in different ambiances
φ_a, φ_s	angles of light propagation in the ambient
	and substrate respectively
$\varphi(\vartheta_\mathbf{0})$	convergence decision function
$\varphi_\mathbf{c}$	mapping

λ	wavelength
λ_{M}	factor of the optimizing algorithm
Λ	local extreme satisfactory limit of the λ_{M}
μ, ν	tolerances of the solution
ϑ	vector of regression coefficients
$\vartheta_{\mathbf{0}}$	initial approximation vector of the regression coefficients
$\vartheta_{\mathbf{0}}^{\mathbf{P}}$	initial approximations vector with reduced dimension by meaning of the projection
ϑ^*	ideal solution
$\hat{\vartheta}$	estimator of ϑ
$\rho(R^P, R^S)$	correlation coefficient of images R^P and R^S
σ^2	variance
$\hat{\sigma}^2$	estimator of the variance
Ω	covariance matrix
$\hat{\Omega}$	estimator of the covariance matrix
$\psi(\vartheta_{\mathbf{0}})$	function combining the convergence and local extreme decision functions

8 Figure annex

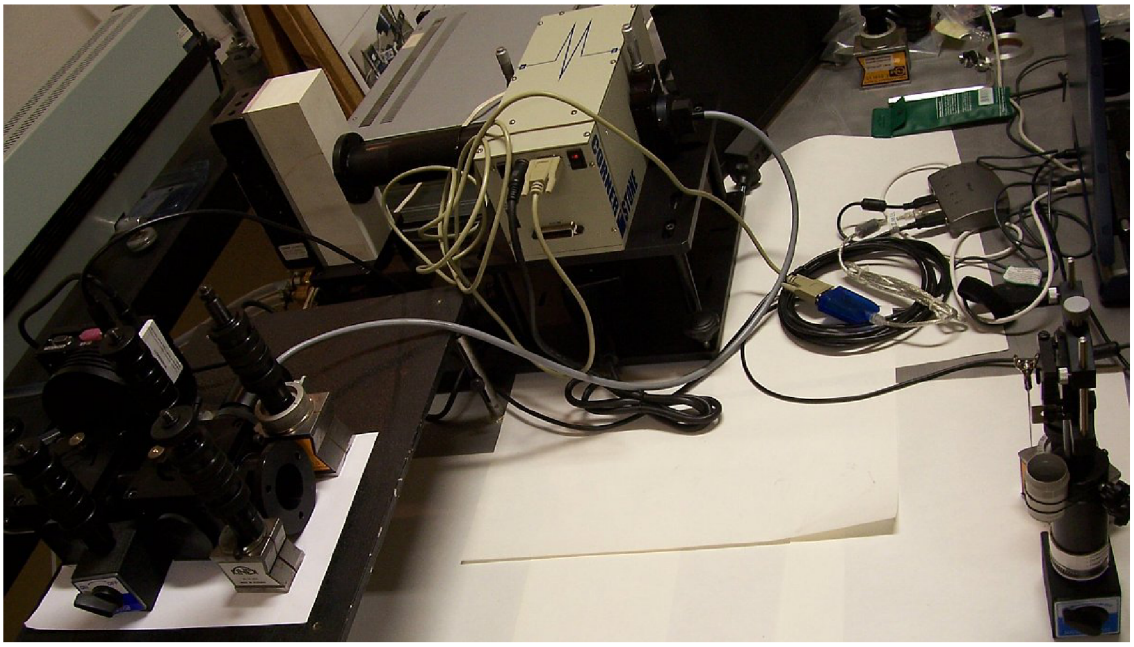

Figure 40: The measuring assembly with a sample holder (in the bottom right corner) that was used for etching the sample.

```
Statistical model sensitivity testing ---- initial parameters

Example
 following vectors
  b_real=[1.52, 5000, 100]
  b_lower_bound=[1.45, 3000, 80]
  b_upper_bound=[1.59, 7000, 120]
  b_delta=[0.05, 200, 5]
  b_lower_tolerance=[15, 5, 5]
  b_upper_tolerance=[3, 6, 8]
 should be written as follows:
1.52
5000
100
1.45
3000
80
1.59
7000
120
0.05
200
5
15
5
5
3
6
8

>>>>>> Begin Parameters <<<<<<
2.0
15000
100
1.55
12000
70
2.45
18000
130
0.03
200
2
0.07
3000
1
0.07
3000
1
>>>>>> End Parameters <<<<<<
```

Figure 41: An input protocol where the set of initial approximations $\mathbf{B}$ and the tolerances of the ideal solution are set.

```
Characteristics of the measurement
The results are classified into following groups:
1 - Other local extreme
2 - Global minimum
3 - Non convergent solution, not extreme
4 - Convergent solution, not extreme
Height: 31
Width:  31
Levels:  31
Type of projection:  d
Frequencies:
>>>>>>> Begin Data <<<<<<<
17,16,16,17,17,17,16,17,17,17,17,17,17,17,17,17,17,17,16,16,16,16,16,16,16,16,16,
16,16,16,16
16,16,16,16,16,16,16,16,16,16,16,16,16,16,16,15,15,15,15,15,16,16,16,16,16,16,16,
15,16,16,16
16,16,16,16,16,16,16,16,16,16,16,16,16,16,16,16,16,16,16,16,17,17,17,17,17,17,17,
17,17,17,17
                        ...
18,18,18,18,18,18,17,18,18,18,18,17,17,17,17,17,17,17,17,17,18,18,18,18,18,18,18,
18,19,19,19
18,18,18,18,18,18,18,18,18,18,18,17,17,17,17,17,17,17,17,17,18,18,18,18,18,18,18,
19,19,19,19
>>>>>>> End Data 1 <<<<<<< Classifications
1,1,1,1,1,1,1,1,1,1,1,1,1,1,1,1,1,1,1,1,1,1,1,1,1,1,1,1,1,1,1
1,1,1,1,1,1,1,1,1,1,1,1,1,1,2,1,1,1,1,1,2,2,2,2,2,2,2,1,2,2,2
2,2,2,2,2,2,2,2,2,2,2,2,2,2,2,2,2,2,2,2,2,2,2,2,2,2,2,2,2,2,2
                        ...
2,2,2,2,2,2,2,2,2,2,2,2,2,2,2,2,2,2,2,2,2,2,2,2,2,2,2,2,2,2,2
2,2,2,2,2,2,2,2,2,2,2,2,2,2,2,2,2,2,2,2,2,2,2,2,2,2,2,2,2,2,2
2,2,2,2,2,2,2,2,2,2,2,2,2,2,2,2,2,2,2,2,2,2,2,2,2,2,2,2,2,2,2
>>>>>>> End Data 2 <<<<<<<
```

Figure 42: The modal characteristics summarized in the output protocol. The frequencies are depicted in the top data set and the types of the most frequently acquired results are depicted in the bottom data set.

```
Output Image properties & range of parameters
Probability threshold: 0.95
Local extreme consideration LM limit: 1
Height: 31
Width:  31
Levels:  31
Excluding parameter type: d
Excluded levels: 0 ( 0.00%)
Excluded levels - list: [ ]
Remained levels: min max: 70.000 130.000
Range:
  b0: [ 1.5500, 12000.0000, 70.0000 ]
  b1: [ 2.4500, 18000.0000, 130.0000 ]
  step: [ 0.0300, 200.0000, 2.0000 ]
  real solution: [ 2.0000, 15000.0000, 100.0000 ]
Tolerances:
  min tol: [ 1.9300, 12000.0000, 99.0000 ]
  max tol: [ 2.0700, 18000.0000, 101.0000 ]
>>>>>>> Begin Data <<<<<<<
0.452,0.452,0.452,0.452,0.452,0.452,0.452,0.452,0.452,0.452,0.452,0.452,0.452,0.4
52,0.452,0.452,0.452,0.452,0.484,0.484,0.484,0.484,0.484,0.484,0.484,0.484,0.484,
0.484,0.484,0.484,0.484
0.484,0.484,0.484,0.484,0.484,0.484,0.484,0.484,0.484,0.484,0.484,0.484,0.484,0.4
84,0.516,0.516,0.516,0.516,0.516,0.516,0.516,0.516,0.516,0.516,0.516,0.516,0.516,
0.516,0.516,0.516,0.516
0.516,0.516,0.516,0.516,0.516,0.516,0.516,0.516,0.516,0.516,0.516,0.548,0.548,0.5
48,0.548,0.548,0.548,0.548,0.548,0.548,0.548,0.548,0.548,0.548,0.548,0.548,0.548,
0.548,0.548,0.548,0.548
0.548,0.548,0.548,0.548,0.548,0.548,0.548,0.548,0.548,0.581,0.581,0.581,0.581,0.5
81,0.581,0.581,0.581,0.581,0.581,0.581,0.581,0.581,0.581,0.581,0.581,0.581,0.581,
0.581,0.581,0.581,0.581

         ...

0.581,0.613,0.613,0.613
0.581,0.581,0.581,0.581,0.581,0.581,0.581,0.581,0.581,0.581,0.581,0.581,0.581,0.5
81,0.581,0.581,0.581,0.581,0.581,0.581,0.581,0.581,0.581,0.581,0.581,0.581,0.581,
0.581,0.613,0.613,0.613
0.581,0.581,0.581,0.581,0.581,0.581,0.581,0.581,0.581,0.581,0.581,0.581,0.581,0.5
81,0.581,0.581,0.581,0.581,0.581,0.581,0.581,0.581,0.581,0.581,0.581,0.581,0.581,
0.581,0.613,0.613,0.613
0.581,0.581,0.581,0.581,0.581,0.581,0.581,0.581,0.581,0.581,0.581,0.581,0.581,0.5
81,0.581,0.581,0.581,0.581,0.581,0.581,0.581,0.581,0.581,0.581,0.581,0.581,0.581,
0.613,0.613,0.613,0.613
>>>>>>> End Data <<<<<<<
```

Figure 43: The frequent characteristics summarized in the output protocol.

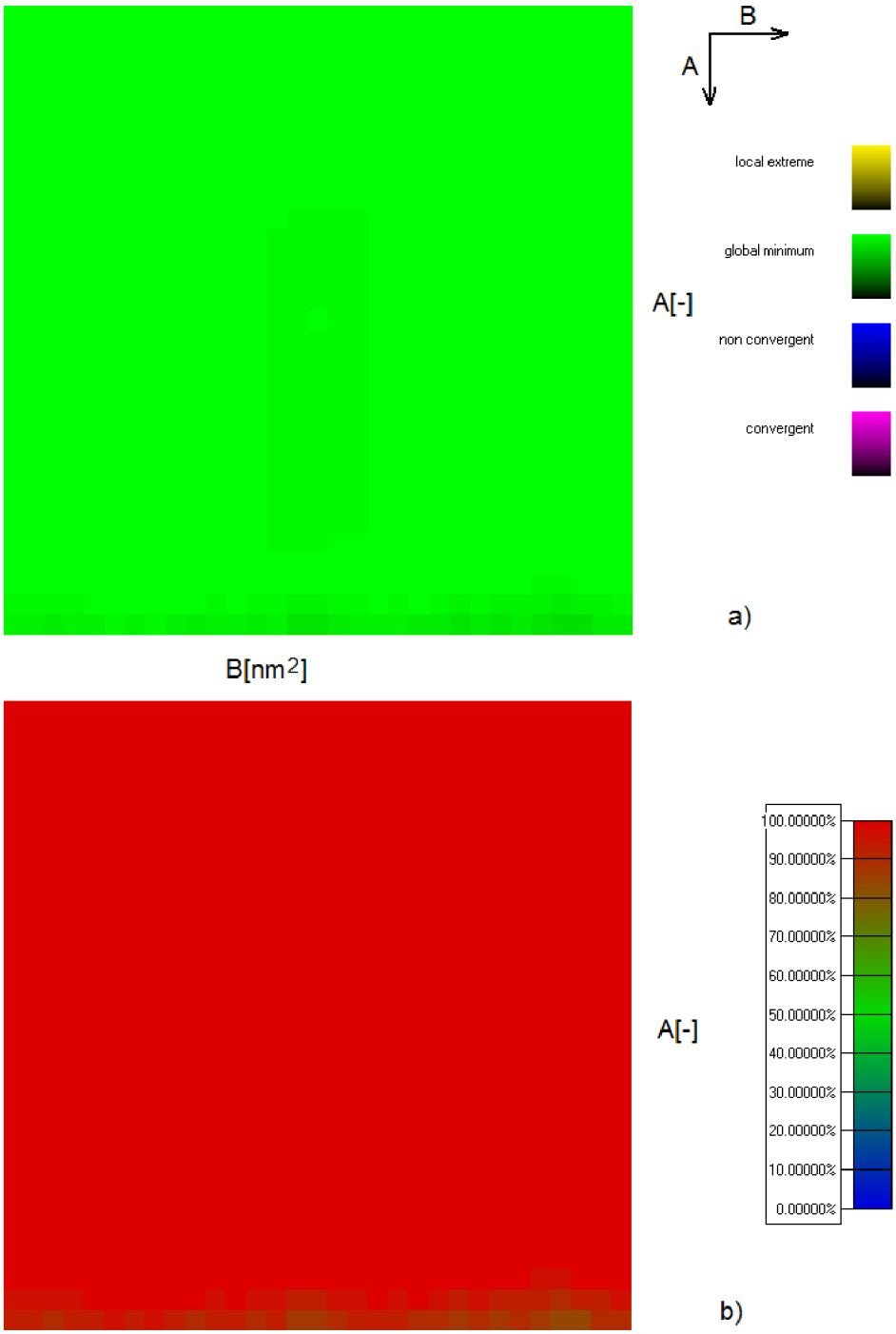

Figure 44: An example of $\mathbf{B^p}$ of 150nm thick SiO_2 film on silicon substrate when all coefficients were unfixed and where the thickness d was omitted.
a) The modal characteristics shows what type of the result (see the legend) was acquired most often. The lighter is the color, the higher is the frequency of the acquired result.
b) The frequency characteristics expresses the rate of acquired global minims to all types of results at each particular setting, i.e. at each setting of A and B regardless on the thickness d.
The example shows that global minimum was the most frequent acquired result within the whole chosen set of initial approximations $\mathbf{B}$.

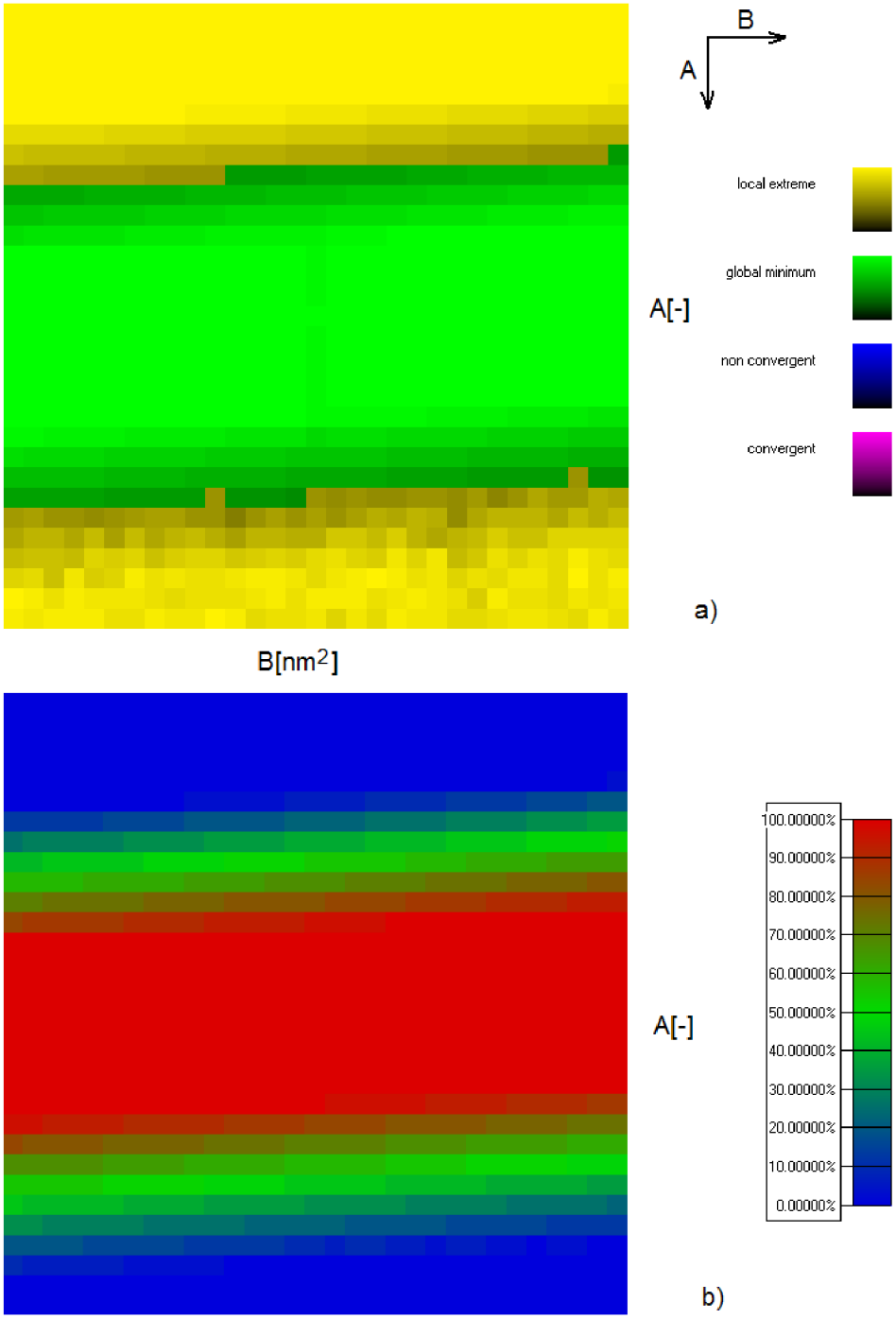

Figure 45: An example of $\mathbf{B^p}$ of 460nm thick SiO_2 film on silicon substrate when all coefficients were unfixed and where the thickness d was omitted.
a) The modal characteristics shows what type of the result (see the legend) was acquired most often. The lighter is the color, the higher is the frequency of the acquired result.
b) The frequency characteristics expresses the rate of acquired global minims to all types of results at each particular setting, i.e. at each setting of A and B regardless on the thickness d.
The region where mostly the global minimum was acquired is narrower in comparison to the detected region in Fig. 44.

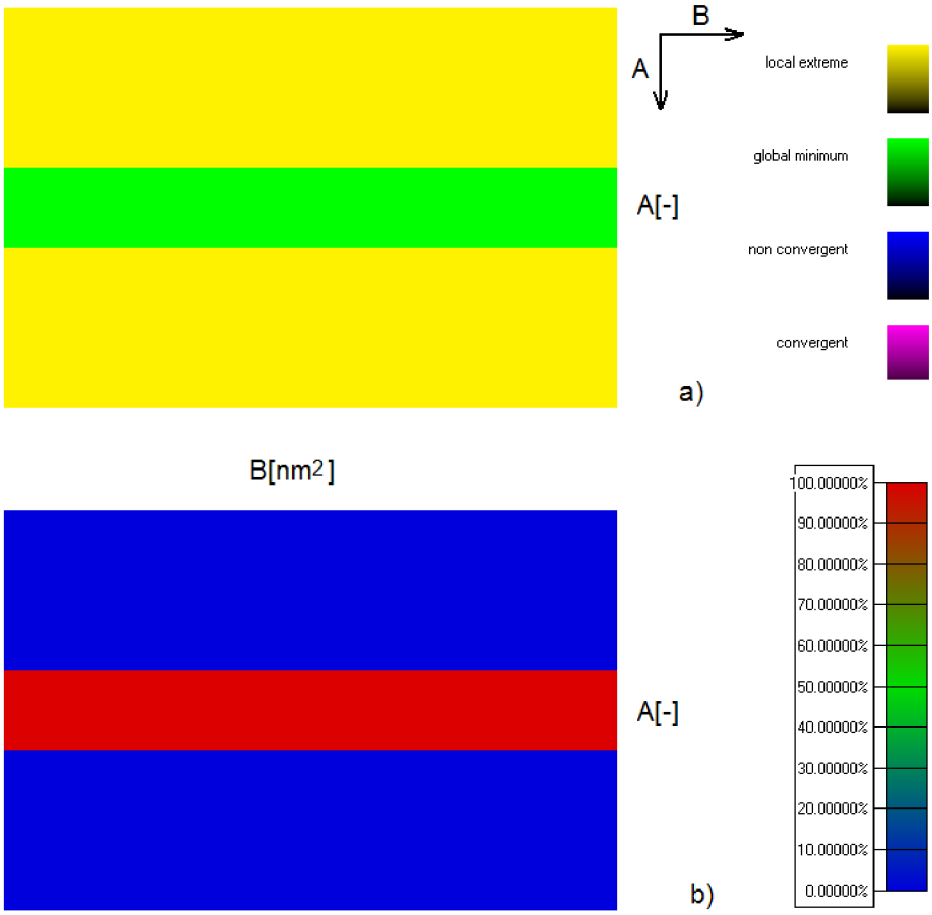

Figure 46: An example of $\mathbf{B^P}$ of 100nm thick SiO_2 film on silicon substrate when the coefficient A was fixed and where the thickness d was omitted.
a) The modal characteristics shows what type of the result (see the legend) was acquired most often. The lighter is the color, the higher is the frequency of the acquired result.
b) The frequency characteristics expresses the rate of acquired global minims to all types of results at each particular setting, i.e. at each setting of A and B regardless on the thickness d.
The detected range of A is very narrow and hence estimating the optical properties of such film with fixed A could be very difficult.

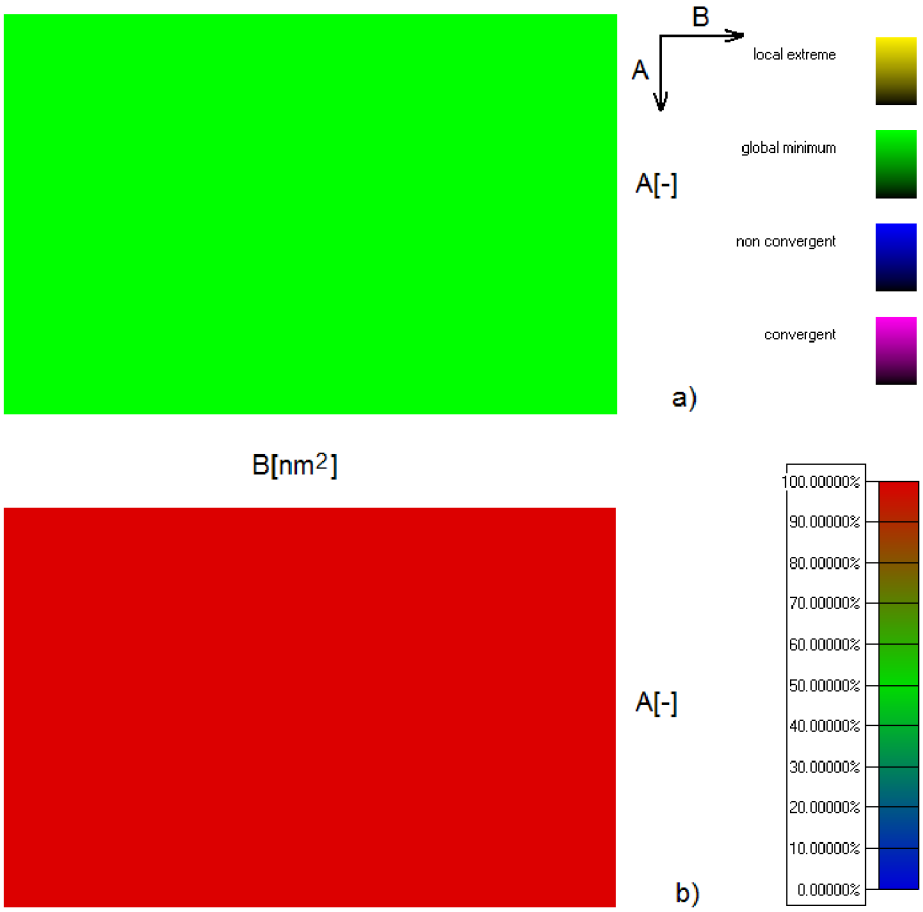

Figure 47: An example of $\mathbf{B^p}$ of 460nm thick SiO_2 film on silicon substrate when the coefficient A was fixed and where the thickness d was omitted.
a) The modal characteristics shows what type of the result (see the legend) was acquired most often. The lighter is the color, the higher is the frequency of the acquired result.
b) The frequency characteristics expresses the rate of acquired global minims to all types of results at each particular setting, i.e. at each setting of A and B regardless on the thickness d.
The calculations of the coefficients was successful in each point of measurement because the global minimum was reached from every initial approximation as depicted.

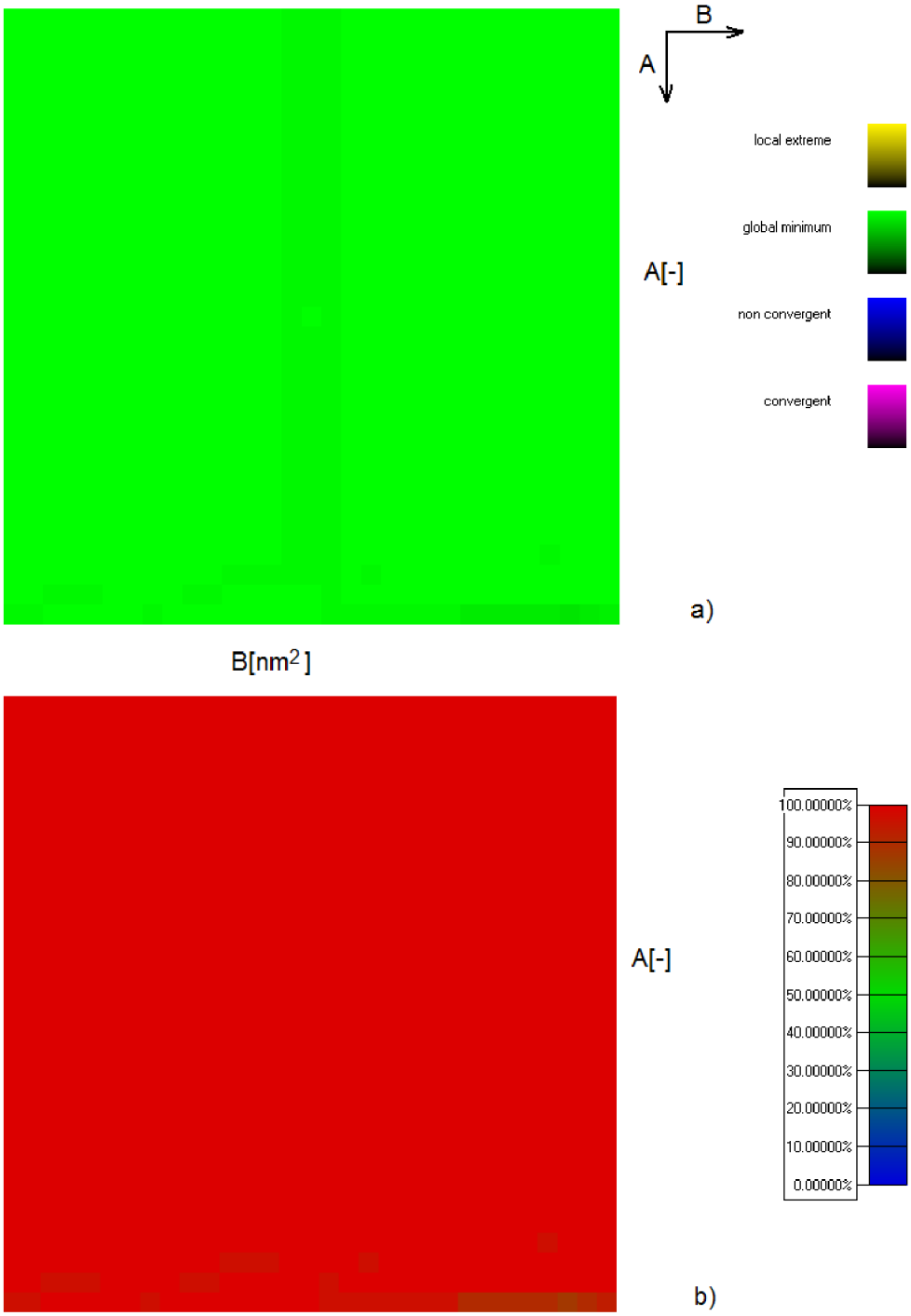

Figure 48: An example of $\mathbf{B^p}$ of 150nm thick PMMA film on silicon substrate when all coefficients were unfixed and where the thickness d was omitted.
a) The modal characteristics shows what type of the result (see the legend) was acquired most often. The lighter is the color, the higher is the frequency of the acquired result.
b) The frequency characteristics expresses the rate of acquired global minims to all types of results at each particular setting, i.e. at each setting of A and B regardless on the thickness d.
Again, an example of highly successful measurement.

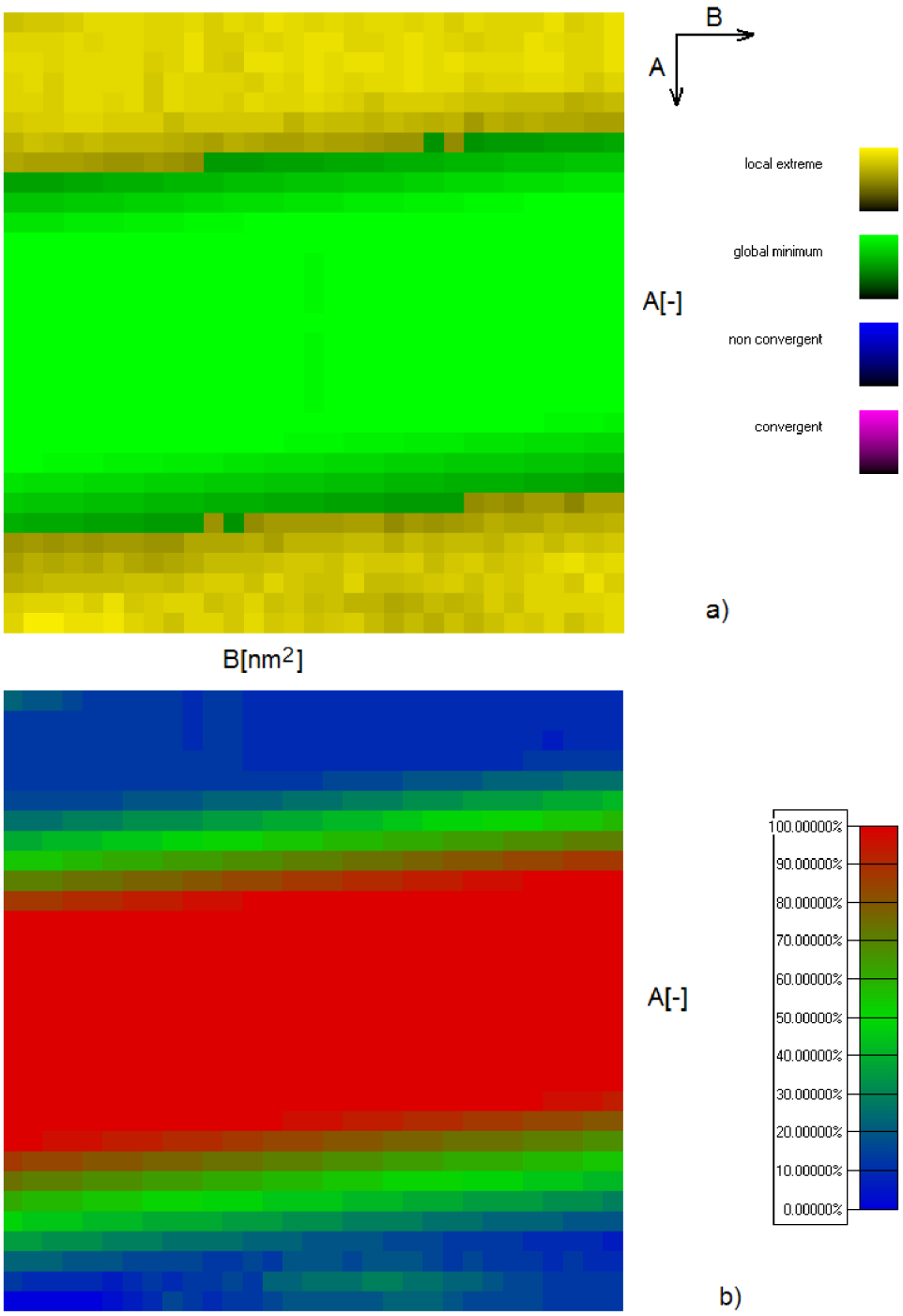

Figure 49: An example of $\mathbf{B^P}$ of 460nm thick PMMA film on silicon substrate when all coefficients were unfixed and where the thickness d was omitted.
a) The modal characteristics shows what type of the result (see the legend) was acquired most often. The lighter is the color, the higher is the frequency of the acquired result.
b) The frequency characteristics expresses the rate of acquired global minims to all types of results at each particular setting, i.e. at each setting of A and B regardless on the thickness d.
An example of analysis that showed that high reliability results can be acquired when the A started from a narrower interval surrounding the A_{id} as depicted in b).

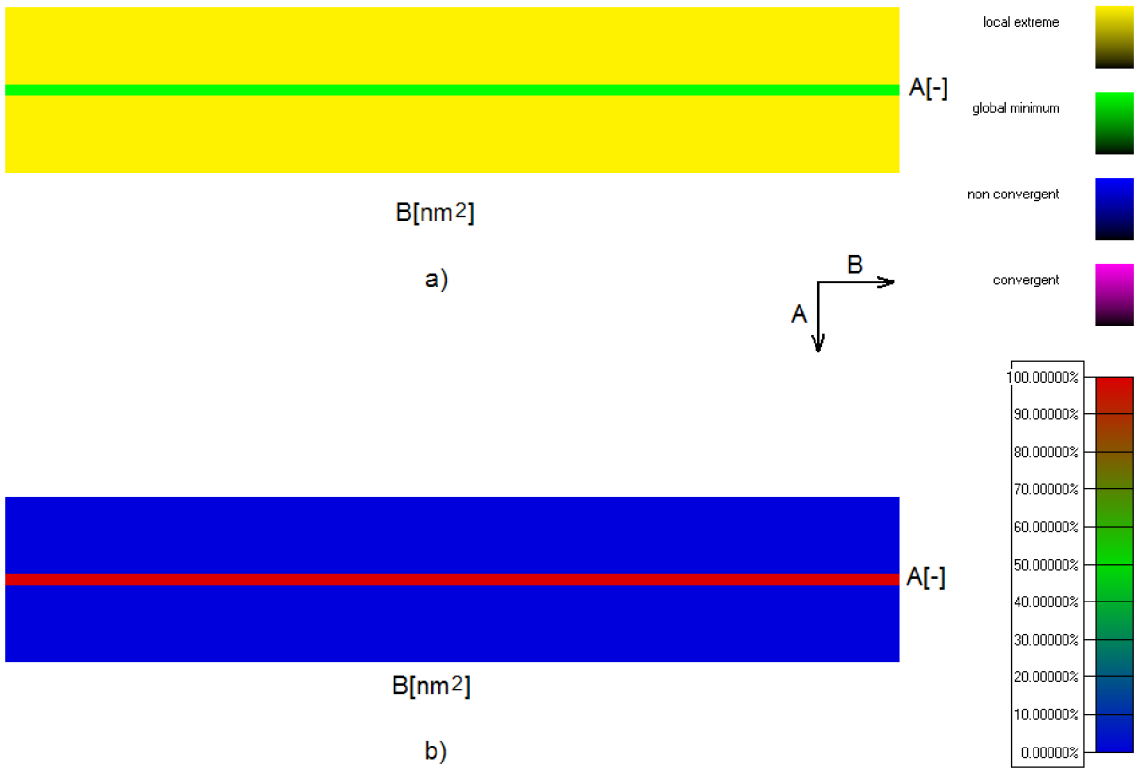

Figure 50: An example of $\mathbf{B^P}$ of 130nm thick PMMA film on silicon substrate when the coefficient A was fixed and where the thickness d was omitted.
a) The modal characteristics shows what type of the result (see the legend) was acquired most often. The lighter is the color, the higher is the frequency of the acquired result.
b) The frequency characteristics expresses the rate of acquired global minims to all types of results at each particular setting, i.e. at each setting of A and B regardless on the thickness d.
It is too difficult to measure optical properties of such film when A is fixed even if it is set very close but not precisely to A_{id}.

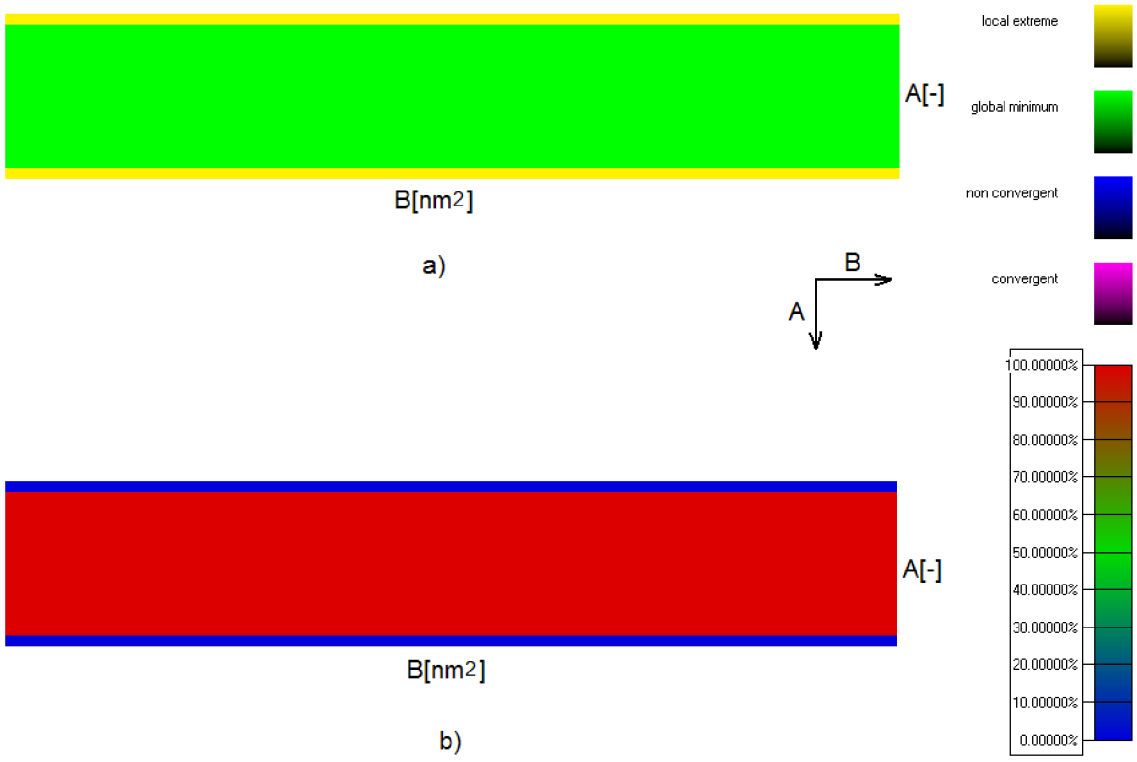

Figure 51: An example of $\mathbf{B^p}$ of 460nm thick PMMA film on silicon substrate when the coefficient A was fixed and where the thickness d was omitted.
a) The modal characteristics shows what type of the result (see the legend) was acquired most often. The lighter is the color, the higher is the frequency of the acquired result.
b) The frequency characteristics expresses the rate of acquired global minims to all types of results at each particular setting, i.e. at each setting of A and B regardless on the thickness d.
The fixed value of A can be set more liberally in order to measure the optical properties precisely in comparison to Fig. 50.

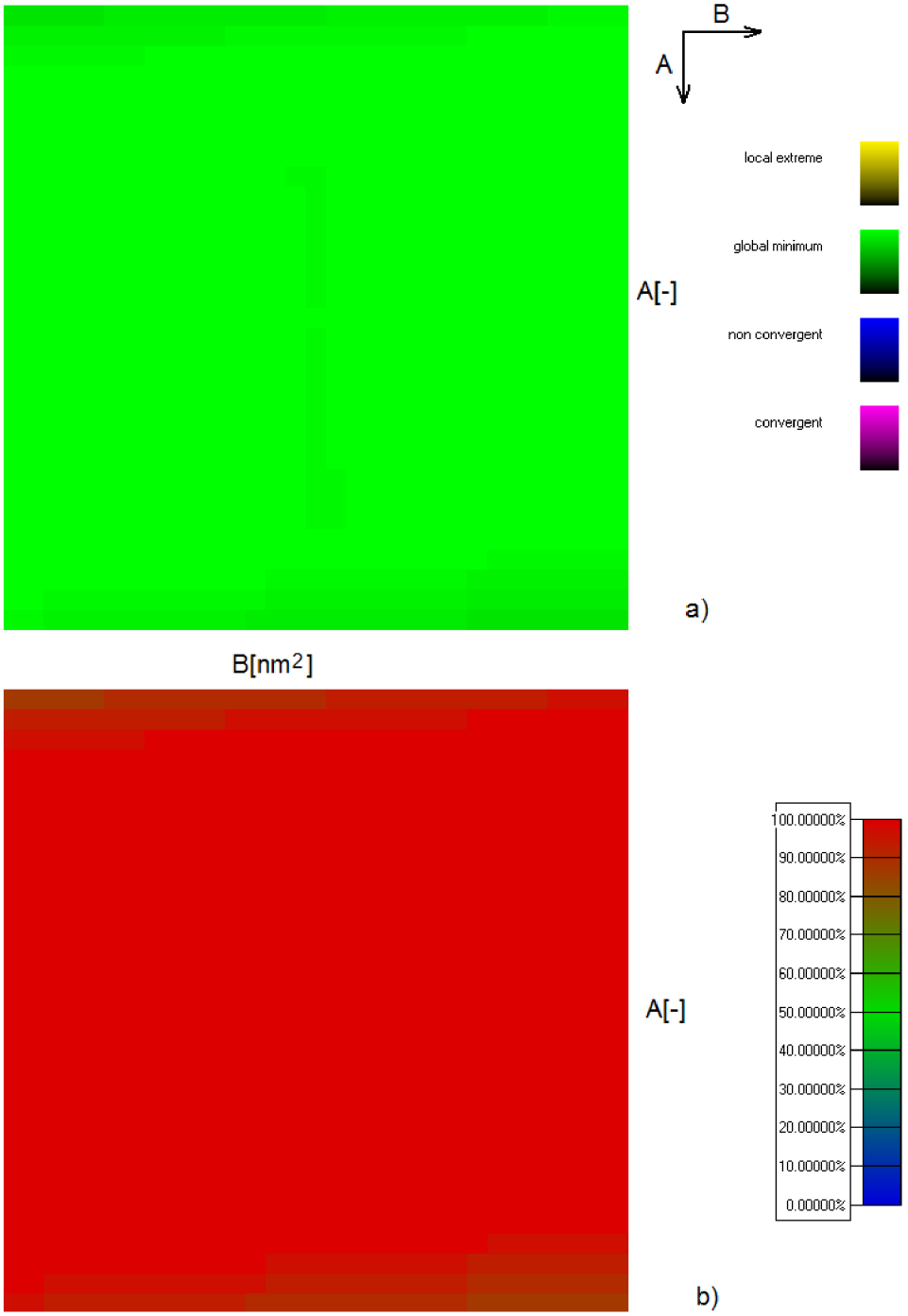

Figure 52: An example of $\mathbf{B^P}$ of 150nm thick Si_3N_4 film on silicon substrate when all coefficients were unfixed and where the thickness d was omitted.

a) The modal characteristics shows what type of the result (see the legend) was acquired most often. The lighter is the color, the higher is the frequency of the acquired result.

b) The frequency characteristics expresses the rate of acquired global minims to all types of results at each particular setting, i.e. at each setting of A and B regardless on the thickness d.

Again, the initial approximation can be set to quite imprecise values and still only the global minimum can be acquired.

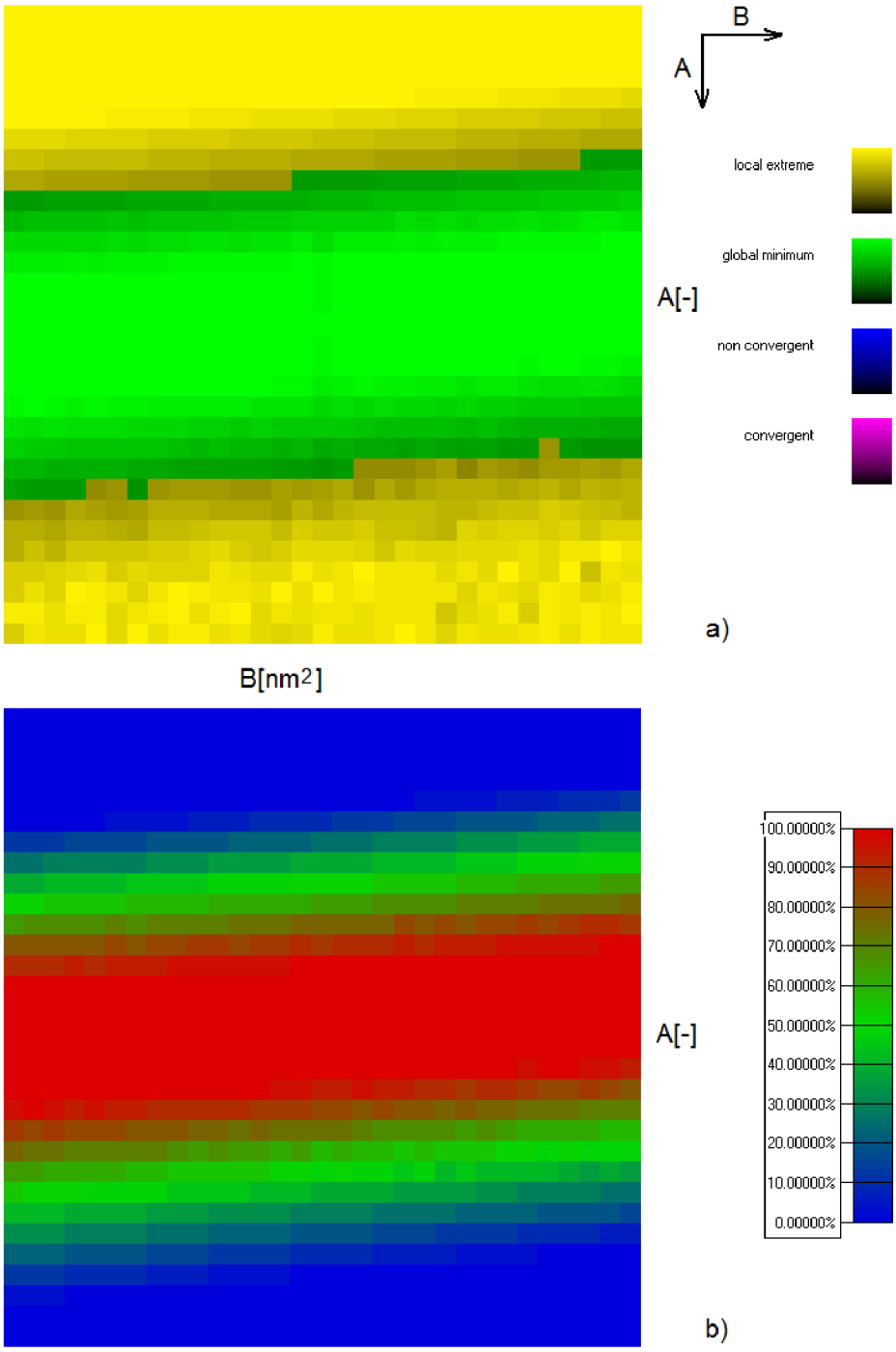

Figure 53: An example of $\mathbf{B^p}$ of 500nm thick Si_3N_4 film on silicon substrate when all coefficients were unfixed and where the thickness d was omitted.
a) The modal characteristics shows what type of the result (see the legend) was acquired most often. The lighter is the color, the higher is the frequency of the acquired result.
b) The frequency characteristics expresses the rate of acquired global minims to all types of results at each particular setting, i.e. at each setting of A and B regardless on the thickness d.
The A has to be known quite precisely to fit successfully the reflectance model to reflectance spectra of 500nm thick Si_3N_4 film deposited on a silicon substrate.

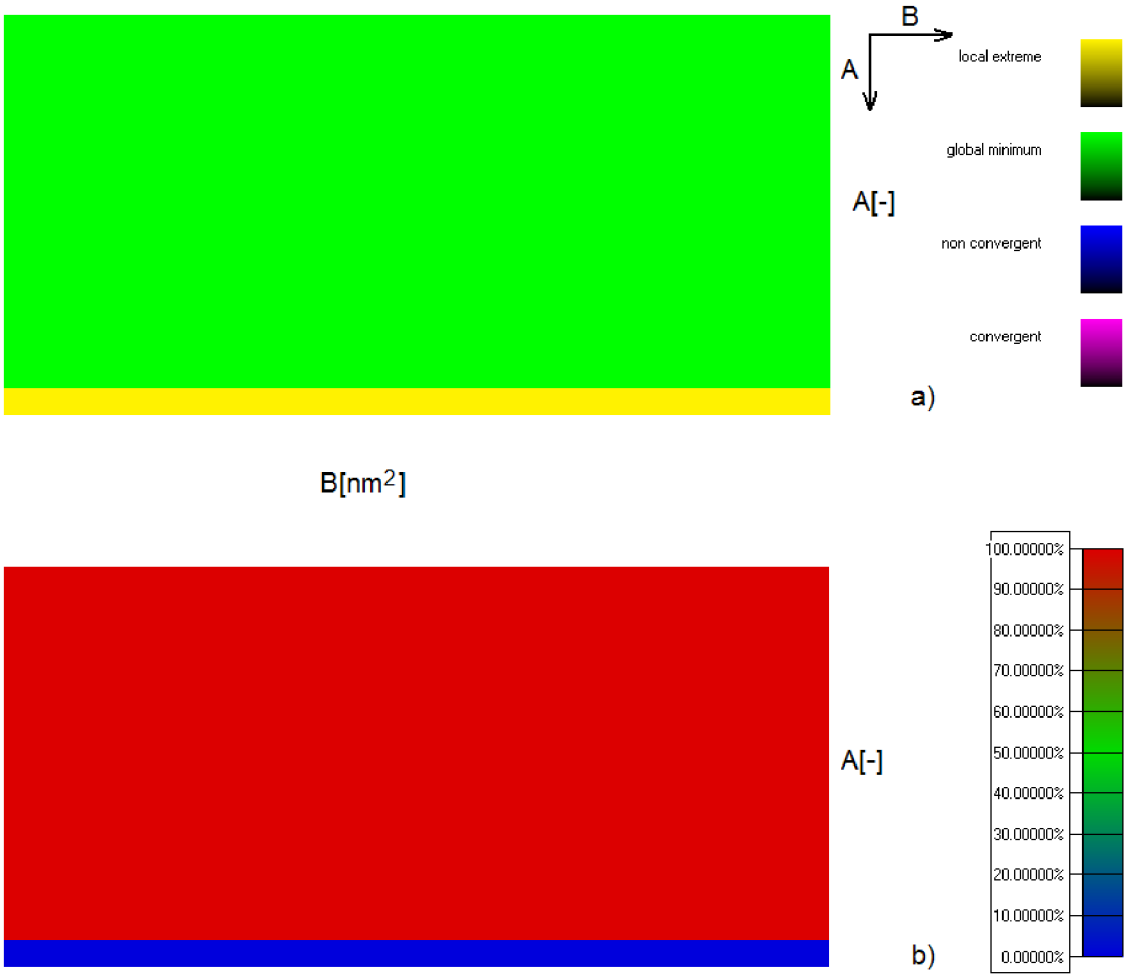

Figure 54: An example of $\mathbf{B^P}$ of 140nm thick Si_3N_4 film on silicon substrate when the coefficient A was fixed and where the thickness d was omitted.
a) The modal characteristics shows what type of the result (see the legend) was acquired most often. The lighter is the color, the higher is the frequency of the acquired result.
b) The frequency characteristics expresses the rate of acquired global minims to all types of results at each particular setting, i.e. at each setting of A and B regardless on the thickness d.
The analysis of Si_3N_4 showed that fixing the A to values close to A_{id} can guarantee acquiring results very close to the ideal solution, i.e. measuring the optical properties very precisely.

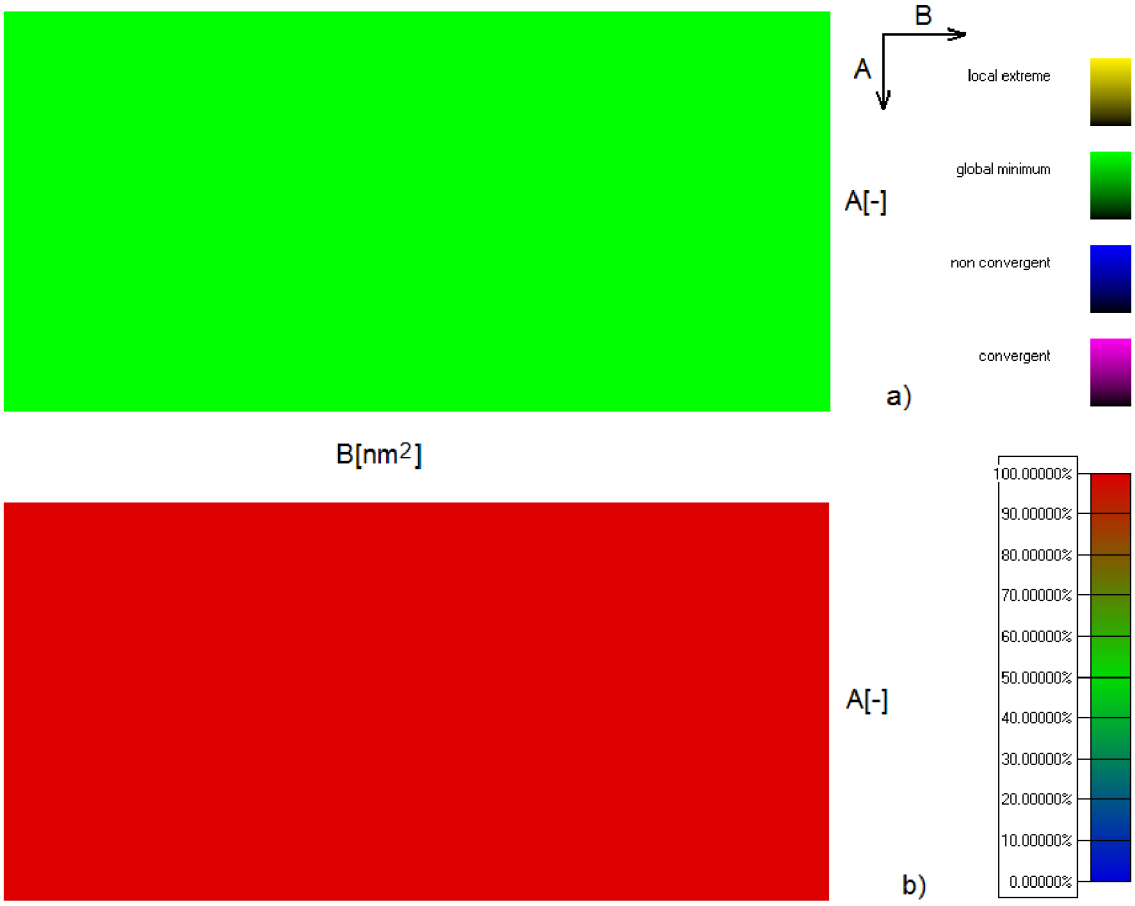

Figure 55: An example of $\mathbf{B^P}$ of 400nm thick Si_3N_4 film on silicon substrate when the coefficient A was fixed and where the thickness d was omitted.
a) The modal characteristics shows what type of the result (see the legend) was acquired most often. The lighter is the color, the higher is the frequency of the acquired result.
b) The frequency characteristics expresses the rate of acquired global minims to all types of results at each particular setting, i.e. at each setting of A and B regardless on the thickness d.
The analysis of Si_3N_4 showed that fixing the A to values close to A_{id} can guarantee measuring the optical properties very precisely.